Identifications of Genetic and Epigenetic Targets to Improve Cancer Therapies

Yunyi Wang
St. Hugh's College
University of Oxford

Supervised by Professor Yang Shi and Dr Carol Leung

A thesis submitted to the examination for the degree of Doctor of Philosophy

Trinity Term 2025

Abstract

Cancer remains a global health burden. Despite advances in our understanding of cancer biology and the development of cancer treatments, including radiotherapy, chemotherapy, hormonal therapy, targeted therapy, and immunotherapy, persistent limitations in efficacy due to tumour heterogeneity, therapy resistance, and immune evasion underscore the need for developing novel cancer therapies.

This thesis presents an integrated approach to identify and characterise new genetic and epigenetic targets for cancer therapy. Firstly, we identified UDP-xylose synthase 1 (UXS1) as a novel genetic target in non-small cell lung cancer (NSCLC) cells with high expression of UDP-glucose dehydrogenase (UGDH), revealing a metabolic vulnerability with therapeutic potential. We also identified type I protein arginine methyltransferases (PRMTs) as epigenetic targets capable of enhancing T cell function, providing a potential strategy to improve adoptive cell transfer therapies. Finally, we elucidated novel mechanistic insights into lysine-specific demethylase 1 (LSD1), a known cancer therapy target, and explored its functional interplay with metabolic pathways.

Collectively, these findings advance our understanding of cancer biology and identify therapeutic targets across genetic and epigenetic domains. The work provides a foundation for developing novel cancer therapies that address current limitations.

Declaration

Except where acknowledgement is made below and in the text or figure legends, the work described in this thesis was performed by the author in the Ludwig Institute for Cancer Research or the Wellcome Trust Centre for Human Genetics at the University of Oxford.

The following individuals have made contributions to part of this research:

- Dr Chen Zhou (Harvard Medical School, University of Oxford) analysed and prioritised the selective essential genes (Chapter 2).
- Dr Berna Bou Toyah (University of Oxford) helped with the cloning and expansion of UGDH expression plasmids (Chapter 2).
- Professor Skirmantas Kriaucionis (University of Oxford) performed the intracellular metabolite measurement experiments (Chapter 2).
- Richard Lisle and Robbie Crickley helped visualise immunostaining samples using confocal microscopy (Chapter 2).
- Dr Yuanqin Yang (University of Oxford) culled the mice used in the experiments and helped with the drug screening and subsequent validation experiments (Chapter 3).

The work reported in this thesis has not been submitted for any other degree in this or any other university or institute of learning. All sources used have been cited in the bibliography. Grammar in this thesis has been reviewed and corrected with the assistance of Grammarly.

Acknowledgements

The past four years have been both challenging and profoundly rewarding. None of this would have been possible without the support and guidance of numerous individuals to whom I owe my deepest gratitude. And I am particularly indebted to several individuals that I would like to thank here.

First and foremost, I would like to express my sincere gratitude to my supervisors, Professor Yang Shi and Dr Carol Leung, for their guidance. Yang is a remarkable scientist with a great work ethic and dedication to research. He always believes in me and encourages me to try out my ideas, which has been invaluable to my growth as a researcher. And Carol has provided me with helpful advice with her expertise in immune oncology, and she has always been on hand to provide support. I am deeply grateful for the mentorship.

I want to extend my sincere appreciation to all past and current members of the Shi lab for their continuous support and for making the working environment so enjoyable and cheerful. I am deeply thankful to Dr Yuanqin Yang and Dr Berna Bou Toyah for patiently teaching me various lab techniques and engaging me in stimulating scientific discussions. I am also grateful to Dr Chen Zhou for her advice on research and beyond. My heartfelt appreciation also goes to Felice Wallner and Dr Matthew Harris, who joined the lab together with me, for being such great benchmates and making my time in the lab running experiments less dull. Thank you all!

In addition, I could not have completed my work without the contributions of many collaborators. I am especially indebted to Professor Skirmantas Kriaucionis for his help with mass spectrometry, Richard Lisle and Robbie Crickley at the light microscopy facility for their help with imaging, and our exceptional lab support team for their continuous technical assistance.

This work has been funded by the Ludwig Institute of Cancer Research. I am grateful to the institution for allowing me to pursue my research with cutting-edge technologies and resources.

Lastly, I would like to extend my gratefulness towards my parents, Yingding Wang and Jun Wu. Thank you for your unconditional love and support. Knowing I will always have a safety net to catch me makes me stronger and more courageous. And to my partner, Dr Qiuchen Qian, who has pursued a DPhil degree in the UK with me. Thank you for handling my breakouts and reminding me there is life beyond lab experiments.

I have spent the past 20 years studying and pursuing higher degrees. This submission of this thesis marks the end of my life as a student. This journey was not without obstacles, but each challenge has shaped me into a better individual. Now is the start of a new chapter. I will carry the lessons, resilience, and relationships I have obtained, and I am ready for more challenges ahead.

Table of contents

List of Tables

List of Figures

List of abbreviations

1C	One-carbon
53BP1	p53 binding protein 1
5-FU	5-Fluorouracil
ACC	Acetyl-CoA carboxylase
ADC	Antibody-drug conjugate
ADCC	Antibody-dependent cellular cytotoxicity
ADCP	Antibody-dependent cellular phagocytosis
ADMA	Asymmetric dimethyl arginine
ALK	Anaplastic lymphoma kinase
ALL	Acute lymphoblastic leukaemia
AML	Acute myeloid leukaemia
APC	Antigen-presenting cell
ATP	Adenosine triphosphate
BAX	Bcl-2 associated X-protein
BCL2	B-cell lymphoma/leukaemia 2
BFP	Blue fluorescent protein
BRCA1	Breast cancer gene 1
BRCA2	Breast cancer gene 2
BRD4	Bromodomain-containing protein 4
Breg	Regulatory B cell
BRG1	Brahma-related gene 1
CAR	Chimeric antigen receptor
CML	Chronic myelogenous leukaemia
CoREST	Co-repressor for element-1-silencing transcription factor
CRT	Chemoradiotherapy
CTL	Cytotoxic T lymphocyte
CTLA-4	Cytotoxic T-lymphocyte-associated protein 4
CXCR3	CXC motif chemokine receptor 3
DC	Dendritic cell
DepMap	Cancer Dependency Map
DKO	Double knockout
DMSO	Dimethyl sulfoxide
DNA	Deoxyribonucleic Acid
DNMT	DNA methyltransferase
DSB	Double-strand break
dsRNA	Double-stranded RNA
dUMP	Deoxyuridine monophosphate
ECAR	Extracellular acidification rate
ECM	Extracellular matrix
ED	Enzymatically dead
EDTA	Ethylenediaminetetraacetic acid

EGFR	Epidermal growth factor receptor
EMT	Epithelial-mesenchymal transition
ER	Endoplasmic reticulum
ER	Oestrogen receptor
EZH2	Enhancer of zeste 2 polycomb repressive complex 2 subunit
FA	Fatty acid
FACS	Fluorescence-activated cell sorting
FAD	Flavin adenine dinucleotide
FASN	Fatty acid synthase
FBS	Foetal Bovine Serum
FDA	Food and Drug Administration
F-dUMP	Fluorodeoxyuridine monophosphate
FUTP	Fluorouridine triphosphate
G6P	Glucose-6-phosphate
GADD45	Growth arrest and DNA-damage-inducible protein
GAG	Glycosaminoglycan
GAR	Glycine arginine rich
GCK	Glucokinase
GDP	Guanosine diphosphate
GFP	Green fluorescent protein
GLDC	Glycine decarboxylase
GLUT	Glucose transporter
GLS1	Glutaminase
GPX4	Glutathione peroxidase 4
gRNA	Guide RNA
GSH	Glutathione
GTP	Guanosine triphosphate
GzmB	Granzyme B
H3K27ac	Histone 3 lysine 27 acetylation
H3K27me3	Histone 3 lysine 27 trimethylation
HA	Hyaluronan
HAS	Hyaluronan synthase
HAT	Histone acetyl transferase
HDAC	Histone deacetylase
HER2	Human epidermal growth factor 2
HIF-1α	Hypoxia-inducible factor-1α
HK	Hexokinase
HKDC1	Hexokinase domain-containing 1
HMT	Histone methyltransferase
HR	Hormone receptor
HuR	Hu antigen receptor
IARC	International Agency for Research on Cancer
ICB	Immune checkpoint blockade
IFNa	Interferon-α

IFNg	Interferon- γ
IGF-BP3	Insulin-like growth factor binding protein 3
IL-2	Interleukin-2
IL-10	Interleukin-10
KD	Knockdown
KO	Knockout
KRAS	Kirsten rat sarcoma virus
LAG3	Lymphocyte-activation gene 3
LDHA	Lactate dehydrogenase A
LSD1	Lysine-specific demethylase 1
LUAD	Lung adenocarcinoma
LUSC	Lung squamous cell carcinoma
MAPK	Mitogen-activated protein kinase
MDM2	Murine Double Minute 2
MDR	Multidrug resistance
MDS	Myelodysplastic syndrome
MDSC	Myeloid-derived suppressor cell
METTL14	Methyltransferase 14
MHC	Major histocompatibility complex
MMA	Monomethyl arginine
MRE11	Meiotic recombination 11
MRP1	Multidrug-resistance-associated protein 1
MS	Mass spectrometry
mTOR	Mammalian target of rapamycin
NADPH	Nicotinamide adenine dinucleotide phosphate
NF-kB	Nuclear factor kappa-light-chain-enhancer of activated B cells
NFAT	Nuclear factor of activated T cells
NGS	Next-generation sequencing
NK cell	Natural killer cell
NLS	Nuclear-localisation sequence
NormLRT	Normal likelihood ratio test
NRF2	Nuclear factor erythroid 2-related factor 2
NSCLC	Non-small cell lung cancer
NuRD	Nucleosome remodeling and deacetylase
OVA	Ovalbumin
OCR	Oxygen consumption rate
OE	Over-expression
OXPHOS	Oxidative phosphorylation
PARP	Poly ADP-ribose polymerase
PBMC	Peripheral-blood mononuclear cell
PBS	Phosphate buffered saline
PD-1	Programme death-1
PD-L1	Programmed death-ligand 1
PDK1	Pyruvate dehydrogenase kinase 1

PDO	Patient-derived organoid
PFK	Phosphofructokinase
PHGDH	Phosphoglycerate dehydrogenase
pHGG	Pediatric high-grade gliomas
PG	Proteoglycan
PI3K	Phosphatidylinositol 3-kinase
PIP2	Phosphatidylinositol (4,5)-bisphosphate
PIP3	Phosphatidylinositol (3,4,5)-trisphosphate
PKB	Protein kinase B
PKM2	Pyruvate kinase muscle isozyme M2
PMA	Phorbol 12-myristate 13-acetate
PPARGC1A	Peroxisome proliferator-activated receptor gamma coactivator 1α
PPP	Pentose phosphate pathway
pRb	Retinoblastoma protein
PRC2	Polycomb repressive complex 2
PRMT	Protein arginine methyltransferase
PROTAC	Proteolysis-Targeting Chimera
PSAT1	Phosphoserine aminotransferase
PTEN	Phosphatase and tensin homolog
R5P	Ribose 5-phosphate
RNA	Ribonucleic acid
ROS	Reactive oxygen species
RT-qPCR	Reverse transcription quantitative polymerase chain reaction
SAM	S-adenosylmethionine
SCD1	Stearoyl-CoA desaturase 1
SCLC	Small cell lung cancer
SDMA	Symmetric dimethyl arginine
SEPHS2	Selenophosphate Synthetase 2
SHMT2	Serine hydroxy methyltransferase
SHP2	Src homology 2 domain-containing phosphatase 2
shRNA	Short hairpin RNA
SREBP	Sterol regulatory element-binding protein
SSB	Single-strand break
STAT3	Signal transducer and activator of transcription 3
SWIRM	Swi3p/Rsc8c/Moira
TAL1	T-cell acute lymphocytic leukaemia protein 1
TAM	Tumour-associated macrophage
TCA	Tricarboxylic acid
TCGA	The Cancer Genome Atlas Programme
TCR	T-cell receptor
TET2	Ten-eleven translocation 2
TF	Transcription factor
TGFb	Transforming growth factor- ß
TIGIT	T cell immunoreceptor with Ig and ITIM domain

TIL	Tumour-infiltrating lymphocyte
Tim-3	T cell immunoglobulin domain and mucin domain 3
TLX	Tailless-like 1
TME	Tumour microenvironment
TNBC	Triple-negative breast cancer
Treg	Regulatory T cell
T-VEC	Talimogene laherparepvec
UDP	Uridine diphosphate
UDP-GlcUA	UDP-glucuronic acid
UGDH	UDP-glucose 6-dehydrogenase
UGT	UDP-glucuronosyltransferases
UTR	Untranslated region
UXS1	UDP-xylose synthase 1
WES	Whole-exome sequencing
WHO	World Health Organisation
WT	Wild-type

Chapter 1: Introduction

In this chapter, I will begin by providing an overview of cancer biology and current therapeutic strategies, then introduce the need for safer and more effective treatments, and discuss the challenges faced in developing novel cancer therapies. I will then examine the application of targeting genetic mutations, followed by introducing three specific fields with therapeutic potential. Finally, I will outline the key aims of this thesis.

1.1 Overview of cancer and current therapies

Cancer remains a significant public health challenge and is among the leading causes of death. According to data from the International Agency for Research on Cancer, 20 million new cases are diagnosed globally each year. It is a complex disease characterised by uncontrolled cell proliferation, which can invade surrounding normal tissues and even metastasise to distant sites. With the increased understanding of tumour-promoting mechanisms, therapies aimed at shrinking tumour size and controlling tumour growth have been developed, including radiotherapy, chemotherapy, hormonal therapy, targeted therapy, and immunotherapy. Despite the remarkable advancements in clinical research, the disease continues to impose a heavy mortality burden, underscoring the need for novel therapies as well as methods for prevention and early detection.

1.1.1 Radiotherapy

High-energy photon radiation induces deoxyribonucleic acid (DNA) damage, including single-strand breaks (SSBs) and double-strand breaks (DSBs). The accumulation of DNA damage imposes a cellular stress that activates the apoptotic pathways and leads to cell death. In addition, radiation also induces the production of reactive oxygen species (ROS) in the cells, such as hydroxyl radicals, superoxide anions and hydrogen peroxide, causing damage to DNA, proteins, and lipids[1]. Consequently, radiation kills

the affected cells. By positioning the radiation beams towards the tumour, clinicians could selectively kill tumour cells while sparing surrounding healthy tissues.

However, radiosensitivity varies by cancer type. For example, lymphoma, myeloma, and neuroblastoma are usually highly sensitive to radiation, while pancreas cancer, breast cancer, bladder cancer and cervical cancer have moderate sensitivity, and glioblastoma, melanoma, osteosarcoma, and renal carcinoma usually do not respond to radiotherapy[2]. This limits the use of radiotherapy for cancer treatment. Radiosensitizers have been developed to address this limitation. These compounds act through multiple mechanisms, including suppressing the production of endogenous radioprotective substances, forming cytotoxic substances through radiolysis, and inhibiting DNA repair pathways[1].

As tumour vascularisation often fails to meet the proliferative demand, the tumour microenvironment (TME) is usually hypoxic. And hypoxia further limits the efficacy of radiotherapy by inhibiting the radiation-induced ROS production, thus minimising the cytotoxic effects of radiotherapy.

In addition, precision targeting is critical to avoid any unintentional exposures of normal cells to the radiation. However, the dynamic changes of the tumour position between imaging and radiation administration complicates this goal. New advancements in image-guided radiation therapy address this limitation and minimise the potential side effects of off-target exposure on adjacent normal cells[3].

1.1.2 Chemotherapy

Chemotherapy targets the rapid proliferation of cancer cells by disrupting mitosis or inducing DNA damage. While the anti-mitotic mechanism is self-explanatory, using

mutagens to cause DNA damage could specifically induce cell death in rapidly dividing cells for three reasons:

1) Rapidly dividing cells tend to have more open chromatin, increasing their susceptibility to mutagens;
2) DNA damage is primarily sensed during S phase (the DNA replication phase) of the cell cycle, which occurs more frequently in proliferating cells;
3) Cancer cells that are rapidly dividing have less time for DNA repair and often harbour pre-existing DNA repair defects, making it even more challenging to repair DNA and avoid DNA damage-induced cell death.

Based on these principles, many chemicals have been developed to treat cancer, including alkylating agents that are chemically reactive to form covalent bonds with DNAs, platinum compounds that can be activated in cells to form reactive intermediates and bind to nucleotides, antimetabolites that inhibit enzymes involved in DNA synthesis and get incorporated into DNAs as a fault base[4], topoisomerase inhibitors that inhibit the release of topoisomerase from topoisomerase-DNA complex and cause DNA SSBs and DSBs [5], and tubulin-binding drugs that inhibit the formation of microtubules, whose reorganisation to form mitotic spindles is essential during mitosis[6.]

For example, 5-Fluorouracil (5-FU) is a widely used chemotherapy drug. It is an analogue of naturally occurring pyrimidine uracil, and it is metabolised inside the cells to form fluorouridine triphosphate (FUTP) and fluorodeoxyuridine monophosphate (F-dUMP). While FUTP is mis-incorporated into ribonucleic acid (RNA) in place of uracil, F-dUMP binds covalently to thymidylate synthase, inhibiting the *de novo* synthesis of thymidine from deoxyuridine monophosphate (dUMP), and further downregulating DNA synthesis and gene expression[7].

Chemotherapy is a cornerstone treatment for cancers, such as lymphoma, breast cancer, lung cancer, leukaemia, and multiple myeloma, with about 25% of new cases receiving it. However, its toxicity towards healthy proliferating cells leads to significant side effects. For example, the hematopoietic cells in bone marrow also proliferate relatively fast. Chemotherapy would give rise to myelotoxicity, where the production of blood cells is inhibited, leading to decreased coagulation, anaemia, and increased susceptibility to infections[8]. Hair follicle keratinocytes are also rapidly dividing. Thus, they will be targeted by chemotherapy, leading to alopecia. And epithelial cells lining the stomach and gut will also be damaged by chemotherapy, leading to nausea, or in more severe cases, gastric perforation, digestive fistulas, and bowel leakage[9].

As many chemotherapies elicit their effect by inducing DNA mutations, they can paradoxically promote secondary malignancies. This is evident by the studies conducted by *Hunter et al.* and *Cahill et al.,* where gliomas that recurred after temozolomide (a DNA alkylating agent) treatment, were found to carry huge numbers of mutations, with the mutation pattern mirroring those induced by temozolomide in experimental systems [10,11].

One potential improvement of chemotherapy is to increase its specificity to cancer cells. Another aspect of advancements is to consider the combined use of radiotherapy and chemotherapy. Synergic effects have been observed in some cancer types to support the use of chemoradiotherapy (CRT) in cervical cancer, non-small cell lung cancer (NSCLC), anal cancer and bladder cancer[12], while a broader application in other cancer types is worth exploring.

1.1.3 Hormonal therapy

Radiotherapy and chemotherapy target cancer cells based on their location or proliferative capacity, which might inadvertently damage nearby healthy cells or other rapidly proliferating normal tissues, causing side effects that limit the drug dosage. In contrast, hormonal therapy targets cancer cells more selectively. Steroid hormones play an important role in regulating cell proliferation and survival via autocrine and paracrine effects, and certain cancer cells, including breast cancer, endometrial cancer, prostate adenocarcinomas, and uterine sarcomas, are dependent on hormonal signals for proliferation. This hormone dependence provides a therapeutic opportunity to selectively target cancer cells while sparing normal tissues, forming the basis of hormonal therapy[13].

The drug molecule works by either inhibiting hormone synthesis or blocking the downstream signalling transduction pathway. One example is the clinical use of tamoxifen, a competitive inhibitor of oestrogen receptors (ERs). It blocks the ER signalling pathways, thus reducing the expression of oestrogen-targeted genes, such as *BCL2* that encodes for B-cell lymphoma/leukaemia 2 (BCL2), an anti-apoptotic regulator, and *PIK3CA* that encodes for phosphatidylinositol 3-kinase (PI3K) of the PI3K/protein kinase B (PKB, AKT)/ mammalian target of rapamycin (mTOR) pathway which promotes cell survival in ER-positive breast cancer [14]. However, as hormones usually regulate multiple physiological systems and interact with other hormones, targeting cancer-driving hormones may lead to systemic side effects, such as headaches, nausea, mood changes and more severely, thrombosis[15].

1.1.4 Targeted therapy

Hormonal therapy is effective only in hormone-driven cancers. In cancers such as triple-negative breast cancer (TNBC), which account for about 15-20% of breast cancers [16], cancer proliferation is not driven by hormones, and hormonal therapy would not selectively induce cell death in these cells. Epidemiological studies have identified breast cancer gene 1 (BRCA1) mutation in 85% of TNBC patients, presenting a genetic vulnerability for therapeutic exploitation[17]. BRCA1 is essential for homologous recombination (HR) repair of DNA DSBs[18]. Cancer cells with mutations in the *BRCA1* gene are more likely to accumulate DNA damage and rely more on Poly-ADP-ribose polymerase (PARP) for DNA repair, making them susceptible to PARP inhibitors. Similarly, mutations in breast cancer gene 2 (BRCA2), another gene involved in DNA repair, are also associated with higher risks of various cancers and cancer cells with mutations in the *BRCA2* gene are also susceptible to PARP inhibitors[19]. This synthetic lethality between BRCA1/2 and PARP underpins the treatment of PARP inhibition in BRCA-mutated cancers. In accordance with these, the clinical use of PARP inhibitors, Olaparib (Lynparza) and Talazoparib (Talzenna), in BRCA-mutated cancers has been approved by the U.S. Food and Drug Administration (FDA)[20].

With the advancement in sequencing technologies, more genetic vulnerabilities have been identified, enabling the development of a new type of cancer therapy, targeted therapy, which selectively kills cancer cells while sparing healthy tissues.

In addition to PARP inhibitors, another targeted therapy used to treat breast cancer is the PI3K inhibitor Alpelisib. The *PIK3CA* gene encodes for the 110 kDa catalytic subunit of PI3K. As the PI3K/ AKT/ mTOR pathway promotes cell proliferation and survival, the gain-of-function mutation in the *PIK3CA* gene leads to tumour development[21]. Alpelisib has been approved to treat PIK3CA-mutated breast cancer. And the combined use of Alpelisib, targeting PI3K, and Fulvestrant, targeting ER, led

to prolonged progression-free survival of patients with PIK3CA-mutated hormone receptor $(HR)^+$/ human epidermal growth factor 2 $(HER2)^-$ breast cancer[21].

The development of targeted therapy is, of course, not restricted to the treatment of breast cancer. B-Raf protein, encoded by the *BRAF* gene, is a critical signal transmitter in the RAS/ RAF/ mitogen-activated protein kinase (MAPK) pathway, and the gain-of-function mutation in the *BRAF* gene is found in 40% to 60% of melanomas, leading to a constitutively activated B-Raf protein[22]. Since the RAS/ RAF/ MAPK pathway regulates essential cellular processes, such as cell growth and survival[23], the BRAF-mutated cancer cells would grow uncontrollably, and B-Raf serves as a good target for the development of targeted therapy. Under this concept, B-Raf inhibitors, Vemurafenib and Encorafenib, have been developed, and they are now approved for treating *BRAF*-mutated melanoma[24].

Once the target is identified, the development of targeted therapy is not restricted to small molecules that inhibit or potentiate the targeted proteins. Antibody-drug conjugates (ADCs) have been made by linking an antibody that recognises the targeted protein on cancer cells to a cytotoxic payload. With the specificity of the antibody, the cytotoxic payload can be selectively delivered to cancer cells, restricting the payload release and cytotoxic effect within the cancer cells.

One example of targeted therapy developed based on this concept is Trastuzumab Deruxtecan for the treatment of HER2-mutated cancers. HER2, encoded by the *ERBB2* gene, is overexpressed in 3% of breast cancer[25], and the constitutively active HER2 receptors in these cancer cells promote cell survival through both RAS/ RAF/ MAPK pathway and PI3K/ AKT/ mTOR pathway[26]. Trastuzumab Deruxtecan consists of an antibody, Trastuzumab, which recognises HER2 on the cell surface, and a topoisomerase inhibitor, Deruxtecan, which causes DNA damage by inhibiting the

release of the enzyme from topoisomerase-DNA complexes. Trastuzumab Deruxtecan has been shown to prolong overall survival of the patients with HER2-mutated cancer.

1.1.5 Immunotherapy

Both the innate and adaptive immune systems are important in controlling tumour growth. This is evident by the increased tumour growth in mouse models following the treatment of neutralising monoclonal antibodies against interferon-γ (IFNg), a key immune cytokine that regulates both innate and adaptive immune responses[27]. Furthermore, mice insensitive to IFNg showed greater susceptibility to methylcholanthrene-induced sarcoma formation[28].

Some innate immune cells, such as natural killer (NK) cells and neutrophils, can elicit cytotoxic effects on targeted cancer cells directly, while other innate immune cells, such as dendritic cells (DCs) and macrophages, initiate adaptive immune responses against cancer cells through tumour-specific antigen presentation and cytokine release[29,30]. In the adaptive immune system, B cells produce tumour-specific antibodies, which aid in the cytotoxic effect of macrophages via antibody-dependent cellular phagocytosis (ADCP) and the cytotoxic effect of T cells via antibody-dependent cellular cytotoxicity (ADCC). Upon recognition of tumour-specific antigens, $CD4^+$ helper T cells enhance immune activity through cytokine secretion, which promotes the activity of B cells and cytotoxic T cells; while $CD8^+$ cytotoxic T cells directly induce apoptosis in targeted cancer cells through the release of cytotoxic molecules, such as perforin and granzymes[29,30]. Collectively, the interplay between innate and adaptive immune systems and between different immune cell types constitutes a robust immune response crucial for controlling tumour growth.

However, tumour cells evolve to evade immunosurveillance through mechanisms such as downregulating the expression of tumour-specific antigens, expressing immune checkpoint inhibitory molecules and secreting molecules to make the TME more immunosuppressive. Given the key role of immune response in regulating tumour growth, therapies targeting dysfunctional anti-tumour immunity have been explored. Here, I will introduce four types of immunotherapies: immune checkpoint blockade (ICB), adoptive cell transfer, cytokine therapies, and oncolytic virus.

Immune checkpoints are molecules of the co-inhibitory signalling pathways. In normal circumstances, these checkpoint molecules on immune cells help to prevent excessive tissue damage from prolonged infection. However, cancer cells utilise this immune regulation mechanism and over-express the ligands for the checkpoint molecules to downregulate T cell function[31]. ICBs are developed to inhibit the interaction between immune checkpoint molecules expressed on T cells and their ligands expressed on cancer cells and tune down the negative signalling pathways in immune cells, thus promoting immune-mediated elimination of malignant cells.

For example, programmed cell death-ligand 1 (PD-L1) on tumour cells interact with programmed cell death-1 (PD-1) expressed on T cells, leading to the recruitment of Src homology 2 domain-containing phosphatase 2 (SHP2) that dephosphorylates proteins involved in TCR signalling pathways and suppresses T cell activation, proliferation, and cytokine production[32]. As expected, a monoclonal antibody that blocks PD-1 increased T cell function in mouse models[33]. And clinical use of PD-1 inhibitors, such as Pembrolizumab (Keytruda) and Nivolumab (Opdivo), has been approved by the FDA in treating multiple cancer types, including melanoma, NSCLC, and kidney cancers[34].

Another example of immune checkpoint molecules is cytotoxic T-lymphocyte-associated protein 4 (CTLA-4, CD152), which elicits its negative regulatory effect by

competing with the co-stimulatory receptor CD28 for binding CD80 and CD86 on antigen-presenting cells (APCs)[35]. Inhibition of CTLA-4 has been shown to increase tumour control in experimental settings[36,37], and the clinical use of Ipilimumab, a monoclonal antibody for CTLA-4, has been approved by the FDA to treat metastatic melanoma[38,39].

Another type of immunotherapy is adoptive cell transfer. As cancer cells release cytokines to render the TME immunosuppressive, the function of tumour-infiltrating T cells is usually downregulated. With the advancement in gene-editing techniques, autologous T cells have been processed and engineered to overcome the negative regulatory signals in the TME and to elicit stronger effector functions to control tumour growth. Currently, there are two main types of adoptive T cell transfer. Chimeric antigen receptor (CAR)-T cells are T cells engineered to express CARs, artificial receptors constructed by linking the variable regions of the antibody targeting a tumour-specific surface protein to the activator of signalling pathways, such as CD28. And T-cell receptor (TCR)-engineered T cells are T cells edited to express TCRs, which recognise antigens that have been processed and presented on the patient's own MHC molecules[40].

The clinical use of both CAR-T cells and TCR-T cells has been explored. For example, CD19-targeting CAR-T cell therapy has been approved by the FDA for treating chemotherapy-resistant B-precursor acute lymphoblastic leukaemia, as CD19 is expressed selectively on the cell membrane of B cells[41]. Similarly, NY-ESO-1 and LAGE-1-targeting TCR-T cell therapy has been approved to treat advanced synovial sarcoma[42].

And the cancer vaccine Sipuleucel constitutes a special type of adoptive cell transfer. In this case, DCs are selected from the patient's peripheral-blood mononuclear cells (PBMCs) and activated to present tumour-specific antigens by a recombinant fusion

protein, PA2024, which consists of prostatic acid phosphatase (a prostate cancer-specific antigen) and granulocyte-macrophage colony-stimulating factor (an immune-cell activator)[43]. The injection of the autologous DCs back to the patients allows the activation of T cell-mediated anti-tumour immune responses by tumour-specific antigens[31].

The applications of cytokine therapies, where cytokines are given directly for their regulatory function on both innate and adaptive immune cells, have also been explored[44]. Examples include the clinical use of interleukin-2 (IL-2) in treating renal cell cancer and advanced melanoma and the use of interferon-α (IFNa) in treating hairy cell leukemia[45.]

Lastly, the clinical use of oncolytic viruses has also been established. The oncolytic virus preferentially infects tumour cells and incorporates eukaryotic transgene payloads into the target cell genome to induce cell death; in addition, it also promotes anti-tumour immunity[46,47]. With our increased understanding of immune-oncology and virology, the oncolytic virus Talimogene Laherparepvec has been developed and approved by the FDA for treating melanoma[47].

1.2 Therapeutic challenges

In Chapter 1.1, I reviewed currently available cancer therapies, including radiotherapy, chemotherapy, hormone therapy, targeted therapy, and immunotherapy. The field has advanced rapidly, and more therapeutic strategies have been developed to reduce tumour burdens and prolong survival. However, cancer is still among the top causes of death globally, with 10 million deaths being attributed to cancer annually according to the World Health Organisation (WHO), suggesting the necessity of developing safer and more effective strategies for treating cancer. In this chapter, I will discuss the various therapeutic challenges, including tumour heterogeneity, drug resistance and the immunosuppressive TME.

1.2.1 Heterogeneity of tumours

Cancer is a complex disease. It is not surprising for the existence of inter-tumoral heterogeneity, where tumour samples showing the same histological features have different genomes, transcriptomes, and epigenomes caused by various environmental factors, germline genetic mutations and somatic mutation profiles[48,49]. On top of that, intra-tumoral heterogeneity is also observed. This is evident in the whole-exome sequencing (WES) experiments by *Harbst et al.*, revealing an average of 489 non-synonymous mutations per tumour, 13% of which were not detected across all samples taken from the same tumour [50]. As the genome has a size of about 6 billion base pairs, and that the cancer genome is relatively unstable due to the exposure to mutagens and/or the dysfunction in DNA repair pathways, spontaneous new mutations could appear in individual cancer cells, and the clonal evolution and selection afterwards lead to the intra-tumoral heterogeneity observed.

However, sequencing a heterogeneous population is less informative. Bulk sequencing of mixed cell populations obscures critical molecular targets, complicating both drug

development and patient stratification since some clones might over-express a particular protein that can be targeted, while other clones might not, rendering these cells resistant to the treatment. For example, the clinical study by *Piotrowska et al.* showed that both epidermal growth factor receptor (EGFR)-wild type (WT) and EGFR-mutant (T790M) clones existed before the treatment of Rociletinib, an EGFR inhibitor targeting EGFR T790M mutation, and these EGFR WT clones could emerge as the dominant source of drug resistance[51].

One potential solution would be the 'dose and rest' administration regime, where the treatment is given to the patients for only a short time, followed by a resting period before the subsequent treatment to minimise the selective pressure for drug-resistant clones. This is validated in a patient-derived xenograft model of melanoma, where a complex dosing schedule consisting of intermittent doses of a BRAF inhibitor reduced drug resistance and improved survival [52].

1.2.2 Drug resistance

A major therapeutic challenge arises when cancer cells develop resistance to treatments. Some cancers have primary drug resistance and respond poorly to the current cancer therapies. In this case, new cancer vulnerabilities need to be identified for the development of new treatments that could selectively cause cell death in these cells. While some cancer cells have acquired resistance. This means the tumour has developed resistance during or after the course of the treatment. The above-mentioned NSCLC patients with both EGFR WT and EGFR-mutant clones are a good example. In this case, the change between therapy types might be necessary to identify the effective therapeutic strategy and to avoid clonal expansion of the drug-resistant clones.

However, some cancer cells have a multi-drug resistance (MDR) phenotype, meaning that they are resistant to multiple treatments, and the switch between therapy types will not improve prognosis. This could be due to mutations in the cancer cells that lead to the increased activity of efflux pumps (e.g., P-glycoprotein and multidrug-resistance-associated protein 1)[53], the reduced drug influx, the activation of detoxifying proteins (e.g., cytochrome P450 mixed-function oxidases), the activation of DNA repair pathways for repairing drug-induced DNA damage and the disruption of apoptotic pathways[54]. These adaptations render tumours resistant to conventional approaches, including radiotherapy, chemotherapy, hormonal therapy, or small-molecule targeted therapy, which will not elicit their beneficial effect. In such cases, immunotherapy may represent a promising alternative, as it operates through distinct mechanisms independent of traditional drug sensitivity pathways.

1.2.3 Immunosuppressive TME

The efficacy of immunotherapies could also be limited due to the immunosuppressive TME with inhibitory cytokines and chemokines, such as transforming growth factor-ß (TGFb) and interleukin-10 (IL-10), which inhibit the cytotoxic function of NK cells and T cells found in the TME[55,56]. The TME also consists of various cells that suppress the effector function of immune cells, including regulatory T cells (Tregs) that tune down immune response by releasing TGFb and IL-10 and expressing CTLA-4[57], regulatory B cells (Breg)[58], tumour-associated macrophages (TAMs) and myeloid-derived suppressor cells (MDSCs) [59]. These components collectively establish a profoundly suppressive milieu that compromises immunotherapy efficacy.

Two promising strategies have emerged to address these limitations. Firstly, identifying these inhibitory pathways and targeting them to enhance immune-mediated tumour control, as done by various ICBs, can help neutralise these inhibitory signals. Another

aspect of improvement would be to edit T cells based on our increasing knowledge of T cell biology and function to generate therapeutic T cells with enhanced capacity for tumour infiltration and resistance to immunosuppression.

In conclusion, the challenges of tumour heterogeneity, drug resistance, and the immunosuppressive TME outlined in this chapter underscore the critical need for better therapeutic strategies. Developing solutions to these barriers represents an essential step towards more effective cancer treatments.

1.3 Cancer genetics

In Chapter 1.3, I will discuss the rationale and methods for targeting cancer genetic vulnerability for the development of cancer therapies. I will then introduce two types of genes, 'tumour-suppressor genes' and 'proto-oncogenes', where mutations are usually found.

1.3.1 Targeting gene mutations for cancer treatment

Cancer has been described as a genetic disease characterised by accumulated mutations. This concept is supported by multiple lines of evidence. For example, agents that caused DNA damage and mutations also caused cancer, and the introduction of total genomic DNA from human cancers into phenotypically normal NIH3T3 cells would convert them into cancer cells[60]. The identification of the *HRAS* gene, which encodes for H-Ras protein, as the first cancer-driving gene further confirmed the genetic basis of cancer[61].

Genetic alterations in cancer can be in various forms, including substitutions of a single base pair, insertions or deletions of small or large segments of DNA, chromosome rearrangements, and more dramatically, alterations in chromosome numbers[62]. While exogenous mutagens, such as tobacco smoke and UV light, can cause mutations, endogenous replication errors also contribute to the accumulation of DNA mutations. Recently, the importance of acquired DNA sequences from exogenous sources, such as human papillomavirus, Epstein-Barr virus, hepatitis B virus, human T lymphotropic virus and human herpes virus, in cancer development has been investigated. This understanding has led to the development of prophylactic vaccines that reduce cancer risk by preventing viral infections[63].

Up to now, research has identified at least 350 out of the 22,000 protein-coding genes with recurrent somatic mutations in cancer, representing 1.6% of all protein-coding genes in the human genome; the mechanism of how these mutations lead to cancer development has been studied, and the potential of targeting these mutations for cancer treatment has been explored[64]. While studies in the mouse models using a retroviral screening approach have identified more than 3000 genes with the potential to contribute to cancer development, suggesting the possibility of more cancer-driving mutations that could be targeted for developing novel therapies. In addition, mutations in the non-coding regions, such as the promoter region of the *TERT* gene and the 5' untranslated region (UTR) of the *MTG2* gene[65], may also contribute to cancer, further increasing the number of potential drug targets. Sequencing technologies and the availability of various sequencing data sets, such as the The Cancer Genome Atlas Program (TCGA) data set, allow us to identify cancer-driving genetic changes that were not previously studied[66].

1.3.2 Tumour-suppressor genes

Tumour-suppressor genes, as the name suggests, are a group of genes that suppress tumour growth. They are usually involved in cell proliferation, apoptosis, or DNA repair pathways. When functioning normally, they control cell growth, repair DNA mutations, and induce apoptosis upon receiving appropriate signals. A loss-of-function mutation in these genes would drive cancer development. One famous example is the *TP53* gene, which is found to be mutated in 50% of cancers[67]. It is maintained at low levels due to the short half-life of p53 protein and is activated by stress signals, such as DNA damage and hypoxia. It acts as a transcription factor (TF) to alter the expression of multiple proteins, such as p21 and murine double minute 2 (MDM2) in cell cycle regulation[68], growth arrest and DNA-damage-inducible protein (GADD45) in DNA repair pathway, Bcl-2 associated X-protein (BAX) in apoptotic pathway[69], and insulin-

like growth factor binding protein 3 (IGF-BP3) in mitotic pathway[70]. Despite the substantial body of literature documenting the functional significance of *TP53* in various cancer types, no drugs targeting the p53 protein have been approved to be used clinically, probably due to the difficulty in developing a molecule that can enter the nucleus and effectively bind to this nuclear protein[71].

Another important tumour-suppressor is phosphatase and tensin homolog (PTEN), which catalyses the conversion between phosphatidylinositol (3,4,5)-trisphosphate (PIP3) to phosphatidylinositol (4,5)-bisphosphate (PIP2), the reverse action of PI3K. As the PI3K/AKT/mTOR pathway promotes cell survival and inhibits apoptosis, PTEN reverses its action and induces apoptosis, especially anoikis, which is the programmed cell death in cells upon loss of contact with the extracellular matrix (ECM)[72]. The loss-of-function mutation in the *PTEN* gene inhibits the apoptotic pathways and increases the risk of prostate cancer, breast cancer, thyroid cancer, and kidney cancer. Therapeutic strategies targeting this pathway have led to the development of Capivasertib (Truqap), an AKT inhibitor, which is approved to treat cancers with PTEN mutations.

1.3.3 Proto-oncogenes

In contrast to tumour-suppressor genes, proto-oncogenes usually function to promote controlled cell proliferation. For example, kirsten rat sarcoma virus (KRAS) encodes for the K-Ras protein, a GTPase that catalyses the conversion of guanosine triphosphate (GTP) to guanosine diphosphate (GDP) to initiate the downstream signalling pathway and ultimately activate TFs that regulate genes involved in cell cycle progression and cell proliferation[8373]. However, the ‘gain-of-function’ mutation at C12G produces a constitutively activated protein and disrupts cell cycle regulation. This specific mutation in the *KRAS* gene is particularly prevalent, occurring in about 30% of lung cancers[74]. Building on this understanding, the FDA has approved Sotorasib, a

drug molecule that forms irreversible covalent bonds with cysteine in the mutated K-Ras, for treating lung cancers with KRAS C12G mutation[75].

1.4 Potential cancer hallmarks for targeting

The term ‘cancer hallmarks’ was first raised by Douglas Hanahan and Robert A. Weinberg in 2000. In their first review, they proposed six cancer hallmarks, including ‘self-sufficiency in growth signals’, ‘insensitivity to anti-growth signals’, ‘tissue invasion and metastasis’, ‘limitless replicative potential’, ‘sustained angiogenesis’ and ‘evading apoptosis’[76]. 11 years later, they proposed two more emerging hallmarks, namely ‘reprogramming of energy metabolism’ and ‘evading immune destruction’[77]. Moreover, in the most recent updates in 2022, four emerging hallmarks and enabling characteristics have been proposed, including ‘polymorphic microbiomes’, ‘senescent cells’, ‘non-mutational epigenetic reprogramming’ and ‘unlocking of phenotypic plasticity’[78]. The latter two convey the critical role of epigenetic regulations in cancer development. In Chapter 1.4, I will discuss three key areas, from these proposed hallmarks, with relevance to therapeutic target identifications: metabolic regulation, immune regulation, and epigenetic regulation in cancer.

1.4.1 Metabolic regulation in cancer

Cancer cells exhibit distinct metabolic pathways as compared to normal cells. This phenomenon was first brought to attention by Warburg in 1925[79]. His work revealed that cancer cells preferentially utilise aerobic glycolysis instead of oxidative phosphorylation (OXPHOS) for energy production. Though OXPHOS is more efficient in terms of the average number of adenosine triphosphate (ATP) molecules produced from a given number of glucose molecules, a lot more ATPs can be generated through glycolysis in a given time to meet the energy demands of rapidly proliferating cancer cells. This is achieved by the upregulation of c-MYC, a transcription factor that

promotes the expression of multiple proteins involved in glycolysis, including glucose transporter (GLUT), hexokinase 2 (HK2), phosphofructokinase (PFK), lactate dehydrogenase A (LDHA), and pyruvate dehydrogenase kinase 1 (PDK1). Concurrent downregulation of p53 further promotes glycolysis through the increased GLUT1 and GLUT4 expression[80].

Another key metabolic shift in cancer cells is the increased conversion of glutamine to glutamate, known as glutaminolysis. The upregulation of glutamine metabolism can promote cancer cell survival in two ways. Firstly, glutamine is another source of energy, and by breaking down glutamine, the downstream metabolites can be used in the tricarboxylic acid (TCA) cycle to produce ATP and α-ketoglutarate. Secondly, glutamate can be used to synthesise glutathione (GSH), an important antioxidant molecule that reduces the oxidative stress in cancer cells[81]. This metabolic shift is also attributed to the upregulation of Myc protein, which leads to an increased expression of glutaminase (GLS1) and glutamine transporter Slc1a5 [82].

Lipid metabolism is also altered in cancer cells. This is characterised by the increased uptake of fatty acids (FAs) and the reactivation of *de novo* FA biosynthesis[83,84] Altered lipid metabolism aids in cancer cell proliferation since FA oxidation produces ATPs. In addition, FA is also a critical component of the lipid membrane, which is needed in the mitotic process to form daughter cells. The alteration in lipid metabolism is achieved by the glucose-induced activation of sterol regulatory element-binding proteins (SREBPs), a transcription factor that activates the expression of enzymes involved in lipid metabolism, including acetyl-CoA carboxylase (ACC), fatty acid synthase (FASN), and stearoyl-CoA desaturase 1 (SCD1)[85].

Another source of ATPs comes from one-carbon (1C) metabolism. Not surprisingly, the 1C metabolic pathway is also upregulated in cancer cells to produce more ATPs to support the rapid cell growth. In addition to generating ATPs, the 1C metabolic pathway

is also important for the transfer and cycling of 1C-groups between various acceptor groups. In this way, the nutrient status inside the cells can be sensed and multiple pathways can be regulated accordingly for the ultimate biosynthesis of purines, thymidine, glutathione (GSH) and S-adenosylmethionine (SAM), which are precursors of the production of macromolecules, including proteins, lipids, and nucleic acids[86]. The upregulation of 1C metabolism in cancer cells is mediated by the increased expression of enzymes, such as phosphoglycerate dehydrogenase (PHGDH) under the regulation of cMYC and phosphoserine aminotransferase (PSAT1) under the regulation of nuclear factor erythroid 2-related factor 2 (NRF2)[87].

Other metabolic pathways may also be altered in cancer cells to generate more ATPs or building blocks for macromolecules. Changes in metabolism also alter signalling transduction to support cell proliferation, with recent studies reporting the role of metabolites in signalling pathways[88]. Since the alteration in metabolic pathway is a unique feature for cancer cells and can differentiate them from healthy cells, therapeutic strategies have been developed to target these altered metabolic pathways in cancer cells.

1.4.2 Immune regulation in cancer

Tumour-infiltrating lymphocytes (TILs) play a crucial role in controlling cancer growth[83]. Cytotoxic T cells release molecules, such as granzymes and perforins, to kill cancer cells directly, and T helper cells release stimulatory cytokines to promote the activation and function of other immune cells[89]. Together, they could restrain tumour growth. While this immune surveillance is counterbalanced by regulatory T cells, which release inhibitory cytokines and downregulate T cell functions to prevent excessive tissue damage[90].

Cancer cells evolve to develop strategies to evade such immune surveillance. As mentioned earlier in Chapter 1.1.5, one such strategy is via the expression of inhibitory receptor ligands, such as PD-L1, which bind to immune checkpoint receptors on T cells and downregulate their functions[91,92]. Cancer cells also secrete immunosuppressive cytokines, such as TGFb, which negatively impact the function of TILs and recruit immunosuppressive cell populations to the TME[93]. Cancer cells also evolve to reduce the presentation of tumour-specific antigens on their cell surface to reduce their immunogenicity. These adaptations enable tumours to escape immune destruction despite the inherent capacity of anti-tumour immunity.

As our immune systems have the capability to kill tumour cells selectively, and the mechanism of evading such immune surveillance is a unique feature of cancer cells, multiple cancer therapies have been developed to target the down-regulated immune-mediated tumour control, including ICBs, adoptive cell transfers, cytokine therapies, cancer vaccine and oncolytic virus as mentioned in Chapter 1.1.5. One of the main barriers to the high efficacy of these therapies is T cell exhaustion induced by the immunosuppressive molecules and cell populations in the TME[94]. Thus, overcoming this barrier through approaches that prevent such exhaustion phenotype and enhance T cell function would help to improve current immunotherapies.

1.4.3 Epigenetics in cancer

Gene expression regulation in cancer extends beyond genetic alterations and includes epigenetic reprogramming, where the chromatin structure is reorganised by DNA and histone modifications without changes in the DNA sequence[95].

DNAs can be modified epigenetically to alter gene expression. Generally, a genome-wide hypomethylation with site-specific hypermethylation is observed in cancer cells[96]. The global hypomethylation leads to the decompaction of chromatin and increases the

occurrence of homologous recombination. This ultimately causes the severe genomic instability associated with cancer[97]. While the hypermethylation at the promoters and enhancer regions alters the expression of individual genes to promote cancer development. For example, DNA methylation at the promoter region of the *RB1* gene downregulates the production of retinoblastoma protein (pRb), which inhibits cell cycle progression and maintains DNA integrity, thus promoting the development of retinoblastoma[98].

The fundamental unit of chromatin consists of DNA wrapped around histone proteins, whose post-translational modifications (acetylation, methylation, phosphorylation, and glycosylation) modulate chromatin compaction and decompaction and ultimately also regulate gene expression[99]. Disruptions to these epigenetic mechanisms frequently contribute to oncogenesis. For example, the H3K27M mutation in histone 3 variant H3.3 occur in about 50% of the paediatric high-grade gliomas (pHGG). This mutation inhibits the enhancer of the zeste 2 polycomb repressive complex 2 subunit (EZH2), the catalytic subunit of the polycomb repressive complex 2 (PRC2), resulting in the global reduction of H3K27 trimethylation (H3K27me3) mark that represses gene expression[100,101]. The mutation is also accompanied by a global increase in H3K27 acetylation (H3K27ac) mark. These epigenetic changes ultimately increase the expression of genes in the RAS and MYC axis and promote cancer cell survival[102].

ATP-dependent chromatin remodelling complex is also involved in cancer development via epigenetic mechanisms. For example, mutations in the subunits of the switch/sucrose non-fermentable (SWI/SNF) complex, such as Brahma-associated factor complex 47 (BAF47), Brahma (BRM) and Brahma-related gene 1 (BRG1), inactivate SWI/SNF complex activity, leading to the over-expression (OE) of tumour-driving genes that are usually regulated by the SWI/SNF complex[103,104]. In addition, non-coding RNAs can contribute to tumourigenesis by interacting with the chromatin-modifying complexes[95].

As altered epigenome is another unique feature of cancer cells that can differentiate them from normal cells, drugs targeting epigenetic regulators have been developed, including DNA methyltransferase (DNMT) inhibitors (e.g., Azacitidine and Decitabine), histone deacetylase (HDAC) inhibitors (e.g., Vorinostat and Romidepsin) and histone methyltransferase (HMT) inhibitors (e.g., Tazemetostat). They have been approved for treating various cancer types, including myelodysplastic syndromes, leukaemia, lymphoma, multiple myeloma, and epithelioid sarcoma[105–107].

1.5 Research aims

Despite the increased understanding of cancer biology and the advancement in cancer therapeutic fields, cancer remains a heavy disease burden globally, demonstrating the need for developing novel therapies to overcome therapeutic challenges, including cancer heterogeneity, drug resistance and immunosuppression in the TME.

In this thesis, I aim to identify genetic and epigenetic targets with therapeutic potential and elucidate their mechanistic roles in cancer progression or anti-tumour immunity. I hope to provide scientific evidence to support their translational use in clinical settings.

The objective of Chapter 2 is to identify a genetic target that is selectively essential in a subgroup of cancer cells by mining the gene fitness screen data sets. Through mechanistic studies, we aim to uncover the biological basis for this selective vulnerability and potentially reveal new therapeutic opportunities.

The objective of Chapter 3 is to identify an epigenetic target capable of enhancing the effector function in $CD8^+$ T cells. Elucidating this target will advance our understanding of T cell biology and provide a potential therapeutic strategy to improve the efficacy of adoptive T cell transfer therapies through epigenetic modulation.

The objective of Chapter 4 is to provide deeper mechanistic understandings of lysine-specific demethylase 1 (LSD1), specifically examining the interaction between this epigenetic regulator and hexokinase (HK, a metabolic enzyme) in regulating B16 melanoma cell proliferation. We also aim to explore the therapeutic potential of targeting these pathways to control tumour growth.

Collectively, we would like to identify novel targets for cancer therapy, provide mechanistic insights into these targets and bridge the discovery with its potential clinical application.

Chapter 2: UDP-xylose synthase 1 (UXS1) is a selectively essential gene in NSCLC

2.1 Introduction

2.1.1 Selectively essential gene

Genes that are only important for cancer cell survival but dispensable in normal cells are promising targets for novel cancer therapies. However, determining gene essentiality in normal cells remains challenging due to the limited availability and study of healthy tissues. In contrast, genome-wide CRISPR/Cas9-based fitness screens from the Cancer Dependency Map (DepMap) portal have systematically identified gene essentiality across over 1000 cancer cell lines of diverse origins[108]. We thought it would be a good starting point to study the selectively essential genes that are crucial only in a small group of cancer cell lines. This is based on the assumption that since they are only necessary in a limited number of cancer cell lines, they are less likely to be involved in common pathways, suggesting a lower probability of their involvement in normal cell survival. In fact, many therapeutic targets of U.S. FDA-approved cancer treatments are defined as 'selectively essential' on the DepMap portal. In contrast, many therapies that failed in clinical trials target common essential genes[109], suggesting that new cancer therapeutic targets could be identified from selectively essential genes.

Previously, our lab collected 347 selectively essential genes from the DepMap portal based on the normal likelihood ratio test (NormLRT) score method that measures the distribution of CERES scores (also known as gene effect score) of each gene across cell lines[110], and we prioritised those understudied genes according to their PubMed counts. This allowed us to identify two unknown genes, C11orf53 (POU2AF2) and COLCA2 (POU2AF3), as selective vulnerabilities in POU2F3-dependent tuft cell-like small cell lung cancer[111]. We demonstrated, as did two other publications[112,113], that they function as transcription co-activators for POU2F3[114], showing the effectiveness of our strategy to identify novel cancer vulnerabilities via studying selectively essential genes.

2.1.2 Uridine diphosphate (UDP)-glucose pathway

With the same strategy, we noticed a selectively essential gene, UXS1, whose essentiality was predicted to be associated with the cellular expression level of UDP-glucose 6-dehydrogenase (UGDH) (**Figure 2.1A-B**). Both proteins are involved in the same biochemical pathway, where UGDH is the sole enzyme in humans that converts UDP-glucose to UDP-glucuronic acid (UDP-GlcUA)[115], and UDP-GlcUA is further converted to UDP-xylose by UXS1 in the Golgi apparatus (**Figure 2.2**).

UDP-xylose serves as the substrate in the synthesis of proteoglycans (PGs) and glycosaminoglycans (GAGs)[116], two important components of the ECM and key players during both embryogenesis[117] and in processes, such as chondrogenesis, in the adult organism[118,119]. On top of that, UDP-GlcUA also participates in two additional downstream pathways: production of hyaluronans (HAs) on the cell membrane, as well as glucuronidation reactions in the endoplasmic reticulum (ER), through which endobiotic and xenobiotic are converted to more water-soluble forms for excretion[120].

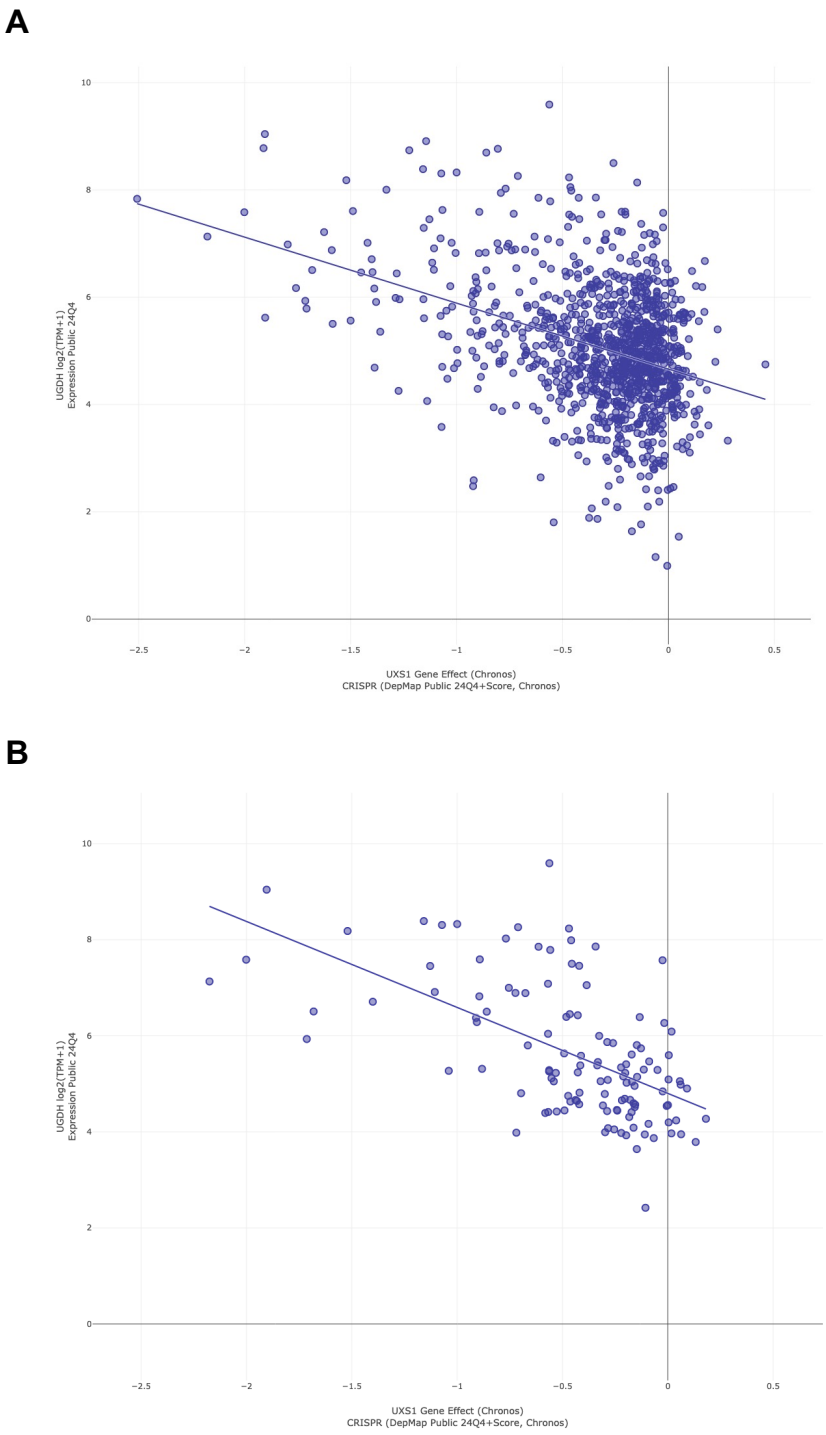

Figure 2.1 UXS1 essentiality in cancer cell lines with different UGDH expressions. CERES score of UXS1, determined by cell proliferation analysis after UXS1 reduction using the CRISPR/Cas9 system, was plotted against the UGDH expression level in cancer cell lines of (A) various origins or (B) lung cancers. The plot was generated with data from the DepMap portal at depmap.org/portal.

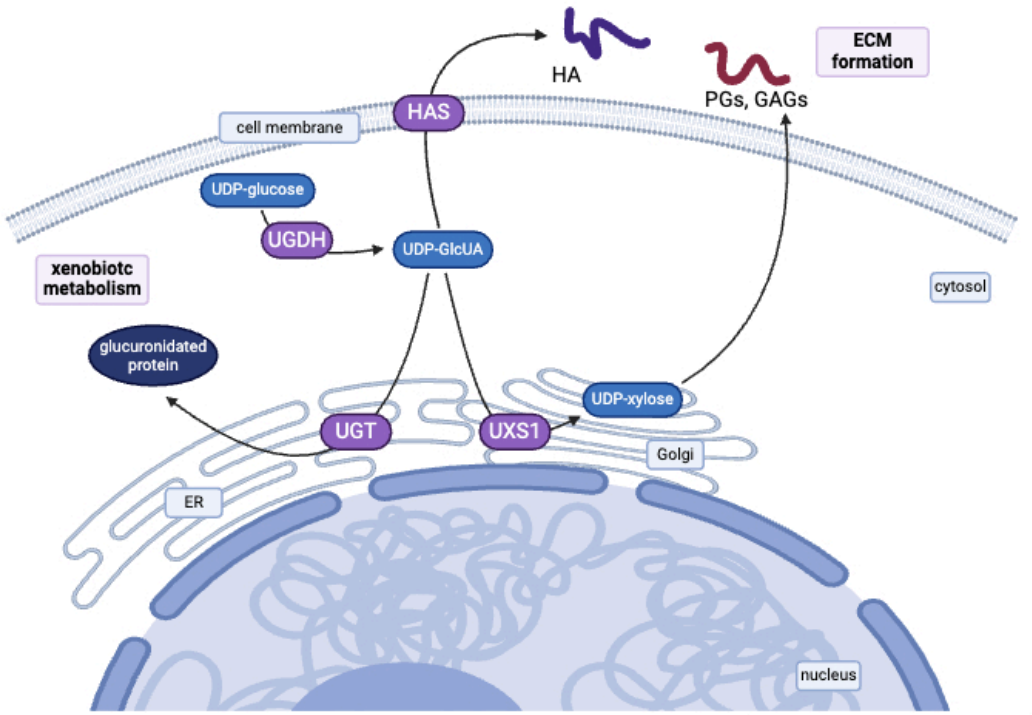

Figure 2.2 Schematic representation of the UDP-glucose pathway.
UDP-glucose is converted to UDP-GlcUA by UGDH in the cytosol. UDP-GlcUA can be used in three pathways: 1) it can be converted to UDP-xylose by UXS1 in the Golgi apparatus for the synthesis of PGs and GAGs; 2) it can be used for glucuronidation reactions catalysed by UGT in the ER; 3) it can be used as the substrate for HA production by HAS on the cell membrane. Abbreviations: ECM, extracellular matrix; ER, endoplasmic reticulum; GAG, glycosaminoglycan; HA, hyaluronan; HAS, hyaluronan synthase; PG, proteoglycan; UDP-GlcUA, UDP-glucuronic acid; UGDH, UDP-glucose dehydrogenase; UGT, UDP-glucuronosyltransferases; UXS1, UDP-xylose synthase 1. Plot was generated with bioRender at biorender.com.

2.1.3 UGDH and its role in cancer

UGDH, the enzyme catalysing the conversion of UDP-glucose to UDP-GlcUA in the UDP-glucose pathway, is highly regulated in normal tissues with its expression restricted to detoxifying organs, such as the liver, kidneys, and intestines[115]. However, UGDH is frequently over-expressed in some cancers, with elevated levels correlating with poor prognosis in lung cancer[121], prostate cancer[122] and breast cancer[123]. One proposed oncogenic mechanism involves UGDH-driven overproduction of downstream GAGs and PGs, which enhances ECM formation, thereby promoting

cancer cell proliferation and migration[124]. Alternatively, recent studies suggest that heightened UGDH activity depletes its substrate, UDP-glucose, thus, relieving the UDP-glucose-mediated inhibition of the Hu antigen receptor (HuR)-SNAI1 messenger RNA (mRNA) interaction; this stabilises SNAI1 mRNA and increases SNAIL protein expression, exacerbating the epithelial-mesenchymal transition (EMT) in the cancer cells[121].

2.1.4 UXS1 and its role in cancer

PGs play an essential role in bone development and homeostasis[125]. Since UDP-xylose, the downstream product of UXS1, is the substrate for PG and GAG synthesis, it is not surprising that mutations in UXS1 would lead to consequent effects on cartilage, perichondral, and bone morphogenesis in both animal models and studies[116,126]. But the involvement of UXS1 in cancer remains incompletely understood. Most papers studying the effect of the UDP-glucose pathway in cancer focus mainly on UGDH, with only a few experiments on UXS1. For example, *Teoh et al* confirmed that UGDH reduction reduced breast cancer metastasis while UXS1 reduction showed no measurable effects on tumorigenesis or metastasis[127]. This suggests that further studies are needed to understand UXS1's relevance in cancer development.

2.1.5 Non-small cell lung cancer (NSCLC)

Analysis of the DepMap portal revealed that the association between UXS1 essentiality and UGDH expression is most pronounced in lung cancer cell lines (**Figure 2.1B**). Thus, we decided to focus on lung cancer cell lines in our study.

According to the latest data from the World Cancer Research Fund, lung cancer is the 4th most common cancer in the UK, with NSCLC constituting approximately 85% of cases[128]. Treatments currently available for NSCLC include surgery, chemotherapy,

and radiotherapy. With the advancements in next-generation sequencing (NGS) and precision medicine, several novel targeted therapies have been developed to provide new treatment options for patients with NSCLC. These novel therapies include Osimertinib that targets EGFR[129], Alectinib that targets anaplastic lymphoma kinase (ALK)[130], Sotorasib that targets KRAS[131], Entrectinib that targets tyrosine-protein kinase ROS1[132], and Dabrafenib and Trametinib that target B-Raf[133]. These novel therapies have helped many patients carrying these specific mutations. However, there is still a subset of lung cancer patients without any of the above-mentioned gene mutations.

Recently, three anti-PD1/ PD-L1 immunotherapies, namely Nivolumab, Pembrolizumab, and Atezolizumab, have been approved for treating NSCLC[134]. However, these therapies benefit only 20% to 40% of patients, leaving a substantial proportion without effective options[135,136]. This underscores the need for novel therapeutic strategies to address unmet clinical needs.

2.1.6 Aims

In this project, we aim to 1) understand the relationship between UXS1-dependency and UGDH expression; 2) study the mechanism of UXS1-dependency in UGDH-high NSCLC cells; and 3) evaluate the possibility of targeting UXS1 for the development of novel cancer therapies.

2.2 Results

2.2.1 UXS1 inhibition caused a stronger effect in UGDH-high cell lines

To validate the DepMap prediction that UGDH-high cells exhibit higher UXS1-dependency, we selected five NSCLC cell lines with different UGDH expression levels. Immunoblot analysis confirmed the differential UGDH expression profile in these cell lines, with NCI-H23 showing the lowest UGDH levels, followed by progressively higher UGDH expression in NCI-H1666, NCI-H647, LUDLU1 and A549 (**Figure 2.3A-B**).

Using the CRISPR/Cas9-mediated gene editing[137], we generated UXS1 knockout (KO) variants of these cell lines. The reduction of UXS1 expression in UXS1 guide RNA (gRNA)-treated cells as compared to non-targeting (NT) gRNA-treated controls was confirmed with reverse transcription quantitative polymerase chain reaction (RT-qPCR) (**Fig. 2.3C**). Cell proliferation was quantified with the CyQuant cell proliferation assay, which measures cellular nucleic acid content as a proxy for cell number. We found that the growth inhibitory effects of UXS1 KO showed a correlation with UGDH expression levels. While NCI-H23 (UGDH-low) exhibited no significant growth reduction upon UXS1 reduction, we observed progressively greater UXS1 KO-mediated growth suppression in cell lines with higher UGDH expression, with relative cell growth in NCI-H1666, NCI-H647, LUDLU1 and A549 reduced by 36.32%, 55.64%, 76.16%, and 78.78%, respectively. (**Figure 2.3D**).

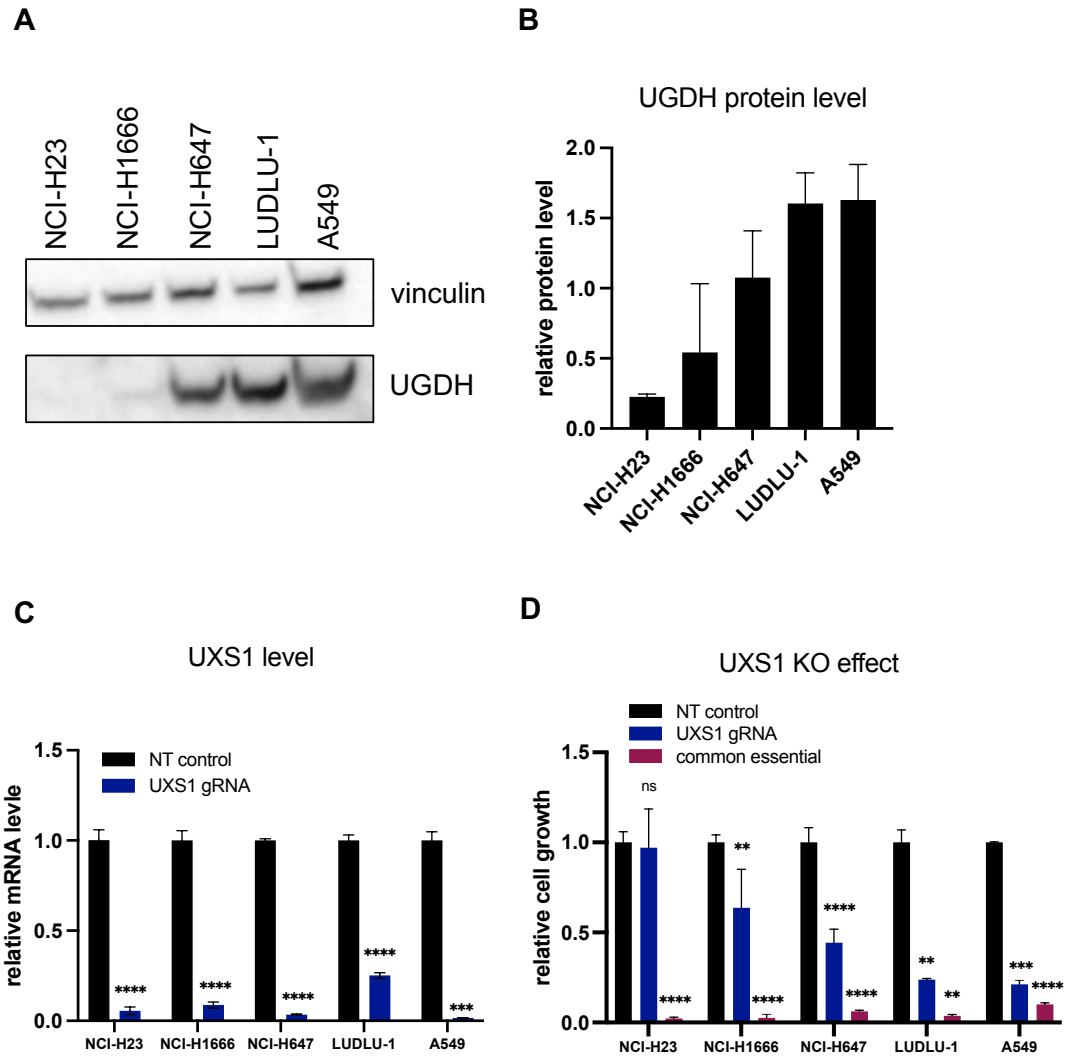

Figure 2.3 UXS1 KO caused a stronger effect in UGDH-high cell lines.
(A) Western blot analysis performed with protein extracts from NCI-H23, NCI-H1666, NCI-H647, LUDLU-1 or A549 showing the UGDH expression level. (B) Quantification of the western blot results in (A) with ImageJ showing relative UGDH expression levels in the five cell lines. (C) Relative UXS1 expression level in cells treated with NT gRNA or UXS1 gRNA measured with RT-qPCR. (D) Relative cell growth, measured by the CyQuant cell proliferation assay, of five cell lines treated with NT gRNA or UXS1 gRNA. Data presented as mean ± standard deviation (SD).

To complement the CRISPR/Cas9 KO experiments, we also performed parallel short hairpin RNA (shRNA) knockdown (KD) experiments in UGDH-high cell line A549 and UGDH-low cell line NCI-H23. RT-qPCR analysis confirmed the significant reduction of UXS1 expression in cells treated with UXS1 shRNA (**Figure 2.4A**). Consistent with the gene KO experiments, UXS1 KD had minimal impact on NCI-H23 proliferation, but it reduced A549 cell growth by 46.83% (**Figure 2.4B**).

To verify the specificity of this effect, we introduced an expression vector into A549 cells to over-express an exogenous shRNA-resistant UXS1 transcript. This UXS1 OE construct successfully rescued the UXS1 loss-mediated growth defects in A549 (**Figure 2.4C**), demonstrating that the observed phenotype was explicitly due to UXS1 depletion rather than any off-target effects.

To further validate the specificity of UXS1 reduction, we introduced a second, independent shRNA sequence (UXS1 shRNA4), which can target both endogenous and exogenous UXS1 transcripts. Cell proliferation was quantified with the 5-bromo-2'-deoxyuridine (BrdU) assay, where BrdU, a thymidine analogue, is incorporated into newly synthesised DNAs and subsequently detected with immunostaining to provide a direct measure of cell proliferation rate. Notably, UXS1 shRNA4 reduced the cell proliferation in UXS1 OE cells by 53.36% (**Figure 2.4D**).

These results strongly support the DepMap prediction that UXS1 exhibits selective essentiality in UGDH-high NSCLC cells. The consistent phenotype across different genetic perturbation methods, coupled with robust rescue experiments, establishes a clear dependence on UXS1 in UGDH-high NSCLC cells.

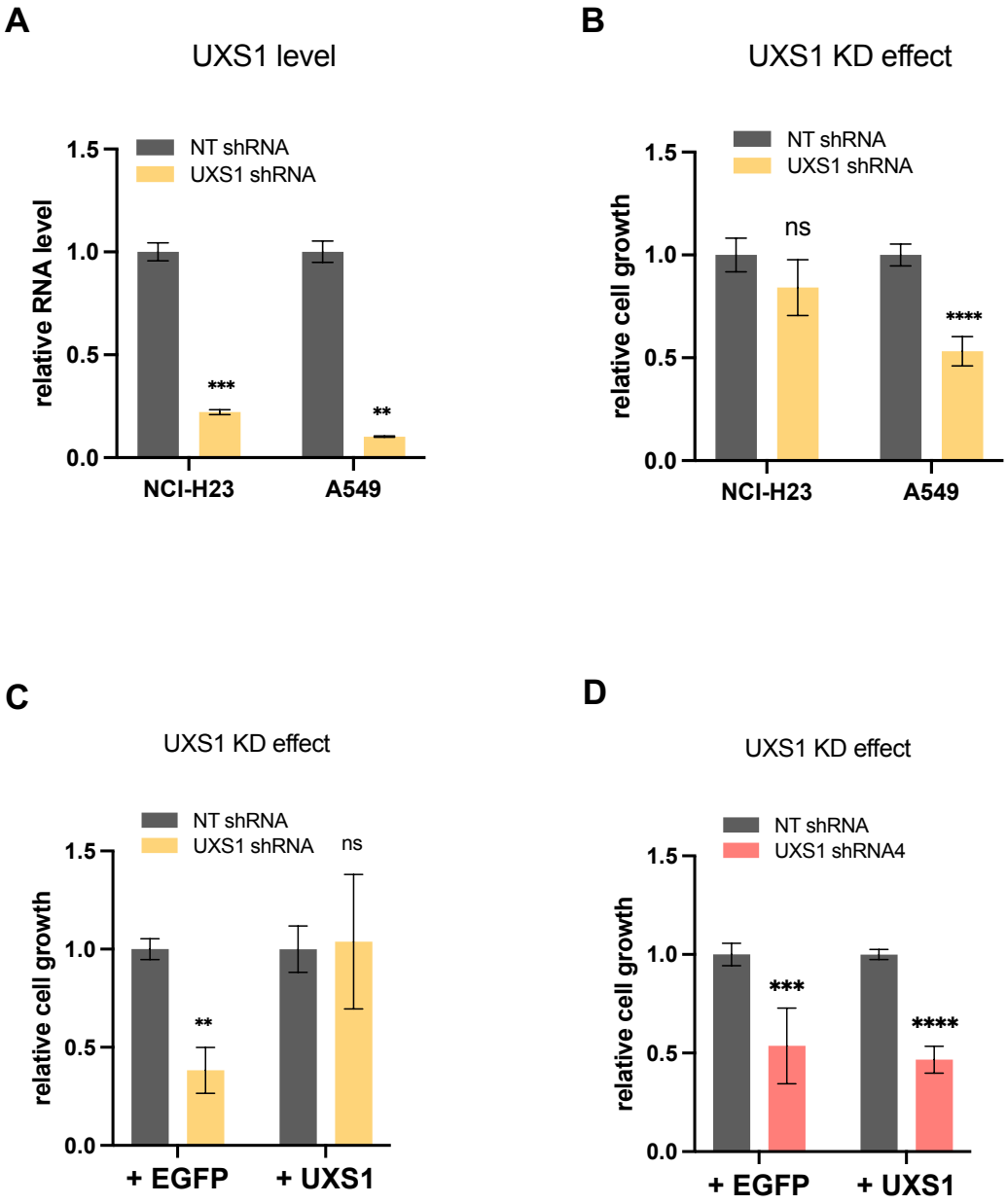

Figure 2.4 UXS1 KD caused a stronger effect in UGDH-high cell lines.
(A) UXS1 expression, measured at mRNA level by RT-qPCR, in NCI-H23 and A549 cells treated with NT shRNA or UXS1 shRNA. Relative cell proliferation, measured with the BrdU assay, of (B) NCI-H23 and A549 cells or (C) A549 EGFP OE cells and A549 UXS1 OE cells treated with NT shRNA or UXS1 shRNA. (D) Relative cell proliferation, measured with the BrdU assay, of A549 EGFP OE cells and A549 UXS1 OE cells treated with NT shRNA or UXS1 shRNA4, a shRNA sequence that interferes with the exogenous UXS1 transcript. Data presented as mean ± SD.

2.2.2 UGDH-high cells were not dependent on UXS1 upon UGDH inhibition

To determine whether high UGDH expression level dictates UXS1-dependency, we generated UGDH KO variants of UGDH-high cell lines (i.e., A549 and LUDLU-1) using the CRISPR/Cas9 gRNA system. Immunoblot analysis confirmed the successful UGDH depletion (**Figure 2.5A**). Strikingly, the reduction of UGDH protected the cells from the growth suppression induced by UXS1 KO (**Figure 2.5B-D**). Similarly, UGDH KO also protected A549 cells from growth suppression induced by UXS1 KD (**Figure 2.5E**). To establish causality, we reintroduced WT UGDH into UGDH KO cells, and the exogenous expression of WT UGDH transcript fully restored the UXS1-dependency in UGDH KO A549 cells (**Figure 2.5F-G**). To investigate the importance of the enzymatic activity in the UGDH rescue phenotype, we reintroduced an enzymatically dead (ED) UGDH into UGDH KO A549 cells. We found that ED UGDH could not re-sensitise the cells to UXS1 loss (**Figure 2.5F-G**), demonstrating that UGDH's enzymatic activity is essential for maintaining UXS1-dependency. These results establish a direct and activity-dependent relationship between UGDH expression and UXS1-dependency in NSCLC cells.

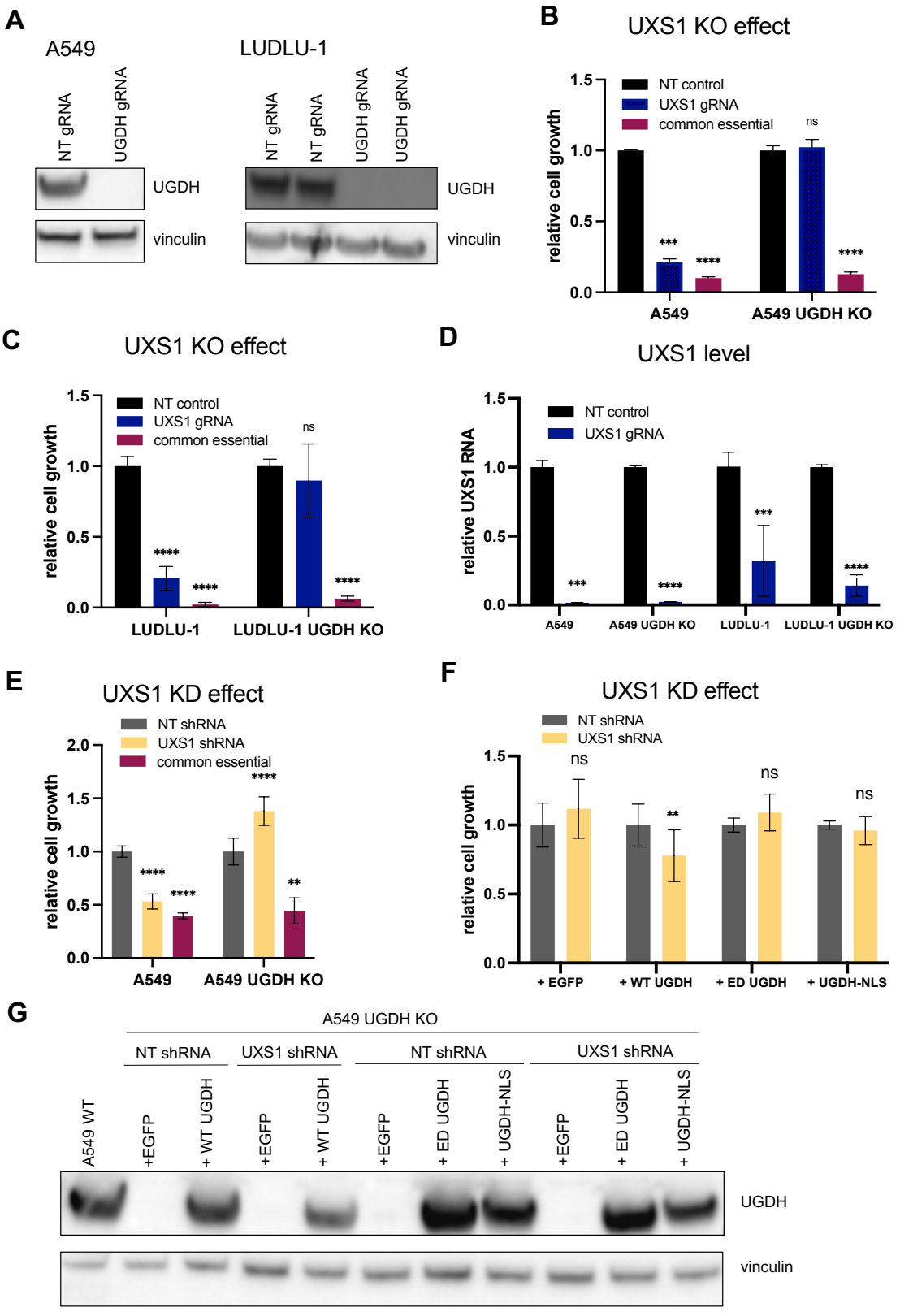

Figure 2.5 UXS1-dependency was regulated by UGDH expression.

(A) Immunoblot performed with protein extracts from A549 and LUDLU-1 cells treated with NT gRNA or UGDH gRNA. Relative cell growth, measured by the CyQuant assay,

(*Figure 2.5 continued*) of (B) A549 and UGDH KO A549 cells or (C) LUDLU-1 and UGDH KO LUDLU1 cells treated with NT gRNA or UXS1 gRNA. (D) UXS1 expression, measured at mRNA level by RT-qPCR, in A549, UGDH KO A549, LUDLU-1 and UGDH KO LUDLU-1 cells treated with NT gRNA or UXS1 gRNA. (E) Relative cell growth, measured by the BrdU assay, of A549 and UGDH KO A549 cells treated with NT shRNA or UXS1 shRNA. (F) Relative cell growth, measured by the BrdU assay, of A549 UGDH KO cells over-expressing EGFP, WT UGDH, ED UGDH or UGDH with nuclear-localisation sequence (NLS). Data presented as mean ± SD.

2.2.3 Subcellular localisation of UGDH was important for determining UXS1-dependency

Consistent with previous reports[138], we found that UGDH localised to both nuclear and cytoplasmic compartments in WT A549 cells (**Figure 2.6**). To investigate whether the subcellular localisation of UGDH influences UXS1-dependency, we engineered UGDH KO A549 cells to express a nuclear-targeting UGDH variant (**Figure 2.6**). Nuclear-restricted UGDH did not restore UXS1-dependency (**Figure 2.5F-G**), indicating that the cytoplasmic UGDH activity is essential for maintaining UXS1-dependency. These results suggest that the enzymatic function of UGDH in the cytoplasmic compartment, rather than potential nuclear functions, mediates the observed UXS1-dependency.

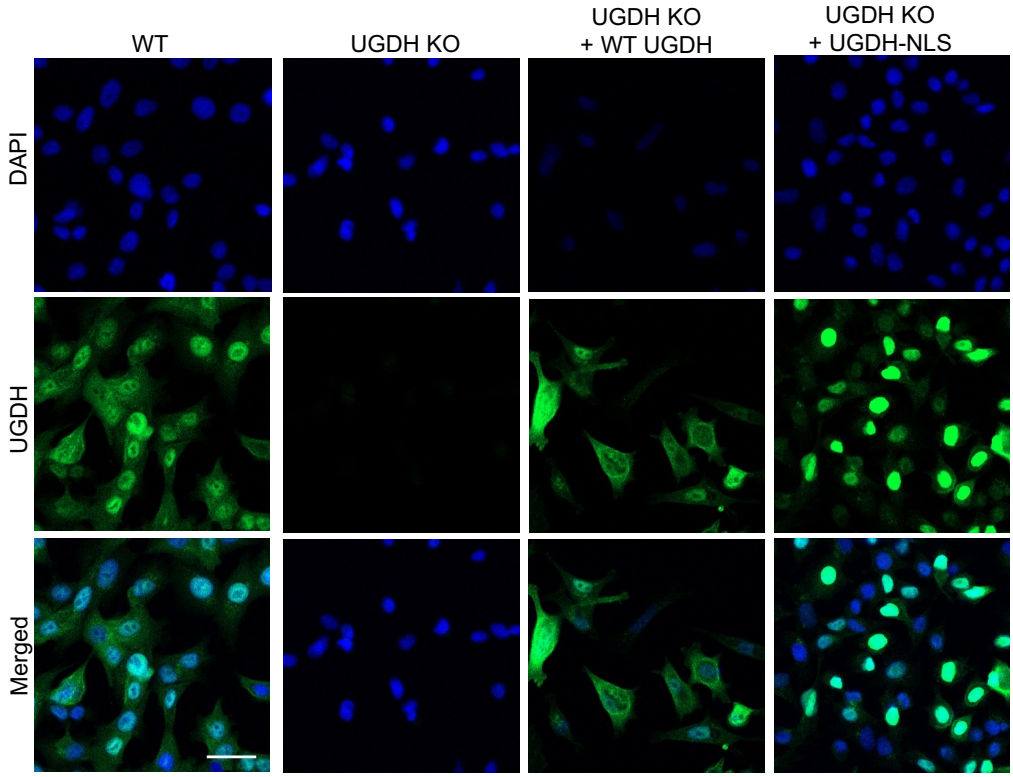

Figure 2.6 Subcellular localisation of UGDH.
Immunostaining of UGDH in WT A549 cells, UGDH KO A549 cells, and UGDH KO A549 cells with exogenous expression of WT UGDH or UGDH-NLS. Scale bar: 10 μm. Abbreviations: WT, wild-type; KO, knockout; NLS, nuclear-localisation sequence; DAPI, 4',6-diamidino-2-phenylindole.

2.2.4 UGDH-high cells did not require more UDP-xylose or its downstream derivatives

To elucidate the mechanistic basis of UXS1-dependency in UGDH-high cells, we hypothesised that UGDH-high cell lines might require more UDP-xylose or its downstream derivatives to sustain proliferation. This model would predict that UGDH loss should resemble the UXS1 depletion phenotype in UXS1-sensitive cell lines. However, analysis of the DepMap data revealed that none of the UXS1-dependent cells were dependent on UGDH (CERES scores <-1) (**Fig. 2.7A**). Consistent with this, genetic ablation of UGDH in A549 cells, a UXS1-sensitive cell line, did not inhibit cell proliferation (**Fig. 2.7B**). These findings demonstrate that neither UDP-xylose depletion nor reduced flux through the UDP-glucose pathway could fully explain the observed

UXS1-dependency in UGDH-high cells, suggesting the existence of alternative mechanisms linking UGDH expression to UXS1-dependency.

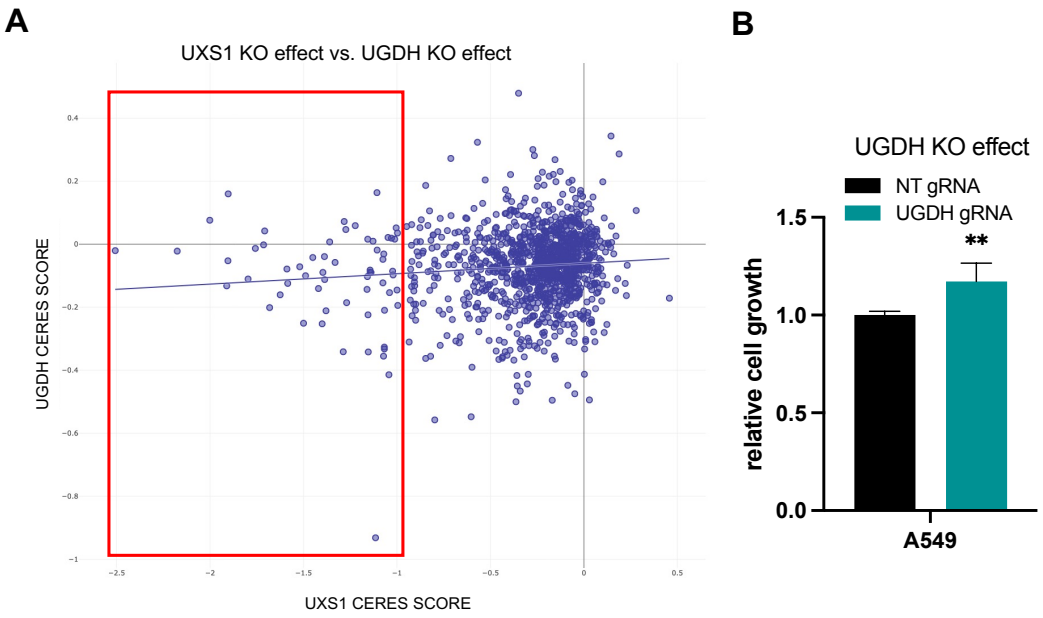

Figure 2.7 UGDH KO effects in cancer cells.
(A) Graph of UGDH CERES score against UXS1 CERES score plotted with the DepMap Public 24Q4 data. UXS1-sensitive cell lines are circled in red. (B) Relative cell growth, measured by the CyQuant proliferation assay, of A549 cells treated with NT gRNA or UGDH gRNA. Data presented as mean ± SD.

2.2.5 UXS1-dependency in UGDH-high cells was due to UDP-GlcUA accumulation

Since UXS1-dependency in UGDH-high cells could not be explained by UDP-xylose or its downstream pathway products, we hypothesised that UXS1 loss led to a toxic accumulation of the intermediate metabolite, UDP-GlcUA, specifically in UGDH-high cells. To test this model, we quantified the intracellular UDP-GlcUA levels in WT and UGDH KO A549 cells following UXS1 KD. Strikingly, UXS1 KD induced a 4-fold increase in UDP-GlcUA level in WT cells from 138.45 µM to 554.17 µM, while UGDH KO completely abrogated this UDP-GlcUA accumulation (**Figure 2.8A**).

We also engineered A549 cells to exogenously over-express SLC35D1, the membrane transporter for UDP-GlcUA, in A549 cells, and examined the effects of UDP-GlcUA supplementation. Notably, 1 mM UDP-GlcUA selectively impaired proliferation only when combined with UXS1 inhibition in UGDH KO A549 cells. (**Figure 2.8B**). These results demonstrate that UXS1 loss in UGDH-high cells causes a cytotoxic UDP-GlcUA accumulation in the cells, and UGDH-high cancer cells depend on UXS1 to prevent the toxic build-up of UDP-GlcUA, uncovering a novel metabolic vulnerability in these cancer cells.

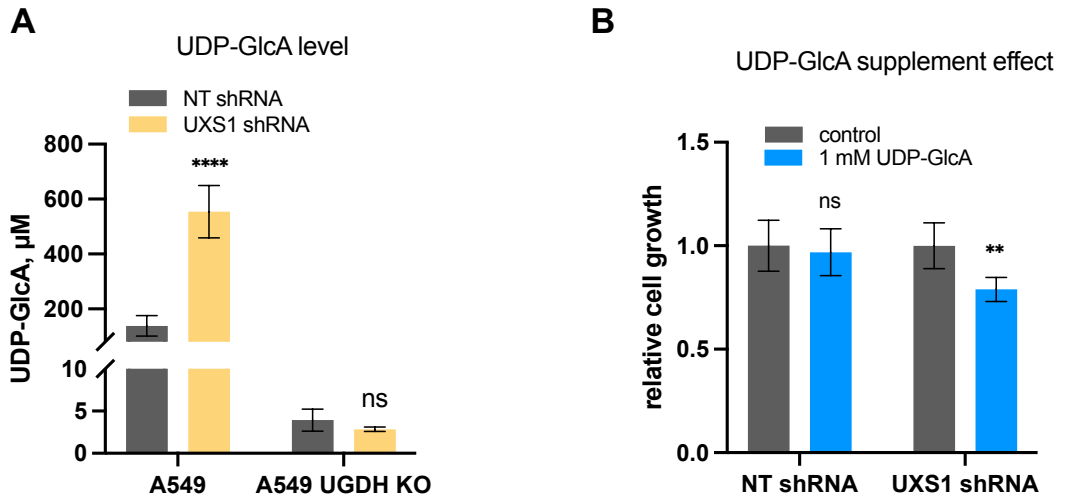

Figure 2.8 UXS1-dependency in UGDH-high cells was due to UDP-GlcUA accumulation.

(A) Intracellular UDP-GlcUA level, measured with mass spectrometry (MS) by Professor Skirmantas Kriaucionis, of WT A549 and UGDH KO A549 cells treated with NT shRNA or UXS1 shRNA. (B) Relative cell growth, measured by the BrdU assay, of A549 cells treated with NT shRNA or UXS1 shRNA and supplemented with vehicle control or 1 mM UDP-GlcUA. Data presented as mean ± SD.

2.2.6 UXS1 inhibition did not affect normal cell growth

So far, we have identified UXS1 as a selectively essential gene in UGDH-high cancer cell lines. For UXS1 to be a viable therapeutic target, two key conditions must be met: UGDH expression should be preferentially elevated in tumours compared to normal cells, and normal cells should tolerate UXS1 reduction. Analysis of TCGA data revealed that the two most common subtypes of NSCLC, lung adenocarcinoma (LUAD)

and lung squamous cell carcinoma (LUSC), exhibit significantly higher UGDH expression than matched adjacent normal tissues (**Figure 2.9A**). Importantly, UXS1 KD in non-transformed human bronchial epithelial cells BEAS-2B caused no measurable growth suppression (**Figure 2.9B-C**), demonstrating the selectivity for cancer cells. Together, these results provide strong preclinical evidence that UXS1 inhibitors could achieve therapeutic efficacy against UGDH-high tumours while sparing normal tissues, fulfilling the essential criteria for a promising cancer target.

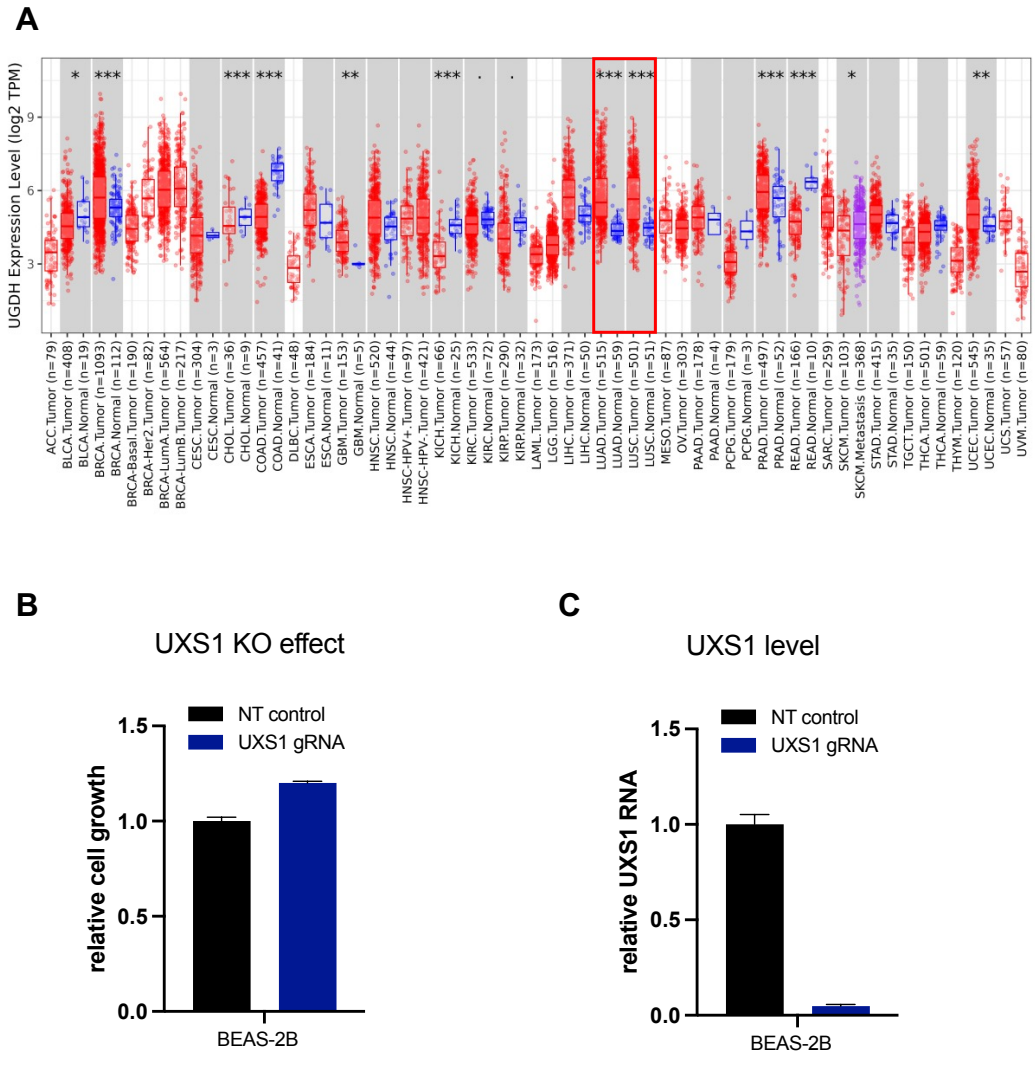

Figure 2.9 UXS1 inhibition in normal cells.
(A) UGDH expression in cancer cells and matched adjacent normal cells plotted with data from TCGA dataset. NSCLCs are circled in red. (B) Relative cell growth, measured by the CyQuant cell proliferation assay, of BEAS-2B cells treated with NT gRNA or UXS1 gRNA. (C) UXS1 expression, measured at mRNA level by RT-qPCR, in BEAS-2B cells treated with NT gRNA or UXS1 gRNA.

2.3 Discussion

2.3.1 Summary of the results

In summary, we leveraged the data from the DepMap portal and validated UXS1 as a selectively essential gene in NSCLC cell lines expressing high levels of UGDH. We also demonstrated that UXS1-dependency arises from the toxic accumulation of UDP-GlcUA in specifically in UGDH-high cancer cells, revealing a previously unrecognised metabolic vulnerability. These findings have important translational implications and support the potential use of UXS1 as a target for developing novel cancer therapy and UGDH as a biomarker for stratifying patients to receive UXS1 inhibition treatment.

2.3.2 Limitations of experiments and prospects

While we established that UDP-GlcUA accumulation leads to UXS1-dependency in UGDH-high cells, the precise mechanisms underlying its cytotoxicity remain to be fully understood. Parallel work published in Nature proposed that UDP-GlcUA toxicity arises from structural and functional disruptions of the Golgi apparatus[139]. Their studies demonstrated that UXS1 KO altered Golgi morphology (as shown by immunostaining) and impaired protein glycosylation patterns, which subsequently downregulated cell-surface proteins, such as EGFR, and this disruption of receptor trafficking attenuated cell proliferation and survival signalling pathways [139]. However, the majority of the accumulated UDP-GlcUA was localised to the cytosol, leaving unresolved mystery of how cytosolic metabolite imbalances propagate to Golgi dysfunction.

An alternative mechanism could involve dysregulated HA production. Although *Doshi et al.* did not observe a significant increase in HA production upon UXS1 reduction in A549 cells, prior work by *Vigetti et al*. showed that elevated cytosolic UDP-GlcUA level enhanced HA production in human aortic smooth muscle cells[140]. Given HA's critical role in the formation of ECM, its influences on cell survival, proliferation, and differentiation have been established[141]. Thus, further investigation into HA dynamics

following UXS1 reduction is required. Specifically, quantifying HA levels across UGDH-high versus UGDH-low cell lines upon UXS1 KO and correlating these results with Golgi integrity and cell viability could clarify whether HA overproduction contributes to the observed cytotoxicity.

Our study focused on establishing the relationship between UXS1-dependency and UGDH expression in NSCLC cells. But we did not explore other cancer types. Independent work by *Doshi et al.* demonstrated that this observation could be generalizable to other tissue types by studying the effect of UXS1 KO in 19 cancer cell lines with different UGDH expression levels and from various tissue origins, including liver cancer, breast cancer, colorectal cancer, kidney cancer, pancreatic cancer, and prostate cancer[139]. Their findings further confirm that the link between UXS1-dependency and UGDH expression is conserved across different lineages, and targeting this metabolic vulnerability could benefit patients with UGDH-high tumours of different tissue origins. This convergence of evidence underscores the translational significance of our discovery and positions UXS1 inhibition as a promising strategy for UGDH-high cancers beyond NSCLC.

2.3.3 Clinical applications

Our findings position UXS1 as a compelling therapeutic target for UGDH-high cancers of different origins, such as breast, lung, and prostate since tumour cells from these tissue types exhibit significantly higher UGDH expression levels than the adjacent normal cells (**Figure 2.9A**). Given that high UGDH expression is associated with poor clinical outcomes, UGDH expression could serve as a predictive biomarker to identify patients most likely to benefit from UXS1-targeted therapies.

However, there are two critical factors that need to be considered. Firstly, the embryonic lethality of $UXS1^{-/-}$ mice shows the potentially important role of UXS1 in

development and normal physiology[142] and the defective chondrocyte organisation and skeletal development in uxs1 mutant zebrafish indicate the essential role of UXS1 in the skeletal system and suggest potential side effects of systemic UXS1 inhibition[143]. In addition, while our data show selectivity of cancer cells, certain normal tissues (e.g., liver and kidney) have baseline UGDH expression (**Figure 2.9A**), suggesting potential side effects of targeting UXS1 on these tissues. Our findings advocate for developing conditional UXS1 inhibition strategies, such as tumour-targeted delivery systems, to maximise therapeutic efficacy while mitigating potential adverse effects.

2.3.4 Cancer metabolism and 'kitchen sink' model

Metabolic reprogramming is one of the emerging hallmarks for cancer[77]. One example is the Warburg effect, where cancer cells shift from OXPHOS to glycolysis to produce ATPs even under aerobic conditions[144]. Recently, the 'kitchen sink' model of toxic metabolites has been proposed to explain how metabolic imbalances can induce cytotoxicity in cancer cells. In this model, when an upstream enzyme excessively produces a metabolite, akin to a water tap turned on excessively, the downstream enzyme functions like a drain to reduce the levels of the potentially toxic metabolites[144]. Our discovery that UGDH-high cells require UXS1 to prevent cytotoxic UDP-GlcUA accumulation aligns with the 'kitchen sink' model. This mechanistic alignment with the 'kitchen sink' model underscores the broader relevance of metabolic flux control as a therapeutic vulnerability in cancer.

The 'kitchen sink' model also identifies other metabolic vulnerabilities in oncogenic contexts. For example, in cancers with elevated SLC7A11 expression, increased selenide uptake promotes selenocysteine biosynthesis to sustain glutathione peroxidase 4 (GPX4) activity and protect the cells from ferroptosis; the increased selenide uptake also creates the cell dependence on selenophosphate synthetase 2 (SEPHS2) for detoxification of the cytotoxic selenide accumulation[145]. Similarly, the

dependence on glycine decarboxylase (GLDC) to metabolise the toxic glycine accumulation in cancer cells with high serine hydroxy methyltransferase (SHMT2) expression[146] is another example of cancer metabolic vulnerability that fulfil the 'kitchen sink' model.

The convergence of these observations with our findings suggests that targeting such metabolic vulnerabilities may represent a generalizable therapeutic strategy. With the emerging technologies in cancer metabolomics, including advanced metabolite profiling techniques and the use of artificial intelligence for data analysis and model prediction, we speculate that additional vulnerabilities within this paradigm will be uncovered in the future, potentially revealing new targets for precision medicine.

Chapter 3: The role of protein arginine methyltransferases (PRMTs) in $CD8^+$ T cells

3.1 Introduction

3.1.1 $CD8^+$ T cell and its role in tumour control

Naïve T cells require two distinct signals for activation: antigen recognition through TCR engagement with peptide-major histocompatibility complex (MHC) complex (signal 1) and co-stimulation through receptors such as CD28 (signal 2). Upon receiving both signals, naïve T cells differentiate to $CD8^+$ effector T cells, also known as cytotoxic T lymphocytes (CTLs), which mediate immune responses through the release of cytokines (e.g., IFNg and IL-2) and direct cytotoxicity through the release of Granzyme B (GzmB) and perforin[147].

However, in chronic infections and in the context of tumour, persistent antigen exposure induces T cell exhaustion, a state characterized by the progressive loss of effector function and upregulation of multiple inhibitory receptors, including PD-1 (CD279), CTLA-4 (CD152), lymphocyte-activation gene 3 (LAG3), T cell immunoglobulin domain and mucin domain 3 (Tim-3), and T cell immunoreceptor with Ig and ITIM domain (TIGIT)[148]. This negative regulation on effector T cell function is a protective mechanism to prevent tissue damage due to excessive immune responses. However, it also reduces the capability of our immune system to control the tumour. This understanding has driven the development of ICB therapies, which aim to prevent T cell exhaustion by blocking the inhibitory receptor pathways using antibodies. To date, the FDA has approved multiple anti-PD-1/ PD-L1 antibodies (e.g., Pembrolizumab and Nivolumab) and anti-CTLA4 antibodies (e.g., Ipilimumab) for treating various cancers, such as melanoma, NSCLC, kidney cancer, cervical cancer and TNBC[149–153]. These therapies have demonstrated remarkable clinical success, though response rates remain limited. This highlights the need for additional strategies to modulate the immune-mediated tumour control.

3.1.2 CAR-T therapy

Other than ICB, another type of immunotherapy is CAR-T therapy, where autologous T cells are taken out from the patients and modified for two purposes: increased tumour antigen recognition and enhanced effector T cell function[154]. This approach has demonstrated remarkable clinical success in treating hematologic malignancies, with FDA-approved CAR-T therapies showing efficacy against large B cell lymphoma[155], B cell acute lymphoblastic leukaemia[156], and follicular lymphoma[157] through targeting the well-defined surface markers, such as CD19 and CD20, on B cells.

However, its use for treating solid tumours is still limited for two reasons. Firstly, target antigen selection is complicated due to the heterogeneity of solid tumours and the lack of tumour-specific epitopes comparable to the lineage markers available in B-cell malignancies. Secondly, the immunosuppressive TME creates multiple barriers, including physical exclusion of immune cells, abundant inhibitory signalling molecules and metabolic constraints, which collectively impair CAR-T cell infiltration and function. These two challenges have limited the clinical implications of CAR-T therapy, highlighting the need to identify novel T cell targets that can enhance tumour infiltration and persistence.

3.1.3 CXC motif chemokine receptor 3 (CXCR3) in $CD8^+$ T cells

CXCR3 is a G protein-coupled receptor. The CXCR3-A isoform that couples with the Gai/Gaq pathway is the predominantly expressed isoform in human $CD8^+$ T cells, and its expression level is rapidly increased upon T cell activation[158]. CXCR3 is activated by three interferon-inducible chemokines, CXCL9 (MIG), CXCL10 (IP-10) and CXCL11 (I-TAC) to promote T cell migration towards antigen-presenting cancer cells and enhance effector T cell function[158].

The importance of CXCR3 in anti-tumour immunity is shown by the study where Cxcr3 KO tumour-bearing mice exhibited significantly reduced responses to anti-PD1 treatment compared to WT counterparts[159]. This finding and its characteristic expression pattern make CXCR3 a reliable marker for identifying effector $CD8^+$ T cells.

3.1.4 Epigenetic regulations in $CD8^+$ T cells

Different subtypes of $CD8^+$ T cells, including naïve T cells, effector T cells, central memory T cells, effector memory T cells and exhausted T cells, exhibit distinct epigenetic landscapes. Emerging research has identified several epigenetic regulators that influence $CD8^+$ T cell activation, differentiation, proliferation, and function, offering promising targets for enhancing adoptive cell transfer therapies.

Ten-eleven translocation 2 (TET2), which regulates DNA demethylation through oxidation of 5-methylcytosine, is a prime example. *Carty et al* showed that TET2 could regulate the methylation status of genes involved in cell proliferation and memory T cell markers, and TET2 KO tend to guide the cells towards a central memory phenotype in $CD8^+$ T cells[160]. In accordance with this, TET2-disrupted CAR-T cells showed better tumour control in a mouse B cell acute lymphoblastic leukaemia model[161]. Similarly, clinical observations revealed that 94% of CAR-T cells in a responding patient originated from a single clone where CAR transgene insertion disrupted TET2, and subsequent experimental disruption of TET2 expression recapitulated this functional enhancement, further confirming the beneficial effect of TET2 inhibition in CAR-T cell function[162].

Another example of epigenetic regulations in T cell function is via DNA methyltransferase 3 alpha (DNMT3A), an enzyme responsible for *de novo* DNA methylation. Conditional KO of DNMT3A in $CD8^+$ T cells led to increased effector T cell

function[163], and DNMT3A-edited CAR-T cells showed reduced exhaustion phenotype and improved anti-tumour activity[164].

Beyond DNA methylation, histone modifications also play crucial roles. The inhibition of SUV39H1, a histone lysine methyltransferase that tri-methylates at H3K9, in CAR-T cells improved tumour control in a mouse leukaemia model[165]. And priming the T cells with inhibitors against LSD1, a histone demethylase, promoted the anti-tumour function of adoptively transferred cells[166].

Collectively, these findings show the central role of epigenetic mechanisms in regulating $CD8^+$ T cell biology. The manipulation of epigenetic regulators, such as TET2, DNMT3A and SUV39H1, represents a promising strategy to enhance the efficacy of CAR-T cell therapies by optimising T cell differentiation, function, and persistence.

3.1.5 PRMTs

PRMTs comprise a family of 11 enzymes that catalyse the transfer of methyl groups to arginine residues on diverse protein substrates in human[167]. The arginine residue consists of a guanidino group that can form hydrogen bonds with other proteins, and the methylation mark reduces the potential for hydrogen bond formation, thus affecting protein-protein interactions. PRMTs are classified into three types based on their products: type I PRMTs generate monomethyl arginine (MMA) and asymmetric dimethyl arginine (ADMA); type II PRMTs generate MMA and symmetric dimethyl arginine (SDMA); and type III PRMTs exclusively generate MMA [168]. PRMTs regulate cellular processes by modifying histone tails to alter chromatin structure and gene expression. In addition, PRMTs also methylate non-histone proteins to modulate their functions directly. With the large variety and number of PRMT substrates, these

enzymes can participate in multiple fundamental biological processes, including cell cycle progression, RNA processing and DNA repair[169].

The involvement of PRMTs in cancer development was first reported by *Cheung et al* in 2007. PRMT1 was found to be involved in the mixed lineage leukaemia (MLL) complex with histone acetylation and methylation function, and the reduction of PRMT1 reduced MLL-induced leukemogenesis in myeloid progenitor cells[170]. Since then, the pathways involved have been studied, and the importance of PRMTs in cancer development has been increasingly recognised[171]. For instance, PRMT1-mediated methylation of p53 binding protein 1 (53BP1) and meiotic recombination 11 (MRE11) at their glycine arginine rich (GAR) motifs alters the protein function and affects their role in DNA repair pathways, potentially contributing to the genome instability and cancer progression [172,173]. In addition, PRMT1 can act with KDM4C to regulate the epigenetic and transcriptional pathways in AML cells, and the pharmacological inhibition of either PRMT1 or KDM4C reduces leukemogenesis *in vivo* [174]. Furthermore, the high PRMT1 expression has been associated with breast cancer, pancreatic cancer, colorectal cancer, lung cancer, hepatocellular cancer, melanoma, esophageal cancer and head and neck cancer; the high PRMT3 expression has been associated with pancreatic cancer; the high PRMT4 expression has been associated with breast cancer, pancreatic cancer, colorectal cancer, ovarian cancer, hepatocellular cancer and AML; and the high PRMT6 expression has been associated with gastric cancer, hepatocellular cancer and lung cancer[175]. The pleiotropic functions of PRMTs and their frequent dysregulation in malignancies position them as attractive targets for therapeutic intervention. After the development of AMI-1, the first PRMT inhibitor, in 2004, more potent inhibitors, including MS023 and GSK3368715, have been developed and could work at a much lower concentration than AMI-1. In addition, more selective inhibitors, such as SGC707 for PRMT3 and TP064 for PRMT4, have been studied. Some PRMT inhibitors have entered clinical trial phases, and a list of clinical trials using PRMT inhibitors is provided in **Table 3.1**.

Inhibitor	Target	Indications	Phase	Clinical trial	Status	Year
GSK3368715	Type I PRMTs	Solid tumour and Diffuse Large B-cell Lymphoma (DLBCL)	I	NCT03666988	Terminated	2022
SCR-6920	PRMT5	Solid tumour and non-Hodgkin lymphoma (NHL)	I	NCT05528055	Active	2022
PRT811	PRMT5	Solid tumour, lymphoma and glioma	I	NCT04089449	completed	2023
PRT543	PRMT5	Solid tumour and haematologic malignancy	I	NCT03886831	completed	2023
JNJ-64619178	PRMT5	Solid tumour, NHL and myelodysplastic syndrome (MDS)	I	NCT03573310	Activte	2025
AMG 193	PRMT5	Solid tumour	I/II	NCT05094336	Active	2025
MRTX1719	PRMT5	Solid tumour	I	NCT05245500	Active	2025
	PRMT5	Glioblastoma	I	NCT06883747	Active	2025
	PRMT5	Solid tumour	I	NCT06672523	Active	2025
TNG908	PRMT5	Solid tumour	I/II	NCT05275478	Active	2025
PF-06939999	PRMT5	Solid tumour	I	NCT03854227	Terminated	2025
GSK3326595	PRMT5	Early stage breast cancer	II	NCT04676516	Completed	2022
AZD3470	PRMT5	Solid tumour	I/II	NCT06130553	Active	2025
	PRMT5	Haematologic malignancy	I/II	NCT06137144	Active	2025
TNG462	PRMT5	Pancreatic ductal adenocarcinoma and NSCLC	I/II	NCT06922591	Active	2025
TNG456	PRMT5	Solid tumour	I/II	NCT06810544	Active	2025
CTS3497	PRMT5	Solid tumour and lymphoma	I/II	NCT06971523	Active	2025
BGB-58067	PRMT5	Solid tumour	I	NCT06589596	Active	2025
BAY 3713372	PRMT5	Solid tumour	I	NCT06914128	Active	2025

Table 3.1 List of PRMT inhibitors in clinical trials.
List of clinical trials for testing the safety and efficacy of LSD1 inhibitors, with the name of the inhibitor used, indications, clinical phases, status, and time of last update.

3.1.6 Aims

While CAR-T cell therapies have demonstrated remarkable clinical success, particularly in haematologic malignancies, there remains room to improve their efficacy and expand their applications to more cancer types. Given the critical role of epigenetic regulation in altering T cell differentiation, function, and persistence, we would like to identify and validate epigenetic targets capable of enhancing T cell function.

We would like to start with a high-throughput drug screen using an epigenetic inhibitor library in mouse primary $CD8^+$ T cells with CXCR3 expression as the readout for effector T cell phenotype. Then, we would like to validate the hits from the screen, understand their mechanisms and evaluate their therapeutic potential in preclinical models.

By bridging epigenetic discovery with CAR-T cell biology, this research aims to expand our knowledge and support the development of next-generation immunotherapies with

enhanced tumour control capabilities and broader clinical applicability across diverse cancer indications.

3.2 Results

3.2.1 Drug screen identified eight hits for CXCR3 regulation in $CD8^+$ T cells

To systematically identify epigenetic regulators critical for T cell function, we performed a drug screen using a commercially available epigenetic inhibitor library (purchased from Cayman Chemical) comprising 158 well-characterised compounds (**Appendix 1**). For the drug screen, mouse primary $CD8^+$ T cells were activated with CD3 and CD28 stimulation and concurrently treated with each inhibitor at 2 μM concentration. Following a 72-hour incubation, we quantified CXCR3 expression using flow cytometry as a readout of effector T cell phenotype (**Figure 3.1A**).

The screen revealed eight compounds that significantly modulated CXCR3 expression levels. Four compounds, A-196, MS023, PRT4165 and CAY1072, increased $\%CXCR3^+$ cells in total $CD8^+$ T cells from a baseline of 25% to above 40%; conversely, four compounds, SGC-CBP30, RVX-208, RGFP966 and RSC-133, reduced $\%CXCR3^+$ cells in total $CD8^+$ T cells from 25% to below 15% (**Figure 3.1B**). The molecular targets for the identified hits are detailed in **Table 3.2**.

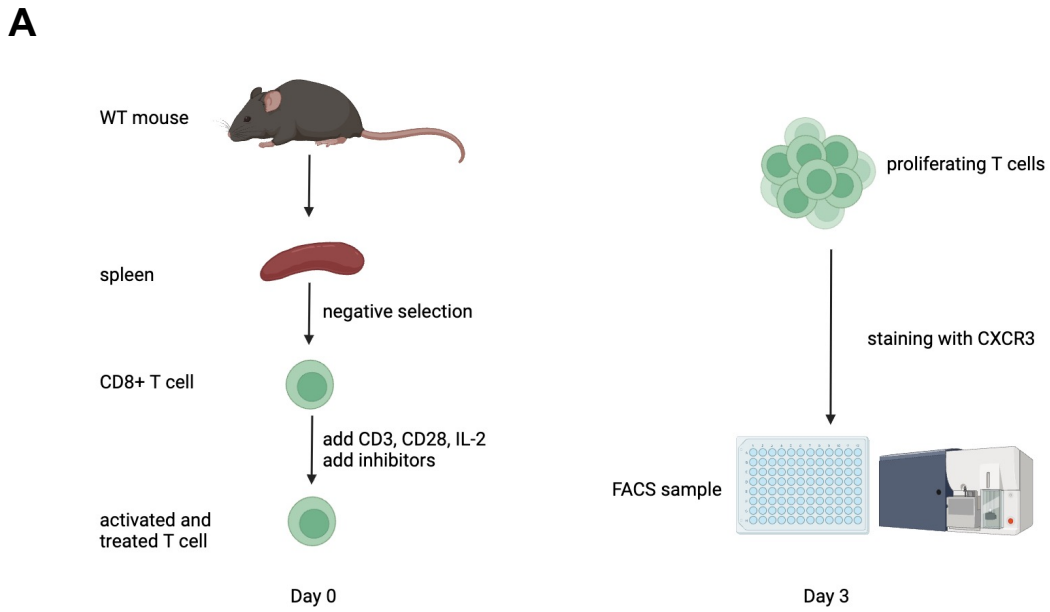

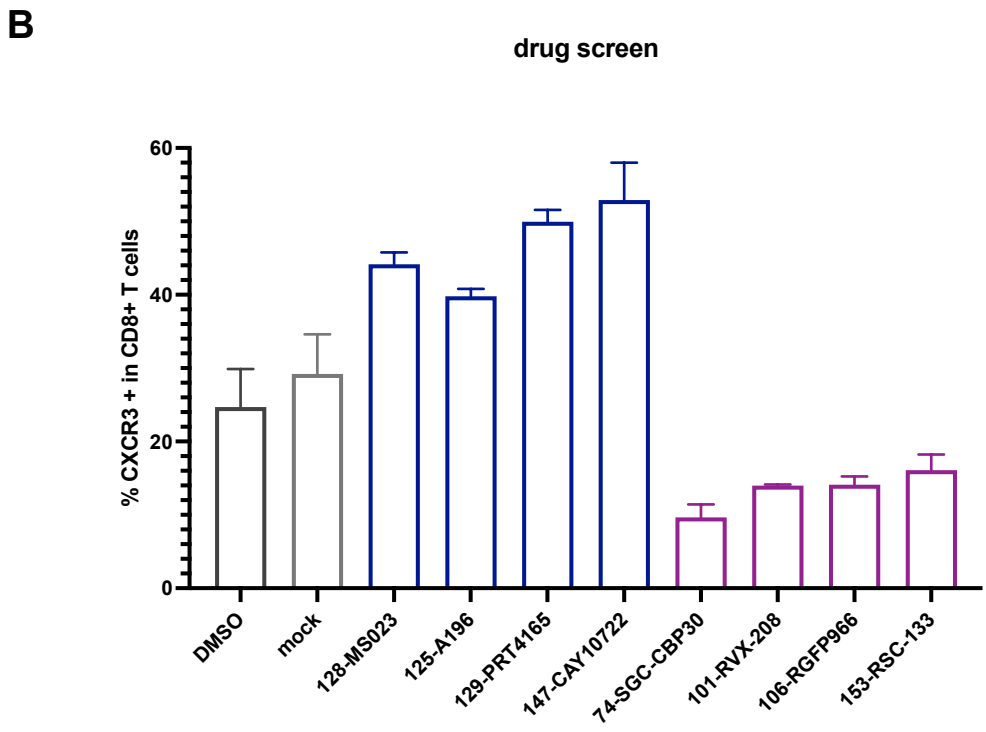

Figure 3.1 Drug screen identified eight hits that regulate CXCR3 expression in CD8$^+$ T cells.

(A) Schematic representation of the experimental design. Plot was generated with bioRender at biorender.com. (B) % CXCR3$^+$ cells, measured with flow cytometry, in CD8$^+$ T cells treated with dimethyl sulfoxide (DMSO) or inhibitors from the Cayman epigenetic inhibitor library for 72 hours.

Name	Target	Target Function
A-196	SUV420H1 and SUV420H2	Lysine methylation[176]
MS023	Type I PRMTs	Arginine methylation[168]
PRT4165	Polycomb repressive complex 1 (PRC1)	Ubiquitination at H2AK119[177]
CAY10722	Sirtuin-3 (SIRT3)	Deacetylation in mitochondria[178]
SGC-CBP30	CREB-binding protein (CBP)/E1A-binding protein (p300)	Transcription co-activator; acetylation[179]
RVX-208	Bromodomain and extra terminal (BET)	Lysine acetylation "reader" [180]
RGFP966	Histone deacetylase 3 (HDAC3)	Histone deacetylation[181]
RSC-133	DNA methyltransferase 1 (DNMT1) and histone deacetylase 1 (HDAC1)	DNA methylation; histone deacetylation; pluripotency[182]

Table 3.2 Hits from the drug screen.
List of hits from the drug screen with their molecular targets and target functions.

3.2.2 MS023 upregulated CXCR3 expression in $CD8^+$ T cells

To validate the screen hits, we performed dose-response analysis by treating mouse primary $CD8^+$ T cells with each candidate compound at concentrations of 1, 2 and 5 μM. CXCR3 expression was quantified by flow cytometry at 24-, 48- and 72-hour timepoints. Among all the hits tested, only the type I PRMT inhibitor MS023 demonstrated consistent upregulation of CXCR3 expression at various concentrations at both 48- and 72-hour timepoints (**Figure 3.2A-H**).

The MS023-induced increase in CXCR3 expression was further confirmed at the transcriptional level, as RT-qPCR analysis revealed that 2 μM MS023 treatment significantly increased CXCR3 mRNA levels by 223.50% after 48 hours and 34.79% after 72 hours compared to DMSO-treated controls (**Figure 3.3A-C**). This concordance between protein and mRNA expression patterns confirms that MS023 mediates its effects through transcriptional regulation of CXCR3 rather than through translational or post-translational modulation of protein expression.

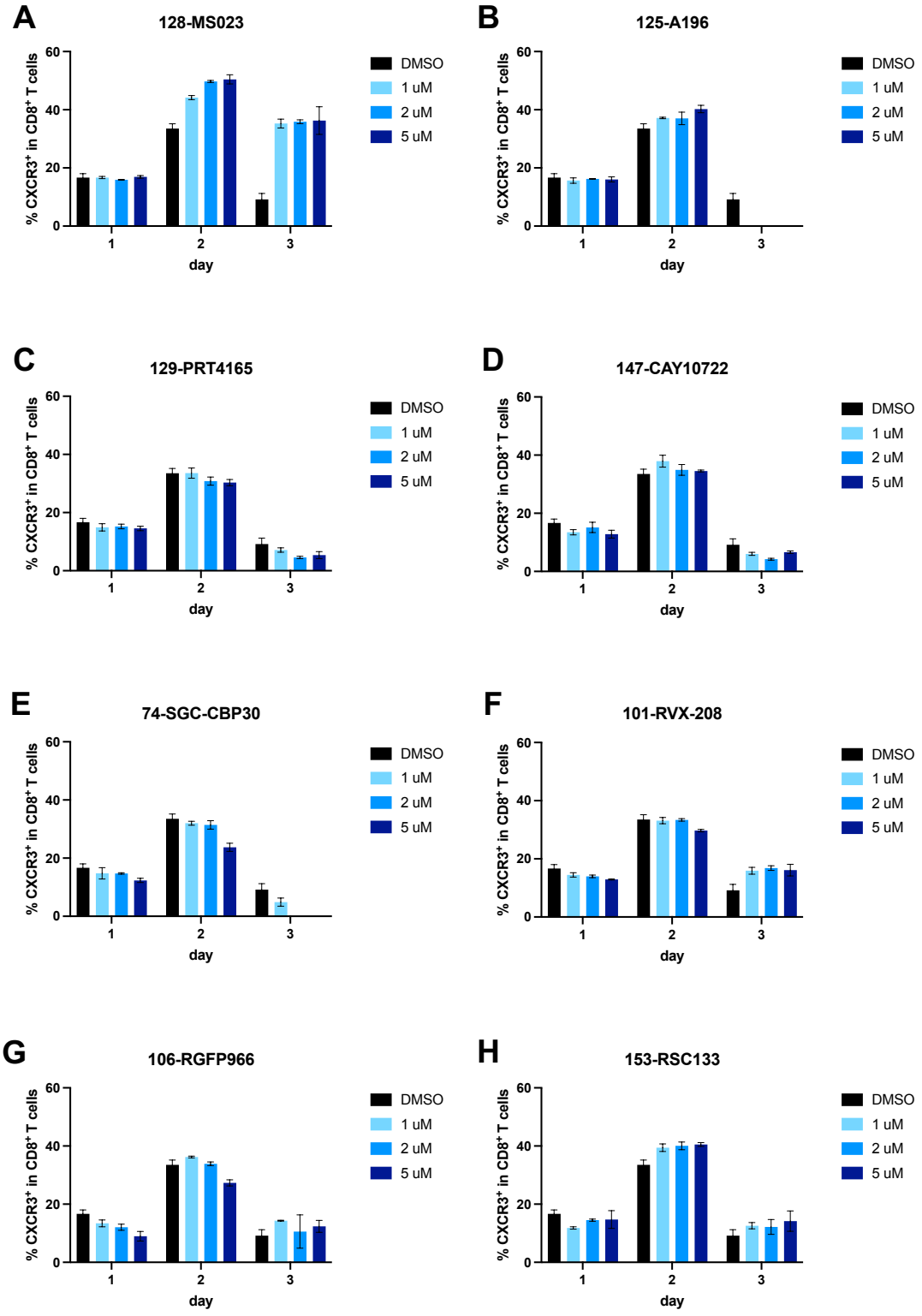

Figure 3.2 CXCR3 expression (protein level) in CD8$^+$ T cells treated with inhibitors.

%CXCR3$^+$ cells in total CD8$^+$ T cells treated with 1, 2 or 5 μM of (A) MS023, (B) A196, (C) PRT4165, (D) CAY10722, (E) SGC-CBP30, (F) RVX-208, (G) RGFP966 or (H) RSC133 for 24, 48 or 72 hours.

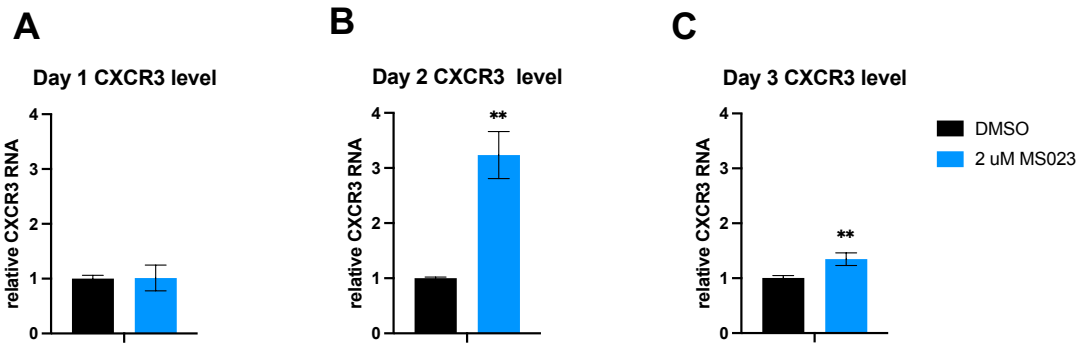

Figure 3.3 CXCR3 expression (mRNA level) in CD8⁺ T cells treated with MS023. CXCR3 expression at mRNA level, as measured by RT-qPCR, in CD8⁺ T cells treated with 2 μM MS023 for (A) 24 hours, (B) 48 hours or (C) 72 hours. Data presented as mean ± SD.

3.2.3 MS023 increased effector molecule production in CD8⁺ T cells

Having established that MS023 upregulates CXCR3 expression, we next investigated whether this epigenetic modulator could enhance the production of effector molecules, another aspect of T cell activation and effector function, in CD8⁺ T cells. We used a stimulation cocktail containing phorbol 12-myristate 13-acetate (PMA) and ionomycin to mimic TCR activation, and we evaluated the effector molecule production following 2 μM MS023 treatment. Notably, 24-hour and 48-hour MS023 exposure significantly increased the expression of key cytokines (e.g., IFNg and IL-2) and cytotoxic molecules (e.g., GzmB and Perforin) in mouse primary CD8⁺ T cells (**Figure 3.4A-B**). These findings demonstrate that MS023 not only increases CXCR3 expression but also potentiates the effector CD8⁺ T cell function, enhancing both the cytokine production and the cytotoxic potential.

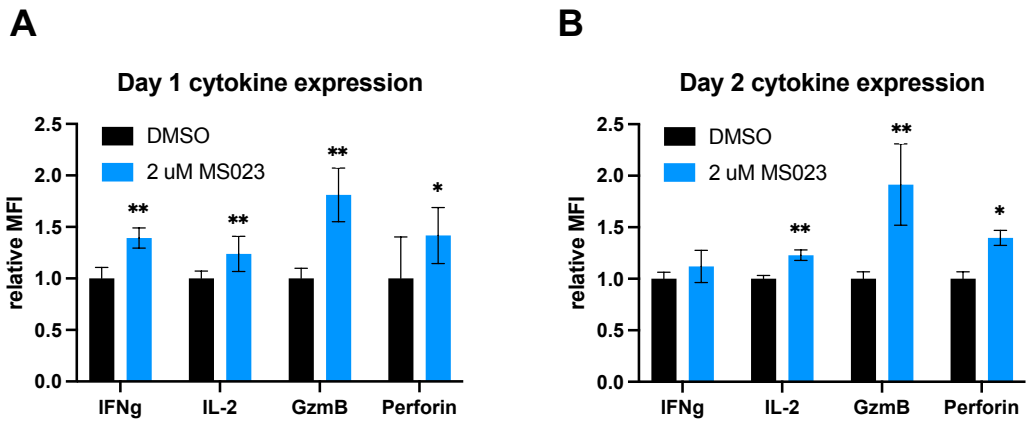

Figure 3.4 MS023 enhanced effector molecule production in CD8⁺ T cells. Relative expression level of the effector molecules (including IFNg, IL-2, GzmB, and Perforin), as measured by flow cytometry, in mouse primary CD8⁺ T cells treated with DMSO or 2 μM MS023 for (A) 24 hours and (B) 48 hours in response to a 4-hour cocktail stimulation treatment. Data presented as mean ± SD.

3.2.4 MS023 increased *in vitro* CD8⁺ T cell killing

After confirming that MS023 boosts CXCR3 expression and effector molecule production in CD8⁺ T cells, we next evaluated its functional impact on direct tumour-killing capacity using *in vitro* co-culture experiments.

We isolated CD8⁺ T cells from OT-1 transgenic mice, which express T cell receptors specific for ovalbumin (OVA) peptide, and we treated them with 2 μM MS023 before co-culturing them with OVA-expressing B16 melanoma cell line (B16-OVA) or MC38 colorectal carcinoma cell line (MC38-OVA) for 16 hours. MS023-treated T cells exhibited increased tumour-killing capacity compared to DMSO-treated controls, with cytotoxicity against B16-OVA rising from 4.00% to 15.67%, and that against MC38-OVA rising from 36.52% to 49.94% (**Figure 3.5A-B**).

These results demonstrate that MS023-mediated epigenetic modulation not only alters CXCR3 expression and effector molecule production but also functionally enhances

the ability of $CD8^+$ T cells to eliminate tumour cells *in vitro*. The differential magnitude of improvement between tumour lines, 4-fold for B16-OVA versus 1.4-fold for MC38-OVA, may reflect inherent differences in their susceptibility to T cell-mediated tumour control, potentially due to variations in antigen presentation, immune evasion mechanisms, or baseline sensitivity to cytotoxic molecules.

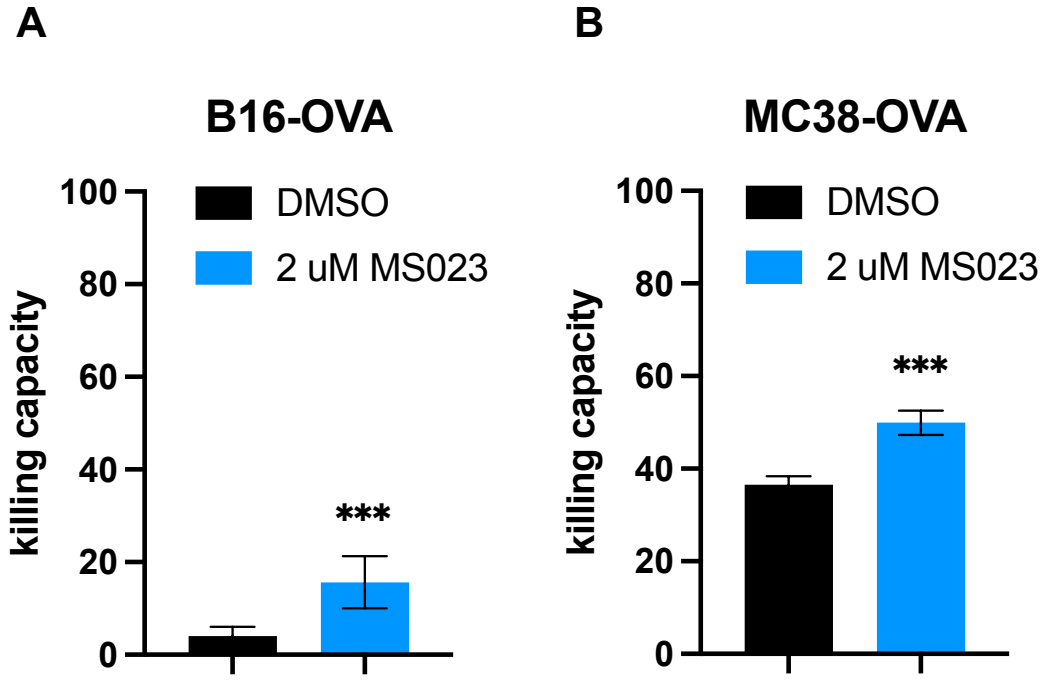

Figure 3.5 MS023 enhanced *in vitro* tumour killing.
Killing capacity, calculated from %dead cells measured with flow cytometry, of primary mouse OT-1 $CD8^+$ T cells pre-treated with DMSO or 2 μM MS023 against (A) B16-OVA cells or (B) MC38-OVA cells. Data presented as mean ± SD.

3.2.5 Pan-type I PRMT inhibitors increased CXCR3 expression and effector molecule production

MS023 functions as a pan-type I PRMT inhibitor targeting five type 1 PRMTs, namely PRMT1, PRMT3, PRMT4, PRMT6 and PRMT8. To validate that the observed increase in CXCR3 expression, effector molecule production and tumour-killing capacity were

specifically mediated through type I PRMT inhibition, we evaluated the effect of GSK3368715, another pan-type I PRMT inhibitor with identical targets. Based on our findings showing maximal CXCR3 upregulation at 72 hours and peak effector molecule production at 24 hours post-MS023 treatment, we focused our analysis on these optimal timepoints.

Treatment with 2 μM GSK3368715 for 72 hours significantly increased CXCR3 expression in primary mouse $CD8^+$ T cells, although to a lesser extent than MS023-induced enhancement (2.14-fold by GSK3368715 versus 2.95-fold by MS023; **Figure 3.6A-B**). Consistent with the increase in CXCR3 expression, 2 μM GSK3368715 also increased IFNg expression and GzmB expression by 19.55% and 26.70%, respectively, 24 hours post-treatment (**Figure 3.6B**). These results confirm that pharmacological inhibition of type I PRMTs consistently augments $CD8^+$ T cell activation and effector function as demonstrated by elevated CXCR3 expression and increased effector molecule production.

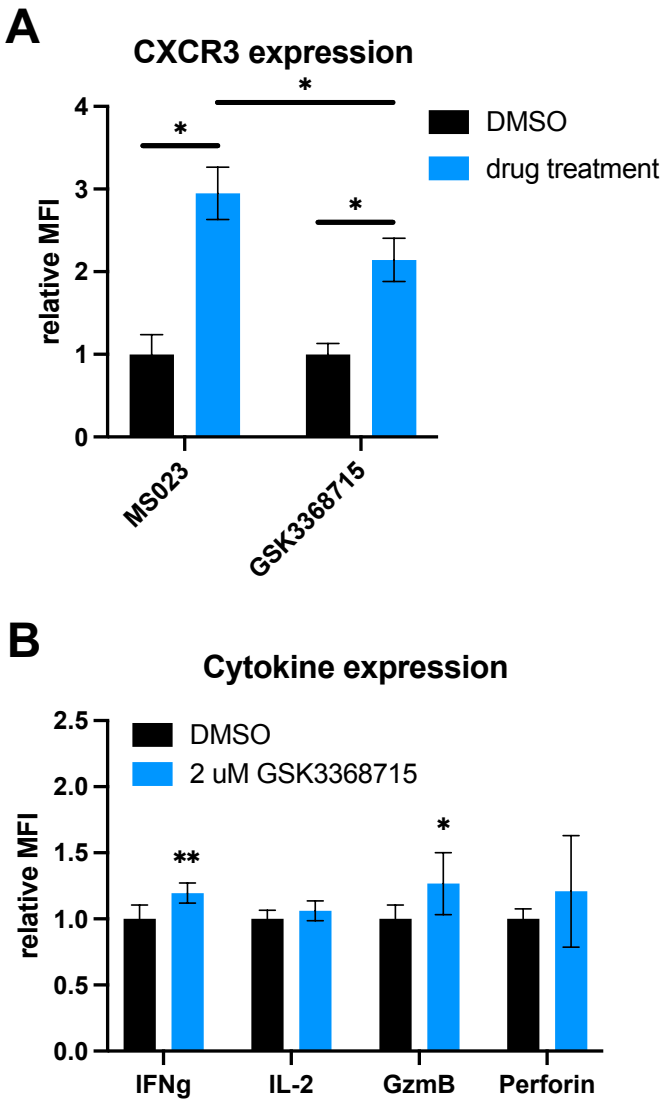

Figure 3.6 Effects of pan-type I PRMT inhibitors on primary CD8⁺ T cells.
(A) Relative CXCR3 expression level, measured by flow cytometry, of $CD8^+$ T cells treated with DMSO, 2 μM MS023 or 2 μM GSK3368715 for 72 hours. (B) Relative effector molecules (IFNg, IL-2, GzmB and Perforin) production level upon stimulation, measured by flow cytometry, of $CD8^+$ T cells treated with DMSO, 2 μM MS023 or 2 μM GSK3368715 for 24 hours. Data presented as mean ± SD.

3.2.6 Single-target type I PRMT inhibitors only increased CXCR3 expression and effector molecule production to a small extent

To identify the specific type I PRMT responsible for modulating $CD8^+$ T cell function, we evaluated the effect or selective inhibitors targeting individual PRMTs, including C-7280948 (PRMT1-sepcific), SGC707 (PRMT3-specific), TP064 (PRMT4-specific), and EPZ020411 (PRMT6-specific). We treated primary mouse $CD8^+$ T cells with 2 μM of each inhibitor, and we found that only TP064 significantly increased CXCR3 expression (**Figure 3.7A**), implicating PRMT4 as the key regulator among type I PRMTs. The PRMT4 inhibitor TP064 also increased the expression of IFNg, IL-2, and GzmB by 39.45%, 13.48%, and 62.34%, respectively (**Figure 3.7B-E**). While other inhibitors did not increase CXCR3 expression significantly, some of them promoted effector molecule expression. For example, PRMT1 inhibitor C-7280948 increased the expression of IFNg, IL-2, and GzmB by 32.43%, 12,34%, and 51.60%, respectively; PRMT3 inhibitor SGC707 increased GzmB expression by 35.78%; and PRMT6 inhibitor EPZ020411 increased GzmB expression by 30.13% (**Figure 3.7B-E**). These results demonstrate that while PRMT4 regulates CXCR3 expression, multiple type I PRMTs contribute to the increased effector molecule production in $CD8^+$ T cells, suggesting both specialised and overlapping roles of type I PRMTs in T cell activation and function.

Given that single-target PRMT inhibitors produced more modest effects compared to pan-type I PRMT inhibitors, we then investigated the effect of simultaneous inhibition of multiple type I PRMTs on $CD8^+$ T cells. Treatment with a combination of four single-target PRMT inhibitors (C-7280948, SGC707, TP064 and EPZ020411) at 2 μM each for 72 hours increased CXCR3 expression level by 50.63% (**Figure 3.8A**). This combinatorial approach also significantly increased the expression of IFNg, IL-2, GzmB, and perforin upon stimulation by 38.47%, 21.63%, 40.27%, and 41.99%, respectively (**Figure 3.8B**). Since none of the single-target PRMT inhibitors alone

could simultaneously increase CXCR3 expression and all four effector molecules measured, these findings demonstrate a synergistic effect of concurrent type I PRMT inhibition.

To understand the individual contributions of each single-target PRMT inhibitor in our combination treatment, we performed a drop-out screen where any one of the inhibitors from the combination treatment was removed each time. Strikingly, we found that the combination treatment without PRMT4 inhibitor TP064 could no longer increase CXCR3 expression (**Figure 3.8C**). This PRMT4-dependent effect extended to the expression of IFNg, IL-2 expression, and Perforin (**Figure 3.8D, E and G**). These results, together with our earlier findings that TP064 alone could increase CXCR3 expression (**Figure 3.7A**), suggest PRMT4 as the central regulator of $CD8^+$ T cell activation and effector function among type I PRMTs. While other PRMTs contribute to specific aspects of T cell function, PRMT4 appears to be required for the coordinated upregulation of both CXCR3 expression and effector molecules production.

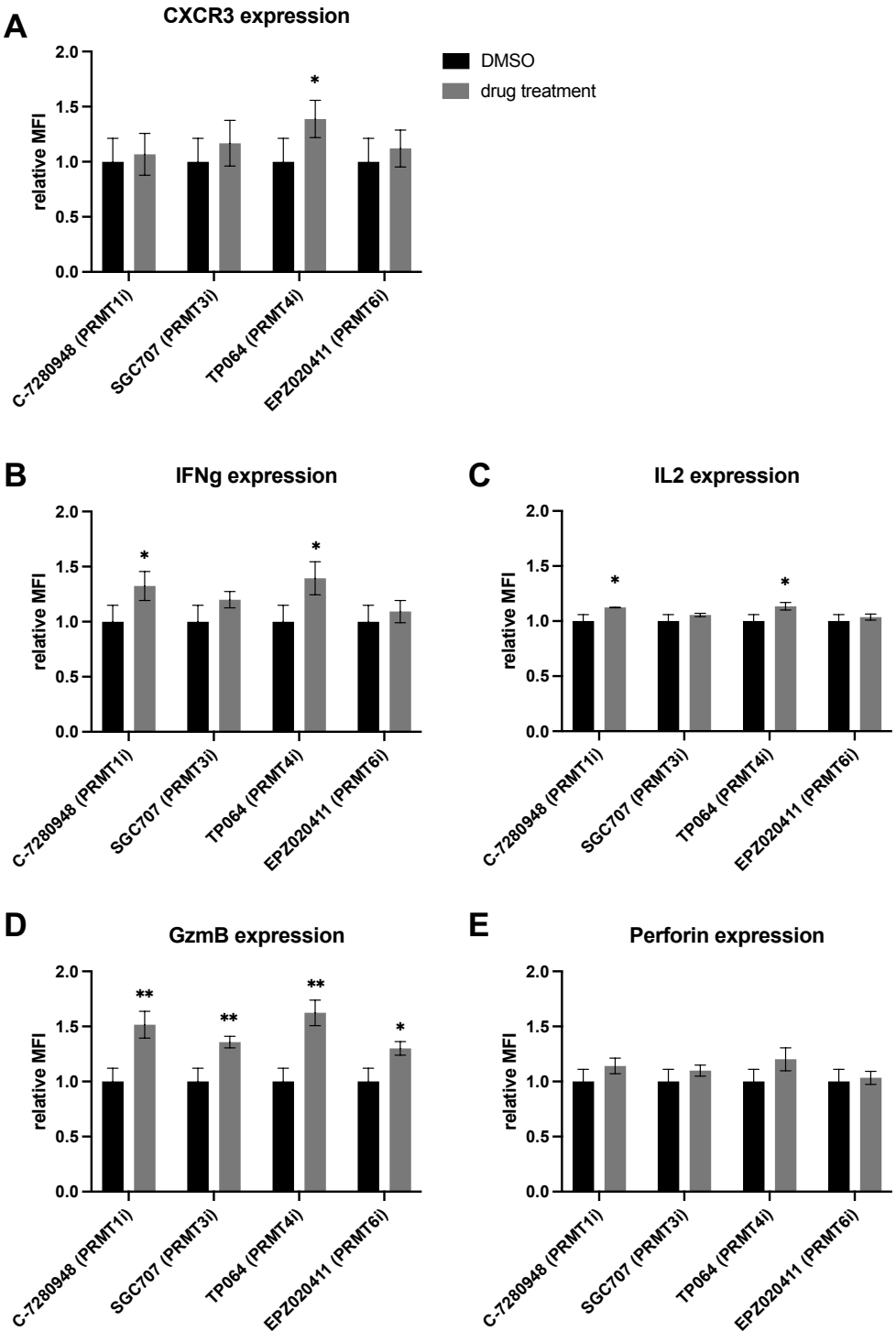

Figure 3.7 Effects of single-target PRMT inhibitors on CD8$^+$ T cells.

(A) Relative CXCR3 expression level, measured by flow cytometry, in primary CD8$^+$ T cells treated with DMSO, 2 μM PRMT1 inhibitor C-7280948, 2 μM PRMT 3 inhibitor SGC707, 2 μM PRMT4 inhibitor TP064, or 2 μM PRMT6 inhibitor EPZ020411 for 72 hours. Relative (B) IFNg, (C) IL-2, (D) GzmB and (E) Perforin expression level upon stimulation, measured by flow cytometry, in primary CD8$^+$ T cells treated with DMSO or above-mentioned drugs for 24 hours. Data presented as mean ± SD.

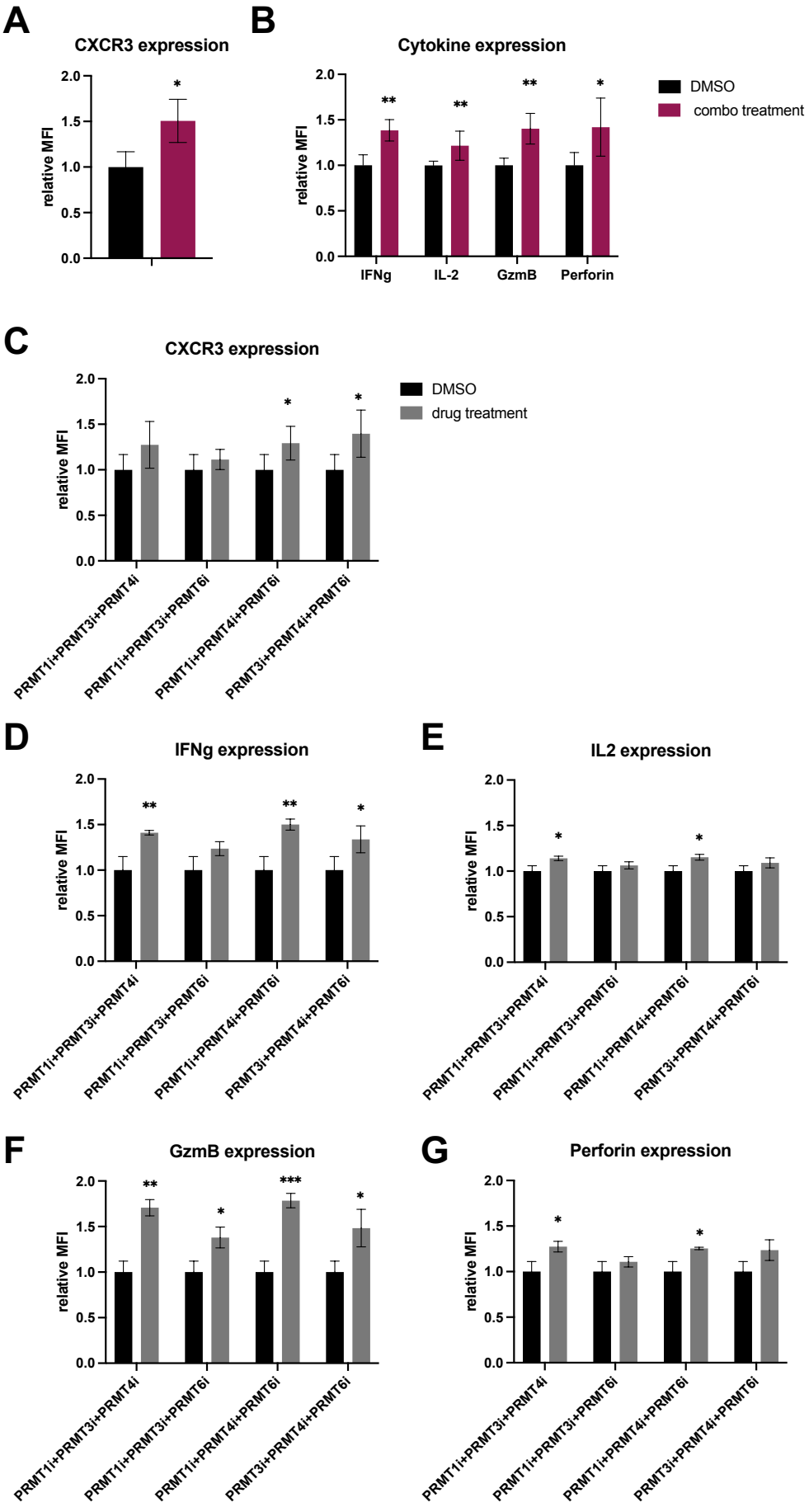
A
CXCR3 expression
relative MFI
2.0
1.5
1.0
0.5
0.0
*
B
Cytokine expression
relative MFI
**
**
**
*
IFNg
IL-2
GzmB
Perforin
DMSO
combo treatment
C
CXCR3 expression
relative MFI
*
*
DMSO
drug treatment
PRMT1i+PRMT3i+PRMT4i
PRMT1i+PRMT3i+PRMT6i
PRMT1i+PRMT4i+PRMT6i
PRMT3i+PRMT4i+PRMT6i
D
IFNg expression
relative MFI
**
**
*
E
IL2 expression
relative MFI
*
*
F
GzmB expression
relative MFI
**
*
***
*
G
Perforin expression
relative MFI
*
*

Figure 3.8 Effects of combination treatment on CD8$^+$ T cells.
(A) Relative CXCR3 expression level, measured by flow cytometry, in primary CD8$^+$ T cells treated with DMSO, or the combination treatment (with 2 μM C-7280948, 2 μM SGC707, 2 μM TP064 and 2 μM EPZ020411) for 72 hours. (B) Relative effector molecule expression level upon stimulation, measured by flow cytometry, in primary CD8$^+$ T cells treated with the above-mentioned drugs for 24 hours. (C) Relative CXCR3 expression level, measured by flow cytometry, in primary CD8$^+$ T cells treated with DMSO or PRMT inhibitors (as labelled on the graph) for 72 hours. Relative (D) IFNg, (E) IL-2, (F) GzmB and (G) Perforin expression level upon stimulation, measured by flow cytometry, in primary CD8$^+$ T cells treated with inhibitors (as labelled on the graph) for 24 hours. Data presented as mean ± SD.

3.2.7 Optimisation of viral infection protocol on primary CD8$^+$ T cells

Although we have tested the effect of inhibiting type I PRMTs with the single-target PRMT inhibitors, we are not certain that the drug inhibited the activity of the specific PRMT. Thus, we would like to validate these findings through genetic KO approaches. However, establishing efficient viral transduction in primary mouse CD8$^+$ T cells is technically challenging.

We first tested the lentiviral infection efficiency on primary mouse CD8$^+$ T cells using the lentivirus encoding mCherry (a red fluorescent protein) as the reporter. We optimised three critical parameters: 1) cell density (ranging from 0.05 to 0.5 million cells per well), 2) the use of retronectin (including method for plate-coating and retronectin concentration ranging from 5-20 μg/cm²), and 3) the use of polybrene. The maximal transduction efficiency was only 2.62%, observed under conditions using 0.05 million cells infected with 1 ml lentivirus in the presence of 5 μg/cm^2 retronectin, followed by centrifugation for 90 minutes (**Table 3.3**). This low efficiency precluded reliable genetic manipulation via lentiviral infection, prompting us to explore gene manipulation with retroviral infection.

We evaluated the efficiency of retroviral infection in mouse primary $CD8^+$ T cells using the retrovirus encoding blue fluorescent protein (BFP) as the reporter. We achieved consistently high infection efficiency exceeding 50% across all tested conditions (**Table 3.4**). This robust performance contrasts sharply with the 2.62% efficiency observed with lentiviral vectors under optimal conditions (**Table 3.3**). Building on these results, we decided to employ retroviral vectors for subsequent genetic manipulation experiments to investigate the functional consequences of PRMT inhibition.

Cell number (million)	Infection protocol	Retronectin concentration (μg/cm2)	% mCherry+
0.05	Virus-bound plate + retronectin	5	2.34%
		10	2.32%
		20	2.03%
0.5		5	0.26%
		10	0.46%
		20	0.74%
0.05	Spin infection + retronectin	5	2.62%
		10	2.24%
		20	2.55%
0.5		5	1.00%
		10	1.38%
		20	0.77%
0.05	Spin infection + polybrene		2.42%
0.5			1.38%

Table 3.3 Lentiviral infection efficiency.
List of lentiviral infection conditions (including changes in cell number, infection protocol, and retronectin concentration) and their corresponding infection efficiency as measured by %$mCherry^+$ cells in total $CD8^+$ T cells.

Cell number (million)	Infection protocol	% BFP+
0.5	virus-bound plate + retronectin	69.30%
0.5	spin infection + retronectin	66.50%
0.5	spin infection + polybrene	58.00%

Table 3.4 Retroviral infection efficiency.
List of retroviral infection conditions and their corresponding infection efficiency as measured by % BFP^+ cells in total $CD8^+$ T cells.

3.2.8 Effects of PRMT KO on $CD8^+$ T cells

To validate our pharmacological findings through genetic manipulations, we cloned the gRNA targeting type 1 PRMT into a retroviral vector construct with BFP expression and puromycin resistance, and we used the CRISPR/Cas9 system to edit the gene expression in primary mouse $CD8^+$ T cells. Following viral infection and selection with 48-hour puromycin treatment followed by BFP^+ gating, we observed that gRNAs targeting PRMT1 and PRMT4 significantly enhanced CXCR3 expression. Specifically, both PRMT1 gRNAs increased CXCR3 expression by 27.69% and 17.66%, and one PRMT4 gRNA increased CXCR3 expression by 8.77% (**Figure 3.9A**). In line with this, PRMT1 gRNA1 also increased the expression of IFNg and IL-2 expression upon stimulation by 12.12% and 7.97%, respectively, and PRMT4 gRNA1 increased the expression of IFNg, GzmB, and Perforin expression by 23.55%, 30.12%, and 20.40%, respectively (**Figure 3.9B-E**). These findings suggest the importance of PRMT1 and PRMT4 in regulating T cell function. Interestingly, gRNAs targeting PRMT6 and PRMT8 selectively enhanced certain effector molecule production without increasing CXCR3 expression (**Figure 3.9B-E**), suggesting potential distinct regulatory roles among type I PRMTs.

These genetic data complement our pharmacological inhibitor experiments. Collectively, these findings establish the critical role of PRMT1 and PRMT4 in regulating $CD8^+$ T cell function. However, we note that the absence of protein-level validation with immunoblot or flow cytometry represents one limitation of our experiments, since we relied on puromycin resistance and BFP expression as proxies for successful gene editing rather than directly quantifying PRMT expression level.

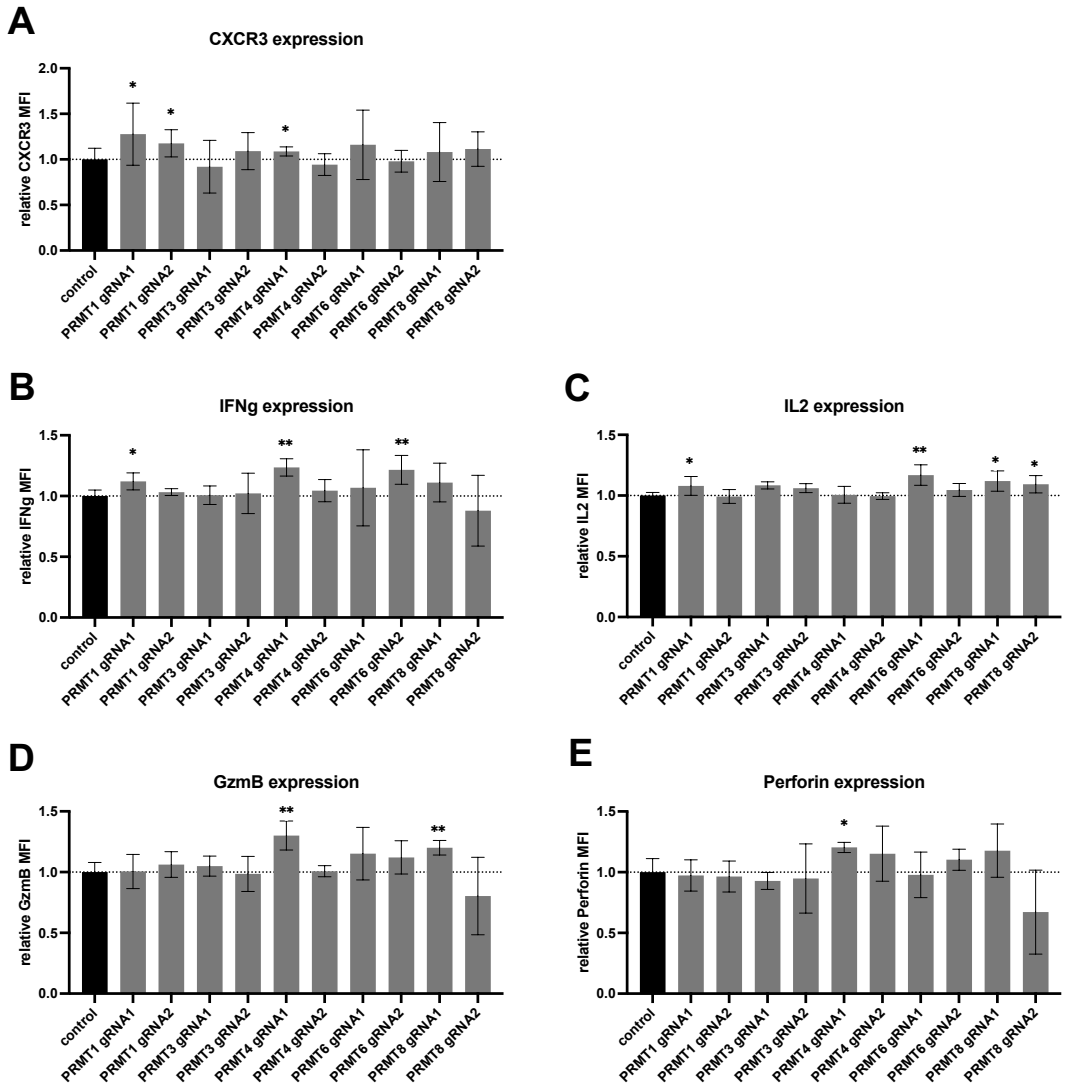

Figure 3.9 Effects of PRMT KO on CD8$^+$ T cells.

(A) Relative CXCR3 expression level, measured by flow cytometry, in primary CD8$^+$ T cells treated with NT gRNA or gRNAs targeting *Prmt1, Prmt3, Prmt4, Prmt6* or *Prmt8* followed by puromycin selection and BFP gating. Relative (B) IFNg, (C) IL-2, (D) GzmB and (E) Perforin expression level upon stimulation, measured by flow cytometry, in primary CD8$^+$ T cells treated with gRNAs as labelled on the graph. Data presented as mean ± SD.

3.2.9 MS023-induced increase in effector molecule production was independent of increased CXCR3 expression

While our previous experiments demonstrate that MS023 treatment increases both CXCR3 expression and effector molecule production in $CD8^+$ T cells, the mechanistic relationship between these effects remained unclear.

To determine whether the production of effector molecules was dependent on CXCR3 upregulation, we isolated $CD8^+$ T cells from $Cxcr3^{-/-}$ mice and tested the effect of MS023 on these cells. Flow cytometry analysis confirmed the expected reduction of CXCR3 expression in KO cells compared to WT controls (**Figure 3.10A**).

We found that treating $CD8^+$ T cells from WT mice with 2 μM MS023 for 24 hours increased the expression level of IFNg, IL-2, GzmB and Perforin by 35.27%, 18.85%, 45.22% and 46.77%, respectively (**Figure 3.10B**). Notably, we found that $Cxcr3^{-/-}$ $CD8^+$ T cells showed comparable or greater MS023-induced enhancement of effector molecule production with the expression level of IFNg, IL-2, GzmB and Perforin increased by 43.13%, 19.12%, 16.68% and 53.47%, respectively in $Cxcr3^{-/-}$ $CD8^+$ T cells receiving MS023 treatment (**Figure 3.10C**). These findings suggest that the mechanism of MS023-induced increase in effector molecule production is independent of CXCR3 upregulation.

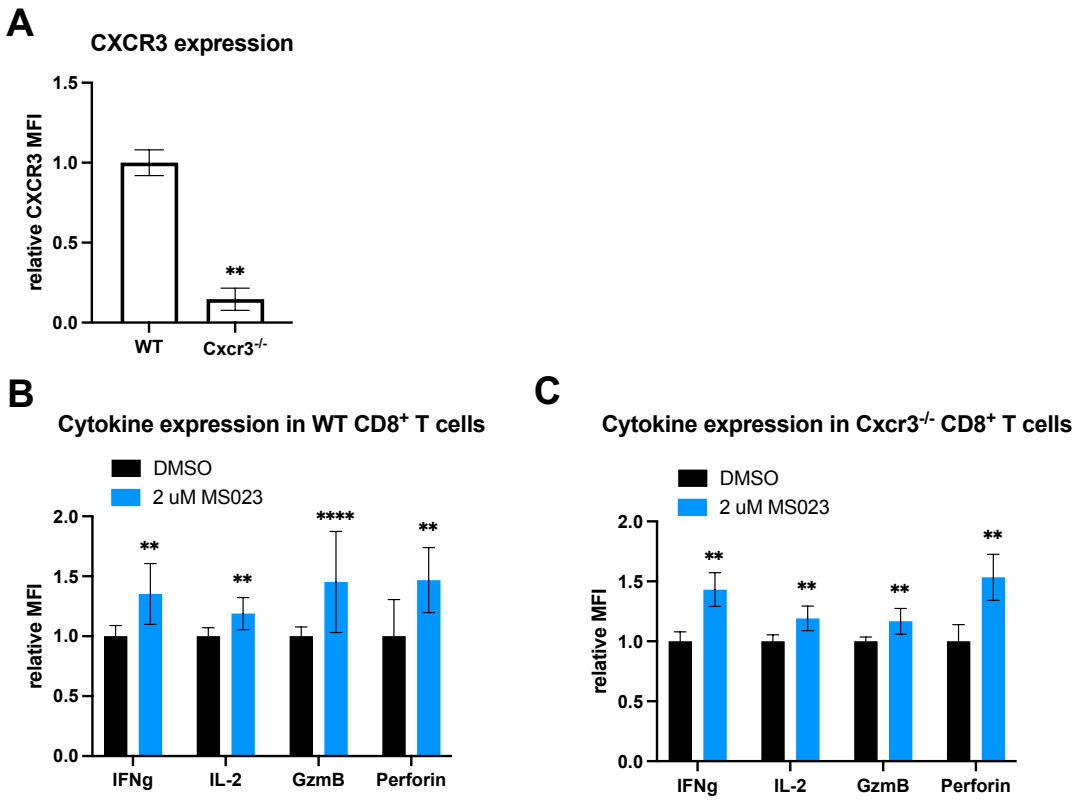

Figure 3.10 Effects of MS023 on Cxcr3$^{-/-}$ CD8^{+} T cells.

(A) Relative CXCR3 expression level, measured by flow cytometry, in primary CD8^{+} T cells from WT mice and Cxcr3$^{-/-}$ mice. (B) Relative effector molecule expression level upon stimulation, measured by flow cytometry, in primary CD8^{+} T cells from (B) WT mice and (C) Cxcr3$^{-/-}$ mice in response to 2 μM MS023 treatment. Data presented as mean ± SD.

3.3 Discussion

3.3.1 Summary of results

In this project, we have identified type I PRMTs as key regulators of $CD8^+$ T cell activation and effector function. Our studies demonstrate that MS023, a pan-type I PRMT inhibitor, significantly enhances CXCR3 expression, effector molecule production and *in vitro* tumour-killing capacity of $CD8^+$ T cells.

Two additional pieces of evidence further support the functional relevance of type I PRMTs. Firstly, GSK3368715, another pan-type 1 PRMT inhibitor, led to a comparable increase in CXCR3 expression. Secondly, the combined inhibition of multiple type I PRMTs (including PRMT1, 3, 4 and 6) synergistically altered T cell function, with PRMT4 emerging as a particularly important regulator through both pharmacological and genetic KO studies.

Collectively, these findings suggest that targeted inhibition of type I PRMTs, particularly through PRMT4 inhibition, may represent a promising strategy to enhance T cell-based immunotherapies.

3.3.2 Limitations of experiments and prospects

While our pharmacological and genetic approaches consistently implicated type I PRMTs in $CD8^+$ T cell regulation, we acknowledge two key limitations in our experiments. Firstly, the absence of direct quantification of PRMT expression level and activity leaves uncertainties regarding the extent of PRMT inhibition achieved with either small-molecule inhibitors or CRISPR/Cas9 editing. Secondly, while our $Cxcr3^{-/-}$ experiments demonstrated that the mechanism of MS023-induced enhancement in $CD8^+$ T cell function is independent of CXCR3 upregulation, the precise molecular mechanisms remain unclear.

Further analysis, such as arginine methylation measurement with stable isotope labelling with amino acids (SILAC) labelling followed by MS analysis, is needed to explore the changes in the arginine methylation pattern following PRMT inhibition and to identify specific methylation targets that mediate the observed T cell enhancements[183]. In addition, RNA sequencing experiments using $CD8^+$ T cells treated with DMSO or MS023 could reveal changes in the transcriptome and identify the downstream effectors of MS023.

These mechanistic insights would advance our fundamental understanding of epigenetic regulation in T cell biology and support the development of selective PRMT-targeted immunotherapies. The differential effects we observed between type I PRMTs suggest that isoform-specific inhibitors may offer precision modulation of desired T cell functions while minimising off-target effects.

3.3.3 Potential mechanisms of PRMT inhibition on T cells

MS-based proteomic studies have identified many T cell signalling components as substrates for arginine methylation in both Jurkat cell lines and primary T cells[184].

Direct modification of transcription factors and cofactors influences T cell differentiation and function. For example, PRMT1-mediated methylation of NIP45, a nuclear factor of activated T cells (NFAT) cofactor protein, facilitates the interaction between NIP45 and NFAT to promote cytokine production in $CD4^+$ T helper cells[185]. Another example is T-bet, a transcription factor involved in differentiation from naïve T cells to effector T cells[184].

In addition, arginine methylation can also indirectly shape T cell function by modulating upstream signalling pathways. For example, nuclear factor kappa-light-chain-enhancer of activated B cells (NF-kB) pathway plays a vital role in $CD8^+$ T cell memory[186], and

PRMT1-mediated methylation of tumour necrosis factor receptor-associated factor 6 (TRAF6) inhibits its activity, thus suppressing the activation of NF-KB and consequently regulating $CD8^+$ T cells indirectly[187].

These established mechanisms provide a conceptual framework for understanding how type I PRMT inhibition might enhance $CD8^+$ T cell effector function in our system. The methylation status of these known substrates or other unidentified PRMT targets could collectively contribute to the observed enhancement in T cell function upon PRMT inhibition.

3.3.4 Clinical use of PRMT inhibitors

Epigenetic regulators have emerged as novel cancer therapeutic targets due to their involvement in various processes involved in cancer development, such as cell cycle regulation, angiogenesis, and cell differentiation. Epigenetic pathways are also involved in drug resistance, allowing the potential use of combinational therapy with chemotherapy.

DNMT and HDAC have been targeted for the development of novel cancer therapies; however, less is understood about inhibiting PRMTs in cancer. Recent advancement shows CBP/p300 mutations could sensitise cells to PRMT4 inhibition[188]. And several studies have revealed potential mechanisms of PRMT regulation in cancer development. For example, PRMT1 plays a key role in DNA damage repair through its modulation of MRE11, a core protein in the Mre11-Rad50-Nbs1 (MRN) complex that senses and repairs DSBs[173]. PRMT4 drives tumour growth in diffuse large B cell lymphoma through its regulation of HATs, creating a chromatin state favourable for oncogene expression[189]. And PRMT6 regulates cell cycle progression by generating the H3R2me2a mark, which inhibits the expression of cell-cycle related genes, such as *p21WAF1*, *p21KIP1*, *p18*, and *p21*[190,191].

The growing recognition of PRMTs as cancer-promoting proteins has spurred interest in developing PRMT-targeted therapies. Several PRMT inhibitors have entered clinical trials, reflecting their potential as novel anticancer agents (**Table 3.1**). While previous studies have primarily focused on PRMT inhibition for direct tumour control[192–194], we raised the possibility of inhibiting PRMT in CAR-T cells to enhance their effector functions, thus increasing the efficacy of CAR-T therapy. However, several critical considerations must be addressed before clinical translation.

Firstly, our current findings only demonstrate short-term enhancement of T cell effector function. The long-term consequences of PRMT inhibition on T cell function and persistence remain unknown. Given that PRMTs regulate epigenetic programmes governing T cell differentiation, PRMT inhibition in CAR-T cells might inhibit the development of memory subsets essential for sustained effects.

In addition, PRMTs have various histone and non-histone substrates[184], including other epigenetic regulators, such as bromodomain-containing protein 4 (BRD4)[195], which is thought to be the driver for multiple genes involved in cancer development. This suggests that PRMT inhibition might cause global effects on $CD8^+$ T cells, and the clinical use of PRMT-edited CAR-T cells might lead to unexpected side effects. Thus, further studies are needed to test the long-term impact and safety of PRMT inhibition in $CD8^+$ T cells before its clinical use.

These concerns underscore the need for comprehensive preclinical studies to evaluate both the durability and safety of PRMT-edited CAR-T cells. Future work could employ longitudinal models to assess the long-term effect of PRMT inhibition in T cells and multi-omics approaches to identify off-target effects of PRMT inhibition.

Chapter 4: The role of HK in LSD1 inhibition-induced phenotype

4.1 Introduction

4.1.1 LSD1

LSD1 (KDM1A, AOF2, and BHC110) was discovered in 2004 as the first histone lysine-specific demethylase[196]. LSD1 is a flavin-dependent amine oxidase that catalyses the oxidative removal of methyl groups from lysine residues on histone H3[197]. This reaction requires flavin adenine dinucleotide (FAD) as a cofactor and generates demethylated histone products along with the by-products, formaldehyde, and hydrogen peroxide.

Structurally, LSD1 contains two functional domains: a C-terminal amine oxidase-like (AOL) domain, within which lies an FAD-binding subdomain, and a Swi3p/Rsc8c/Moira (SWIRM) domain that maintains protein stability and interacts with histone tails. Together, these structural elements enable LSD1 to specifically recognise and modify methylated substrates, making it a critical regulator of chromatin structure and gene expression.

LSD1 exerts its biological functions through the formation of a core complex with histone deacetylase 1/2 (HDAC1/2) and co-repressor for element-1-silencing transcription factor (CoREST)[198]. This core complex serves as the fundamental unit for LSD1-mediated chromatin regulation, where HDAC1/2 and CoREST are indispensable for proper targeting and enzymatic activity. Beyond this core complex, LSD1 also participates in various functional interactions that confer context-specific regulatory roles. For example, in neural stem cells, LSD1 is recruited by the orphan nuclear receptor Tailless-like 1 (TLX) to the promoters of TLX-targeted genes, which are important for self-renewal and neurogenesis[199,200]. While in breast cancer cells, LSD1 associates with nucleosome remodelling and deacetylase (NuRD) complex to regulate TGFb signalling, thus promoting cell proliferation and EMT[201]. And in haematopoietic differentiation, LSD1 interacts with T-cell acute lymphocytic leukaemia

protein 1 (TAL1) to regulate the transcriptional programmes governing erythroid differentiation[202].

As a histone demethylase, LSD1 primarily removes mono- and di-methyl groups from H3K4 to cause chromatin compaction and transcription suppression; on the other hand, its demethylation at H3K9 leads to chromatin relaxation and transcription activation[203,204]. Beyond histones, LSD1 also has non-histone substrates. The tumour suppressor p53 undergoes LSD1-mediated demethylation that modulates its role in transcription activation and apoptosis[205]. LSD1 also targets DNMT1, and the demethylation modification stabilises DNMT1 to maintain DNA methylation patterns[206]. Key signalling molecules, including the transcription factor E2F1[207] and signal transducer and activator of transcription 3 (STAT3)[208], are also substrates of LSD1. Through this broad substrate specificity, LSD1 is involved in diverse biological processes across multiple tissue types, including adipogenesis[209], neurogenesis[210], skeletal muscle differentiation[211,] and hematopoietic cell differentiation[212].

4.1.2 LSD1 and cancer

The role of LSD1 in various genomic, cellular, physiological, and developmental processes has been established. In addition, LSD1 is often overexpressed in cancers, including haematopoietic cancers, such as acute myeloid leukaemia (AML), acute lymphoblastic leukaemia (ALL), chronic myelogenous leukaemia (CML), and myelodysplastic syndrome (MDS), and solid tumours, such as small cell lung cancer (SCLC), colorectal cancer, prostate cancer, and breast cancer[213]. High LSD1 expression correlates strongly with enhanced proliferation, metastatic potential, and poor clinical prognosis.

Mechanistic studies reveal that LSD1 drives oncogenesis through four interconnected pathways. Firstly, LSD1 regulates cell proliferation and cell cycle progression through suppressing the activity of tumour-suppressor p53 and activating proto-oncogene DEK[205,214]. This dual regulation promotes uncontrolled proliferation. Secondly, LSD1 regulates EMT through direct repression of E-cadherin expression [215]. Thirdly, LSD1 promotes the metabolic shift from OXPHOS to glycolysis through suppressing mitochondrial respiration genes (e.g., PPARGC1A) via H3K4 demethylation and stabilising hypoxia-inducible factor-1α (HIF-1α) to upregulate glycolytic enzymes (e.g., PKM2) [216–218] . And lastly, LSD1 also enables immune evasion through suppression of double-stranded RNA (dsRNA) stress that would otherwise trigger interferon responses and increase immunogenicity of the cancer cells[219]. In addition, LSD1 inhibition was also found to increase the expression of hexokinase 1 (HK1) while suppressing the expression of HK2 in mouse melanoma cell line B16 (*Sheng et al.*, unpublished).

The breadth of LSD1's oncogenic mechanisms, combined with its frequent dysregulation across cancer types, makes it a promising therapeutic target. In accordance with this, LSD1-targeted treatments have been developed, and many of them have entered clinical trials.

4.1.3 Hexokinase (HK)

Hexokinases catalyse the first step of glucose metabolism, converting glucose to glucose-6-phosphate (G6P), which serves as a metabolic intermediate for glycolysis to produce ATPs, for glycogen synthesis, and for pentose phosphate pathway (PPP) to produce nicotinamide adenine dinucleotide phosphate (NADPH) and ribose 5-phosphate (R5P), which are essential for nucleotide synthesis.

To date, five HK isoforms have been identified in mammals, namely HK1, HK2, hexokinase 3 (HK3), hexokinase 4 (HK4, also known as glucokinase, GCK), and hexokinase domain-containing 1 (HKDC1) [220,221]. Their characteristics and locations are shown in ***Table 4.1***. HK1 through HK3 and HKDC1 are ~100 kDa proteins believed to have evolved through gene duplication and fusion events from an ancestral 50 kDa hexokinase, while HK4 retains the smaller 50 kDa form.

Among these isozymes, HK1 and HK2 share 72% sequence identity, and both contain a hydrophobic domain that enables them to dock at the mitochondrial outer membrane. However, their expression patterns are distinct. HK1 is ubiquitously expressed across tissue types, whereas the expression of HK2 is highly regulated, with its expression limited to skeletal muscles and adipocytes. Notably, HK2 is frequently over-expressed in cancers, where it promotes tumour development through regulating metabolic pathways, such as the glycolytic pathway and fatty acid $\boldsymbol{\beta}$-oxidation pathway, or through non-metabolic mechanisms, such as stabilising CD133 to enhance cancer cell stemness [222–224].

The remaining isoforms display specialised regulatory features. HK3, which is expressed at low levels in immune cells and lung tissue, is inhibited by physiological concentrations of glucose. HK4 serves as a glucose sensor in the liver and pancreatic β-cells since it has a high Km for glucose and lacks the product inhibition by G6P. It actively converts glucose away when the blood glucose level is high to maintain homeostatic blood glucose. The recently discovered HKDC1 exhibits low enzymatic activity and remains poorly understood[225.]

This functional diversification of HK isoforms enables precise tissue-specific regulation of glucose metabolism, with HK1 maintaining basal metabolic needs, HK2 supporting high-energy demands in muscle and tumours, and HK4 maintaining systemic glucose homeostasis. The differential expression and regulation of these isoforms have

important implications for understanding both normal physiology and pathological conditions, such as cancer.

	HK1	HK2	HK3	HK4 (GCK)	HKDC1
Human gene locus	10q22	2p13	5q35.2	7p15.1–3	10q22.1
Molecular weight (kDa)	100	100	100	50	100
*K*m for glucose (mM)	0.03	0.3	0.003	6	-
G6P inhibition	Yes	Yes	Yes	No	No
Mitochondrial binding	Yes	Yes	No	No	Yes
Major tissue expression	ubiquitous	muscle, adipose	lung, spleen	liver, pancreas	ubiquitous

Table 4.1 Differences between five HK isoforms.
List of five HK isoforms in mammals and their human gene locus, molecular weight, enzymatic activity (measured as Km for glucose), product-induced inhibition, subcellular localisation, and primary tissue type for expression[226].

4.1.4 Aims

In this project, we aim to elucidate the functional consequences of HK isoform change upon LSD1 inhibition, building upon previous findings that LSD1 modulates HK1 and HK2 expression (*Sheng et al.*, unpublished). We would like to understand whether this HK isoform change leads to any of the LSD1 inhibition-induced phenotypes, including reduced cell proliferation, reduced colony formation, activation of anti-viral mimicry pathways and altered metabolism. We would also like to explore the potential for targeting both LSD1 and HK for treating cancer.

4.2 Results

4.2.1 LSD1 inhibition led to HK1 increase and HK2 decrease in B16 cells

Consistent with prior findings from Dr Wanqiang Sheng, we confirmed the significant alterations in HK isoform expression following LSD1 KO in B16 melanoma cell lines. RT-qPCR analysis revealed an increase in HK1 mRNA level by 88.03% accompanied by a decrease in HK2 mRNA level by 44.70% upon LSD1 KO (**Figure 4.1A**). Similarly, immunoblot analysis also showed the increase in HK1 expression and the reduction in HK2 expression in LSD1 KO B16 cells compared to scramble controls (**Figure 4.1B**).

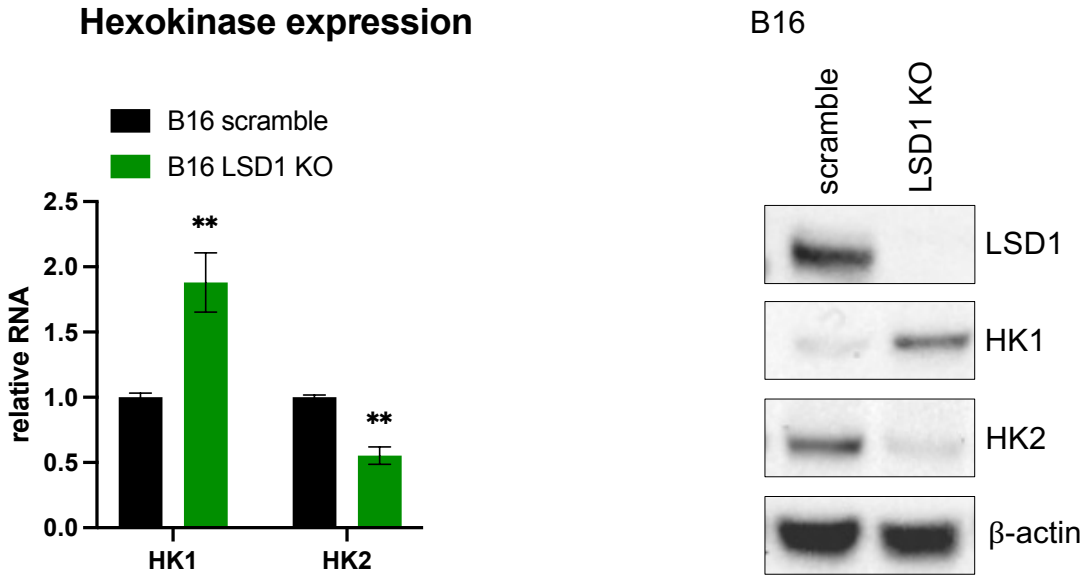

Figure 4.1 Changes in HK expression level upon LSD1 KO in B16.
(A) RT-qPCR and (B) immunoblot performed with RNA and protein extracts from B16 scramble cells or B16 LSD1 KO cells. Data presented as mean ± SD.

4.2.2 HK1 inhibition or HK2 OE in B16 LSD1 KO cells

To dissect the functional consequences of LSD1-mediated HK isoform change, we employed genetic approaches to alter HK isoform expression in B16 cells. Using the CRISPR/Cas9 system[137], we generated an HK1 KO derivative of both B16 scramble and B16 LSD1 KO cell lines. This allows us to differentiate between the effects of HK1 increase and those specific to LSD1 inhibition (**Figure 4.2A**). Single-cell clones of B16

scramble, B16 LSD1 KO, B16 HK1 KO and B16 LSD1 KO with HK1 KO were isolated and validated by immunoblotting to confirm the expected protein expression patterns (**Figure 4.2B**).

To address the functional impact of reduced HK2 expression, we over-expressed HK2 in these cell lines with an OE vector containing mouse HK2 transcript under a CMV promoter. We also transduced cells with an OE vector containing green fluorescent protein (GFP) as controls. Immunoblot analysis verified the successful HK2 OE in treated cells compared to controls (**Figure 4.2C**). These cell lines allow us to further analyse the effect of HK1 upregulation and HK2 downregulation in B16 cells.

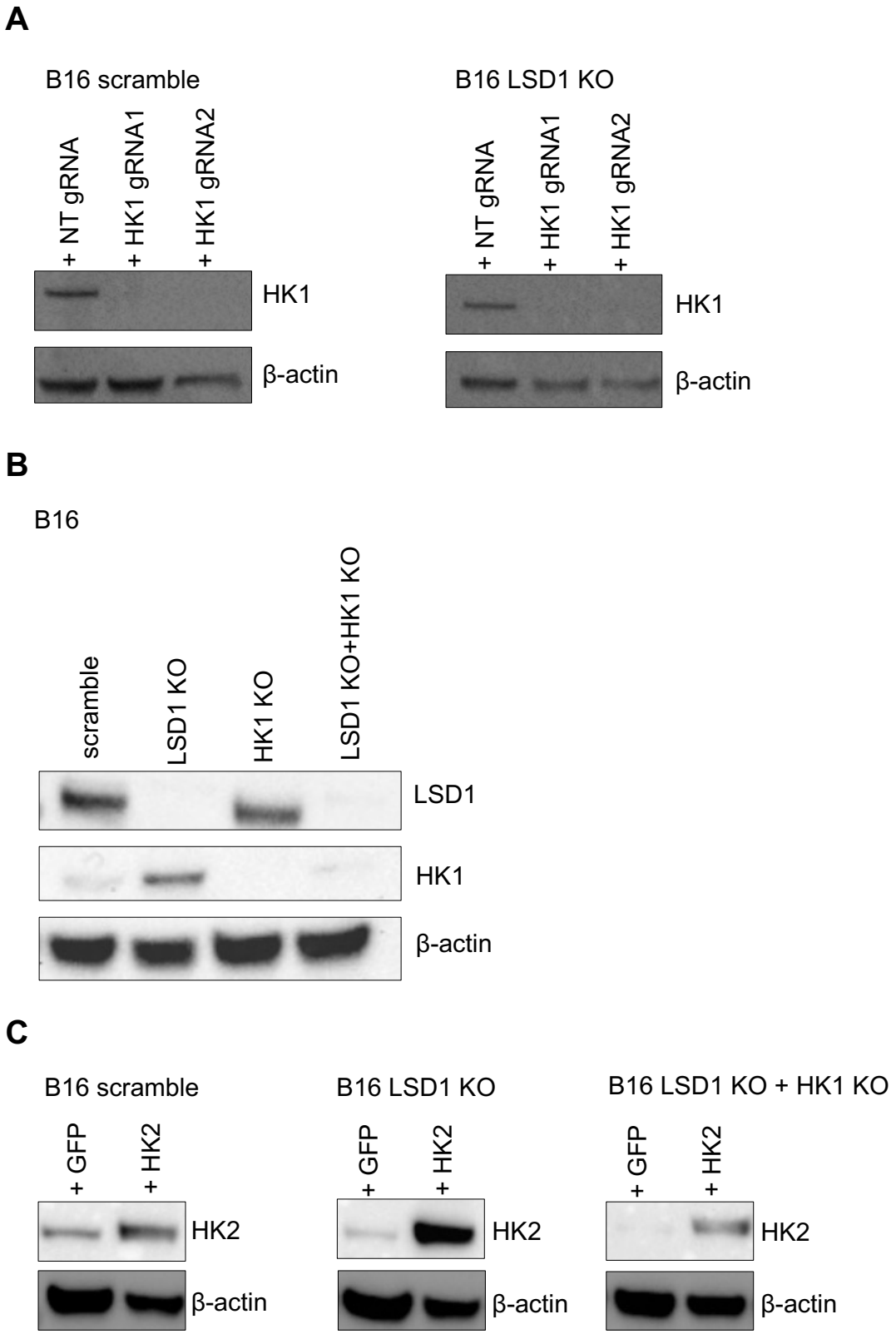

Figure 4.2 HK1 and HK2 expression could be manipulated in B16.
Immunoblot performed using protein extracts from (A) B16 scramble or B16 LSD1 KO cells treated with NT gRNA or HK1 gRNAs, (B) single cell clones with manipulated LSD1 and HK1 expression, and (C) B16 scramble cells, B16 LSD1 KO cells or B16 LSD1 KO with HK1 KO cells infected with lentivirus to over-express GFP or HK2.

4.2.3 HK2 OE in B16 LSD1 KO cells partially restored the growth inhibition

We analysed the phenotype of these engineered cell lines. Consistent with previous studies[219], LSD1 inhibition significantly reduced B16 cell proliferation as quantified by Cell-Titer Glo proliferation assays. This growth suppression was partially restored by HK2 OE, while altering HK1 expression failed to rescue the growth defects (**Figure 4.3A-B**). Similarly, the LSD1-induced reduction in colony formation capability, as demonstrated by crystal violet staining, was partially ameliorated by HK2 OE but was not affected by HK1 reduction (**Figure 4.3C-D**).

The consistent differential effects observed across both proliferation and colony formation suggest that HK2 downregulation, rather than HK1 upregulation, serves as the primary mediator of LSD1 knockout-induced growth inhibition in B16.

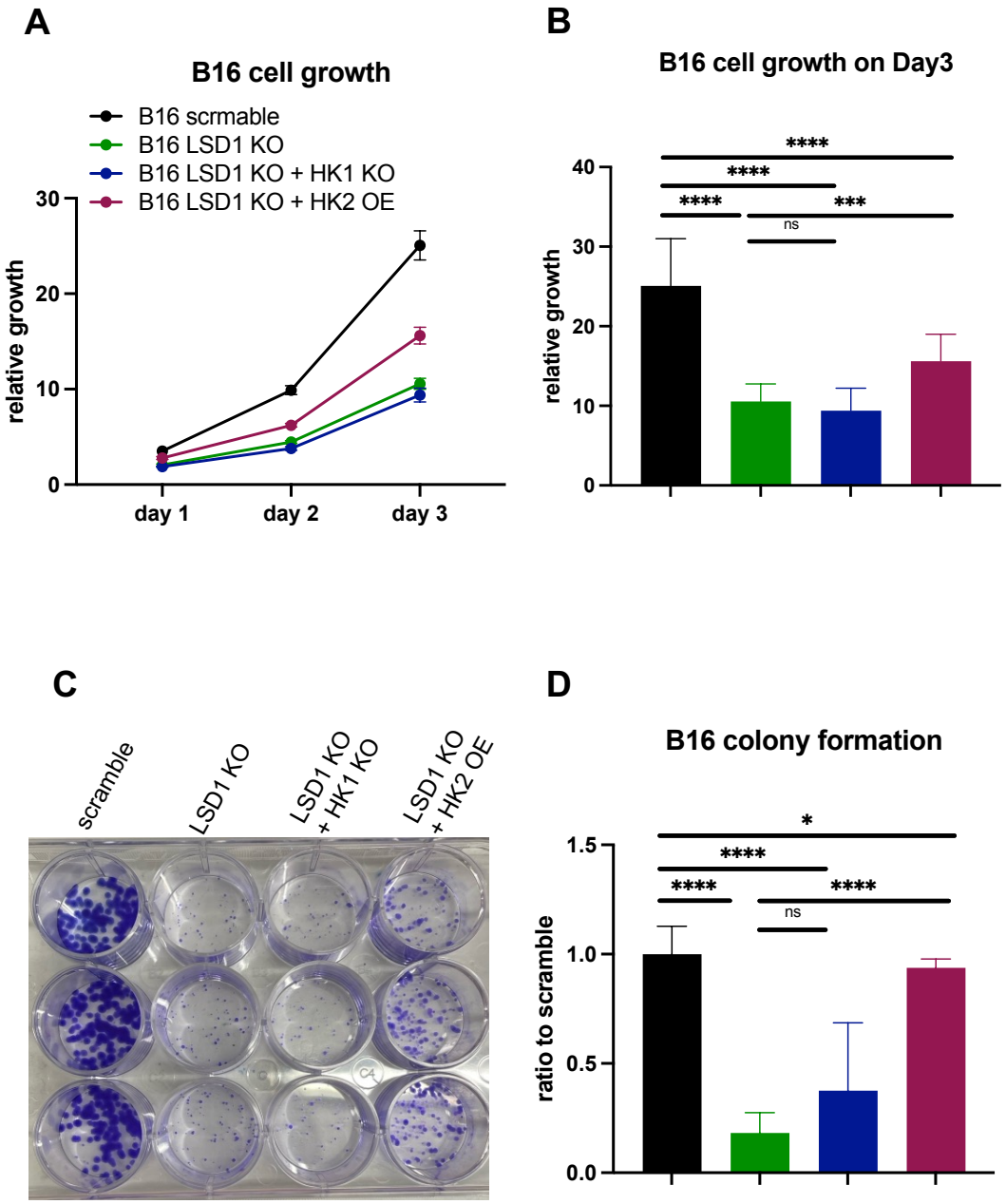

Figure 4.3 B16 cell growth after gene expression manipulation.

Cell growth, as measured by the Cell-Titer Glo proliferation assay, of B16 scramble, B16 LSD1 KO, B16 LSD1 KO with HK1 KO or B16 LSD1 KO with HK2 OE at (A) three time points (24, 48, and 72 hours) or (B) Day 3. (C) Colony formation capability, as measured by Crystal Violet staining, of B16 scramble, B16 LSD1 KO, B16 LSD1 KO with HK1 KO, or B16 LSD1 KO with HK2 OE after 10 days. (D) Quantification of Crystal Violet staining by measuring absorbance at 570 nm. Data presented as mean ± SD.

4.2.4 HK2 OE in B16 LSD1 KO cells partially restored the metabolic shift

Consistent with established links between LSD1 and cancer cell metabolism[217,218], our metabolic analysis also revealed significant alterations in the energy production pathways upon LSD1 KO in B16 cells.

We found that extracellular acidification rate (ECAR), a measurement of cellular glycolysis, was reduced upon LSD1 KO in B16 cells. This reduction was partially restored by HK2 OE, while HK1 reduction caused no significant effect (**Figure 4.4A**), mirroring our observations of the proliferation phenotype.

As cells tend to switch to produce ATP via OXPHOS when the glycolysis pathway is downregulated, we also analysed the oxygen consumption rate (OCR), a measurement of OXPHOS, in B16 cells. Seahorse analysis revealed a modest, though not statistically significant, upward trend in OCR following LSD1 KO (**Figure 4.4B**). This observation suggests that B16 cells may attempt to compensate for the diminished glycolysis by increasing mitochondrial ATP production via OXPHOS but fail to fully offset the metabolic disruption caused by LSD1 loss.

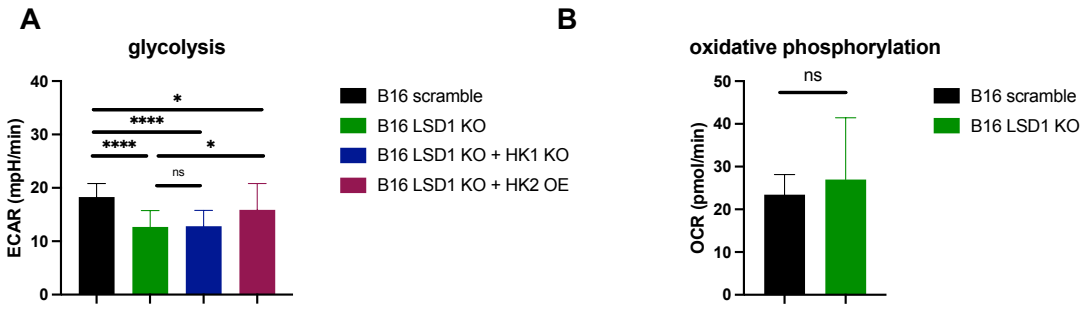

Figure 4.4 Altered metabolic pathways in B16 upon LSD1 KO.
(A) ECAR and (B) OCR, as measured by the Seahorse XF Mito-stress Test, in B16 cells before and after gene expression manipulation. Data presented as mean ± SD. Abbreviations: ECAR, extracellular acidification rate; OCR, oxygen consumption rate.

4.2.5 LSD1 KO and HK1 KO could not be achieved simultaneously

We experienced unexpected technical challenges when attempting to generate B16 clones with concurrent KO of both LSD1 and HK1. Using CRISPR/Cas9 editing, we first established single-cell LSD1 KO clones with LSD1 gRNAs, then we treated the single-cell clones with HK1 gRNAs to further inhibit HK1 expression. Despite the successful generation of single-cell clones, we were unable to obtain clones with complete ablation of both genes. Immunoblot analysis of putative double knockout (DKO) clones showed that they either maintained WT LSD1 levels with complete HK1 KO (clones 3,5,8,9, and 10) or retained residual HK1 expression with complete LSD1 KO (clone 12) (**Figure 4.5A**). We treated clone 12 (LSD1 KO + partial HK1 KO) with HK1 gRNA for a second time. Similarly, we failed to produce complete DKOs, with all three clones showing reduced but detectable HK1 expression alongside LSD1 KO (**Figure 4.5B**).

The consistent failure to obtain complete DKO clones, despite the demonstrated efficacy of LSD1 gRNA and HK1 gRNA in generating single KO clones (**Figure 4.6**), suggests the potential synthetic lethality between LSD1 and HK1 inhibition and implies that simultaneous inhibition of both proteins may be untenable for B16 cell survival. These findings provide compelling, yet indirect, evidence for synergistic essentiality between LSD1 and HK1 in B16 cells. The apparent synthetic lethality has important implications for therapeutic targeting, suggesting that combined inhibition of both pathways may offer potent anti-tumour effects.

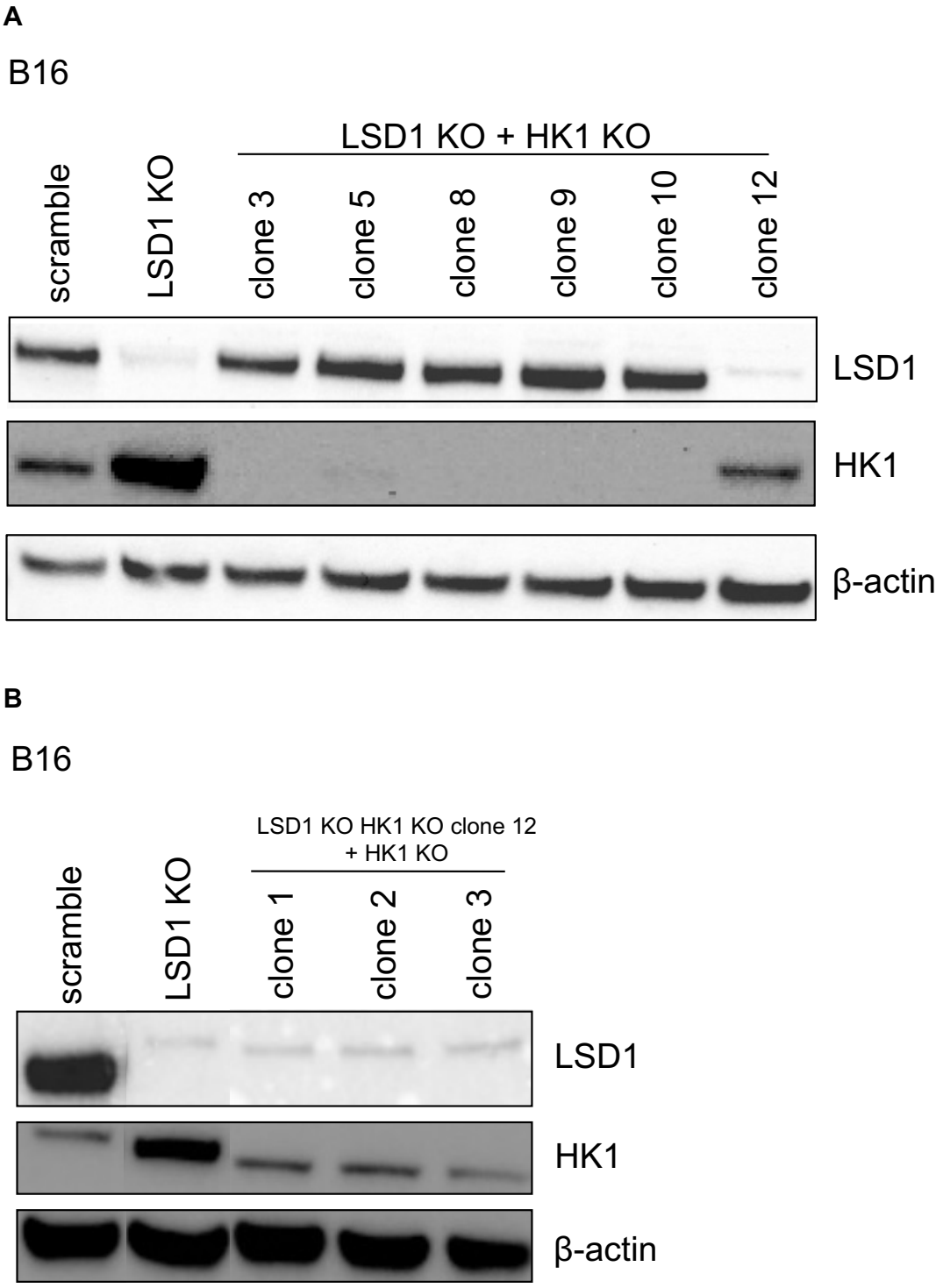

Figure 4.5 Protein expression in LSD1 and HK1 DKO single-cell clones.
Immunoblot performed with protein extracts from B16 scramble, B16 LSD1 KO and (A) B16 LSD1 KO + HK1 KO single-cell clones or (B) B16 LSD1 KO + HK1 KO clone 12 + HK1 KO single-cell clones.

4.2.6 LSD1-dependency did not correlate to HK1 expression in human liver cancer cells

As we were unable to generate B16 single-cell clones with complete KO of both LSD1 and HK1, we hypothesised a potential synthetic lethality of LSD1 and HK1. As not all cancer cell lines are dependent on LSD1[219,227], we further hypothesised that LSD1-dependency may inversely correlate with basal HK1 expression, where cells with lower endogenous HK1 would demonstrate greater dependence on LSD1.

To test this hypothesis, we identified four human liver cancer cell lines (HepG2, Hep3B, SNU398, and SNU475) with similar levels of HK2 and HK4 (GCK) expression but varying HK1 expression (**Table 4.2**) according to DepMap Expression Public 24Q4 data. Immunoblot analysis confirmed this differential HK1 expression pattern, with HepG2 and Hep3B having the lowest endogenous HK1 expression, followed by intermediate expression in SNU398 and highest expression in SNU475 (**Figure 4.6A**).

We performed LSD1 KD experiments in these cell lines. Immunoblot analysis confirmed successful LSD1 reduction in all cell lines treated with LSD1 shRNA compared to NT controls (**Figure 4.6A**). LSD1 KD reduced cell proliferation in HepG2 and Hep3B, two cell lines with low HK1 expression, by 36.82% and 9.85%, respectively. However, a significant reduction of cell proliferation by 23.22% was also observed in SNU475, a cell line with high HK1 expression, after LSD1 KD. While SNU398, with intermediate HK1 expression, showed no significant growth defects upon LSD1 KD (**Figure 4.6B**). These results demonstrate that LSD1 dependence in liver cancer cells does not inversely correlate with basal HK1 expression, as both HK1-high and HK1-low cell lines can be dependent on LSD1 KD, and HK1-low cell lines do not necessarily have LSD1-dependency.

Cell Line Name	log2(TPM+1)		
	HK1	HK2	HK4 (GCK)
HepG2	0.33	5.30	0.00
Hep3B	0.23	6.46	0.03
SNU398	5.41	4.71	0.00
SNU475	6.82	3.99	0.25

Table 4.2 Expression of HK isoforms in four liver cancer cell lines.
List of four liver cancer cell lines, HepG2, Hep3B, SNU398 and SNU475, and their relative expression of HK1, HK2 and GCK. Data from DepMap Expression Public 24Q4 data. HK1, hexokinase 1; HK2, hexokinase 2; HK4, hexokinase 4; GCK, glucokinase.

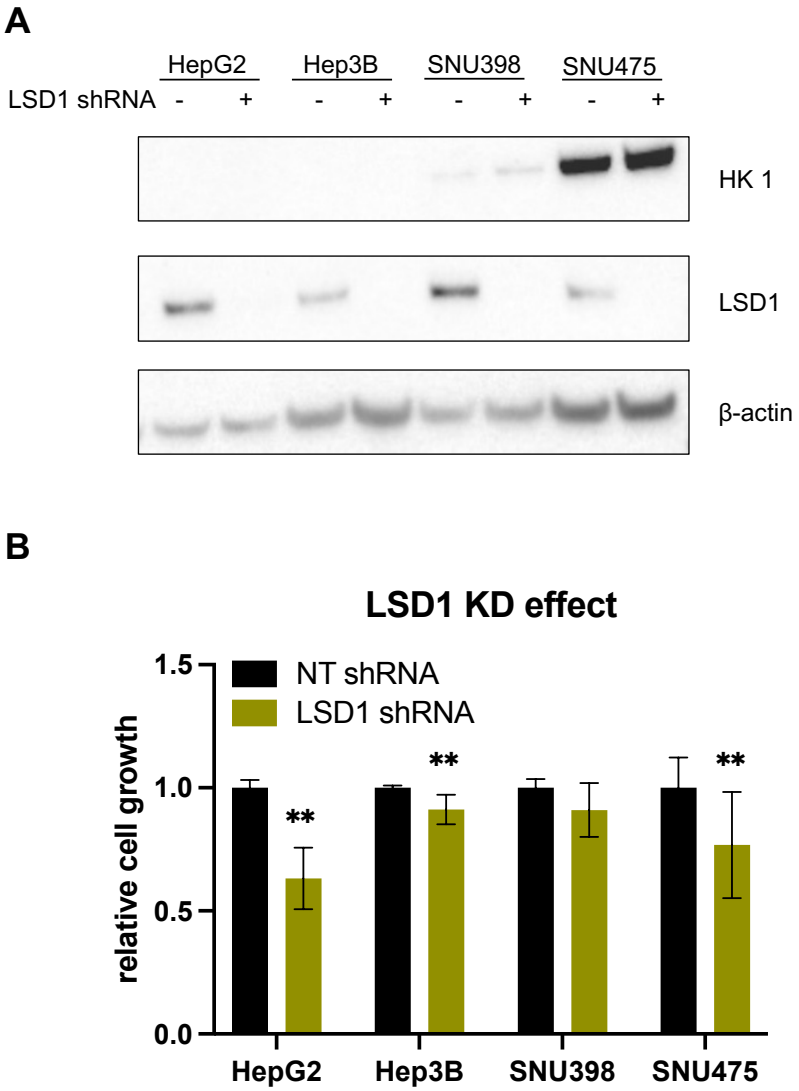

Figure 4.6 Effects of LSD1 KD in liver cancer cell lines.
(A) Immunoblot performed with protein extracts from HepG2, Hep3B, SNU398 and SNU475 cells treated with NT shRNA or LSD1 shRNA. (B) Cell proliferation, measured by the Cell-Titer Glo proliferation assay, of HepG2, Hep3B, SNU398 and SNU475 cells treated with NT shRNA or LSD1 shRNA. Data presented as mean ± SD.

4.2.7 LSD1-dependency did not correlate with changes in HK isoforms in murine cancer cell lines

LSD1 inhibition-induced reduction in proliferation is not generalisable to all murine cell lines, with some cancer cell lines resistant to LSD1 inhibition. For example, MC38, a murine colon cancer cell line, does not show cell growth defects after LSD1 inhibition[227]. Similarly, we found that LSD1 inhibition-induced HK isoforms changes also showed heterogeneity across different murine cancer cell lines. To investigate whether the HK isoform change could be a determining factor for LSD1-dependency in murine cancer cell lines, we investigated the HK isoform change upon LSD1 inhibition in another two LSD1-dependent cell lines, D4M melanoma cell line and LLC lung cancer cell line, and one LSD1-resistant cell line, MC38.

While B16 cells exhibit the characteristic pattern of HK1 upregulation and HK2 downregulation following LSD1 reduction, other LSD1-dependent cell lines display divergent responses. In D4M cells, LSD1 reduction increased HK1 and decreased HK2 expression, mirroring the B16 phenotype. Conversely, LSD1-dependent LLC showed an inverse response, with reduced HK1 and increased HK2 expression upon LSD1 knockout. And in LSD1-resistant MC38 cells, HK1 expression was upregulated without changes in HK2 (**Figure 4.7A-B**).

Collectively, these findings demonstrate that HK isoform change does not reliably predict or determine LSD1-dependency in murine cancer cell lines. The observed variability suggests that the metabolic consequences of LSD1 inhibition are highly context-dependent and are probably influenced by tissue-specific regulatory networks.

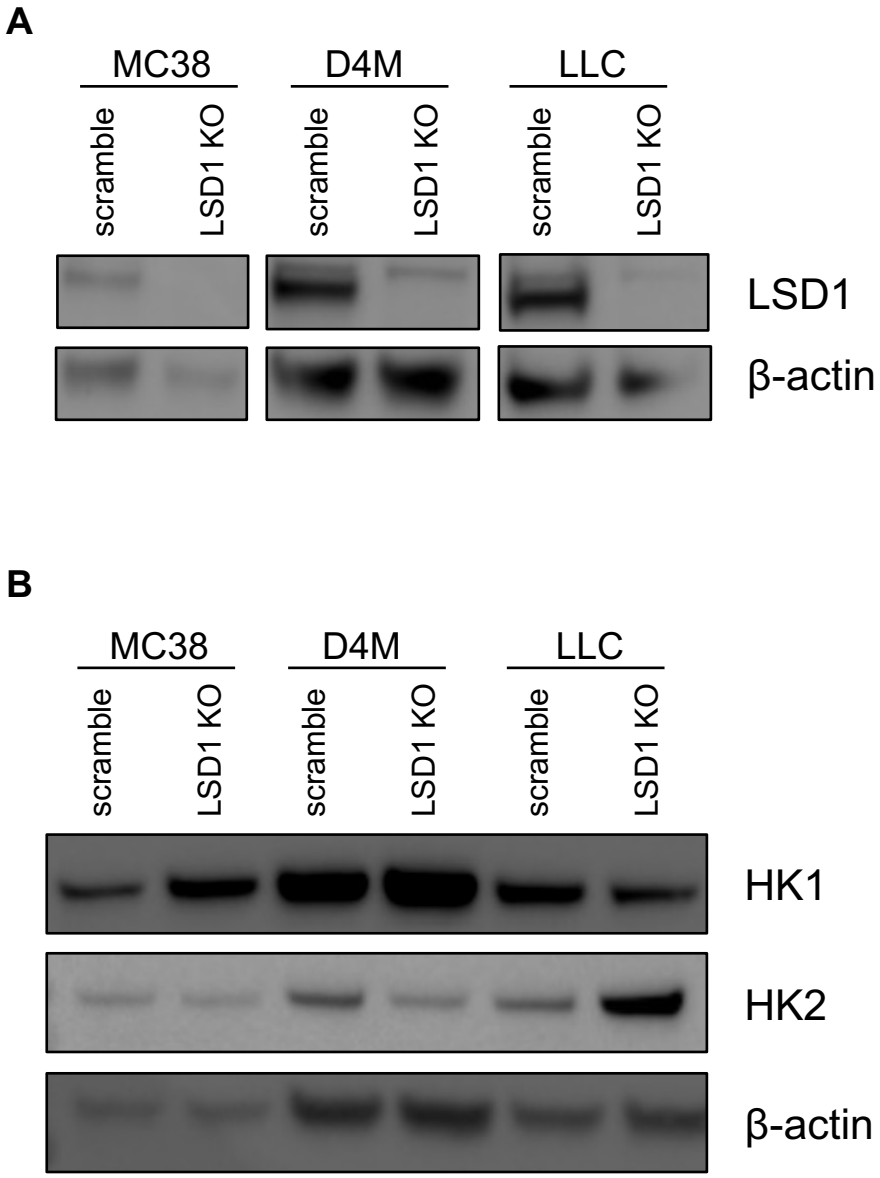

Figure 4.7 Changes in HK isoforms in murine cancer cell lines.

(A-B) Immunoblot performed with extracts from MC38, D4M and LLC cell lines treated with NT gRNA or LSD1 gRNA.

4.3 Discussion

4.3.1 Summary of results

In this project, we showed that LSD1 inhibition in B16 cells induced a characteristic HK isoform change, marked by increased HK1 expression and reduced HK2 expression. Through genetic manipulation, we demonstrated that HK2 OE could partially reverse the LSD1 inhibition-induced phenotypes, including reduced cell proliferation, reduced colony formation and altered metabolism. Our inability to generate single-cell clones with complete KO of LSD1 and HK1 simultaneously raises the potential synthetic lethality between these two proteins and suggests that they may function in complementary survival pathways, though this requires further validation. However, in contrast to our initial hypothesis, LSD1-dependency did not correlate with basal HK1 expression levels across cancer cell lines, indicating that the relationship between LSD1 and HK1 is more complicated.

Further studies are required to explore other phenotypic consequences of LSD1 inhibition and to elucidate the molecular basis of the apparent synthetic lethality between LSD1 and HK1.

4.3.2 Limitations of experiments and prospects

While our experiments demonstrated that HK1 reduction in B16 LSD1 KO cells failed to rescue any of the LSD1 inhibition-induced phenotypic changes, we cannot exclude a functional contribution of HK1 upregulation to LSD1 inhibition due to our inability to achieve complete HK1 KO in LSD1 KO cells. To fully elucidate HK1's role, the effect of HK1 OE in B16 WT cells needs to be studied. In addition, a conditional KD system to transiently inhibit HK1 expression in LSD1 KO cells may be developed to assess HK1-specific effects. These approaches would help determine whether the LSD1-mediated

HK1 upregulation represents an adaptive response, a bystander effect, or an active component of the observed phenotypic changes.

While we characterised the effect of HK isoform change on cell proliferation and metabolic reprogramming, several other aspects of LSD1 inhibition-induced phenotypic changes remain unexplored. Notably, we did not examine whether HK isoform change regulates anti-viral pathway or EMT processes, both of which have been implicated in cancer cells following LSD1 inhibition. Further experiments are required to fully understand the functional consequences of HK isoform change in LSD1-inhibited cells.

Our preliminary analysis of four human liver cancer cell lines with varying HK1 expression only provided initial insights into the link between LSD1-dependency and HK1 expression. To rigorously evaluate HK1 expression as a potential predictive marker for LSD1-dependency, we need to study a broader panel of cell lines representing cancer cells from diverse origins. These results will inform whether HK1 expression could reliably correlate with therapeutic sensitivity to LSD1 inhibition.

4.3.3 Development of LSD1 inhibitors for clinical use.

To date, ten LSD1 inhibitors, including tranylcypromine, ORY-1001, IMG-7289, GSK2879552, CC-90011, SP-2577, ORY-2001, INCB059872, Phenelzine and JBI-802, have entered clinical trials for evaluating their safety and clinical efficacy in cancers, such as AML, SCLC, and Ewing sarcoma, as well as other diseases, such as neurodegenerative and psychiatric conditions (**Table 4.3**).

Despite promising preclinical data, no LSD1 inhibitor has received regulatory approval for clinical use. The clinical translation of LSD1 inhibitors faces two major challenges: patient stratification and therapeutic efficacy optimisation.

Firstly, the absence of reliable predictive biomarkers hinders the identification of patients likely to respond to LSD1 inhibition. Our preliminary investigation suggested HK1 expression as a potential candidate biomarker. Further validation across larger patient cohorts and diverse cancer types is necessary to establish its clinical use.

In addition, monotherapy with LSD1 inhibitors may be insufficient, and combination strategies might be considered. For example, as LSD1 inhibition increases the expression of TGFb, which in later stages facilitates EMT, stimulates angiogenesis, and reduces the cytotoxicity of infiltrated $CD8^+$ T cells in the TME[228], the combined inhibition of LSD1 and TGFb has been explored. This approach overcomes the immunosuppressive effects of TGFb upregulation following LSD1 inhibition and enhances anti-PD1 efficacy in clinical trials[229]. Our findings suggest that simultaneous targeting of LSD1 and HK1 represents another compelling combination. However, the current lack of selective HK1 inhibitors makes it challenging to achieve this combined strategy and necessitates alternative techniques, such as HK1 KD with shRNA or RNA interference.

Inhibitor	Indication	Phases	Clinical trial	Status	Year
Tranylcypromine (TCP, Parnate)	Non-M3 acute myeloid leukemia (AML)	I/II	NCT02717884	Unknown	2016
	AML/ myelodysplastic syndromes (MDS)	I	NCT02273102	Completed	2014
	AML	I/II	NCT02261779	Unknown	2014
Iadademstat (ORY-1001, RG6016, RO7051790)	Small cell lung cancer (SCLC)	I	NCT02913443	Completed	2016
Bomedemstat (IMG-7289)	AML	I/II	NCT02842827	Completed	2016
	Myelofibrosis	I	NCT03136185	Completed	2017
	Essential thrombocythemia	II	NCT04081220	Active	2020
GSK2879552	AML	I	NCT02177812	Terminated	2014
	Relapsed/ refractory SCLC	I	NCT02034123	Terminated	2014
	High risk MDS	II	NCT02929498	Terminated	2016
Pulrodemstat (CC-90011)	Relapsed/refractory solid tumors and Non-Hodgkin lymphomas	I	NCT02875223	Terminated	2016
	SCLC	I/II	NCT03850067	Completed	2019
	Advanced tumours	II	NCT04350463	Completed	2020
Seclidemstat (SP-2577)	Ewing sarcoma	I	NCT03600649	Active	2018
	Solid tumour	I	NCT03895684	Completed	2019
Vafidemstat (ORY-2001)	Mild to moderate Alzheimer's disease	II	NCT03867253	Completed	2019
INCB059872	Advanced malignancies	I/II	NCT02712905	Terminated	2016
	Sickle-cell disease	I	NCT03132324	Terminated	2017
	Relapsed Ewing sarcoma	I	NCT03514407	Terminated	2018
	Solid tumour	I/II	NCT02959437	Terminated	2016
	MDS/myeloproliferative neoplasms (MPN)	I/II	NCT04061421	Active	2019
Phenelzine (Nardil)	Prostate cancer	II	NCT02217709	Completed	2014
	Breast cancer	I	NCT03505528	Completed	2017
JBI-802	Solid tumour	II	NCT05268666	Active	2022

Table 4.3 List of LSD1 inhibitors in clinical trials.
List of clinical trials for testing the safety and efficacy of LSD1 inhibitors, with the name of the inhibitor used, indications, clinical phases, status, and time of last update.

Chapter 5: Discussion

In Chapter 5, I will start by summarising the key findings from Chapter 2-4. I will then discuss the clinical implications of our findings and the limitations of our studies. I will end this chapter by stating future directions focusing on the interplays between epigenetic regulations, metabolic reprogramming, and anti-tumour immune response.

5.1 Summary of key findings

5.1.1 Chapter 2: identification of genetic target in NSCLC cells

Through systematic analysis of DepMap fitness screen data, we identified UXS1 as a selectively essential gene in cancer cells with high UGDH expression. Using CRISPR/Cas9-mediated KO and shRNA KD techniques, we validated this predicted association between UXS1-dependency and UGDH expression in human NSCLC cell lines. Mechanistic studies revealed the requirement of catalytically active and cytoplasm-localised UGDH for UXS1-dependency since ED UGDH or nucleus-localised UGDH failed to restore the UXS1-dependency in UGDH KO cells. We also demonstrated that UXS1 loss leads to a toxic accumulation of UGDH's product, UDP-GlcUA, which explains the selective essentiality of UXS1 in UGDH-high cells.

The translational potential of these findings is supported by TCGA data, showing higher UGDH expression in lung cancer cells compared to adjacent normal cells. This tumour-selective expression pattern positions UXS1 as a promising therapeutic target and suggests that UXS1 inhibition could selectively kill UGDH-high cancer cells while sparing adjacent healthy tissues.

5.1.2 Chapter 3: identification of epigenetic target in $CD8^+$ T cells

Using a drug screening approach, we identified MS023, a pan-type I PRMT inhibitor targeting PRMT1, 3, 4, 6 and 8, as a candidate for enhancing the activation and effector function of primary $CD8^+$ T cells. We demonstrated that MS023 increased CXCR3 expression, effector molecule production and *in vitro* tumour-killing capacity. Similar phenotypic changes were observed using another pan-type I PRMT inhibitor or a combination of multiple single-target PRMT inhibitors, further confirming the regulatory role of type I PRMT in $CD8^+$ T cell activation and function. We also provided some mechanistic insights, showing PRMT4 as the critical isoform among MS023 targets and demonstrating that CXCR3 upregulation is non-essential for the observed functional enhancement. These findings have important translational implications for improving adoptive cell therapies, allowing the immune cells to survive in the immunosuppressive TME.

5.1.3 Chapter 4: mechanistic insights of known targets

We explored a new aspect of the oncogenic function of LSD1, a known cancer therapeutic target, in B16 cells. In addition to its well-characterised roles in p53 modulation, EMT regulation, metabolic reprogramming, and immune evasion, we observed a HK isoform change with HK1 upregulation and HK2 downregulation upon LSD1 inhibition. Through gene-editing experiments, we demonstrated that the observed HK2 reduction partially contributed to both the anti-proliferative effect and metabolic alterations caused by LSD1 inhibition.

A surprising finding was the inability to generate single-cell clones with both LSD1 and HK1 completely KO, despite the successful individual gene ablations. This finding suggests a potential synthetic lethality between LSD1 and HK1 and supports the concurrent pharmacological targeting of both LSD1 and HK1.

5.2 Implications in cancer therapy

5.2.1 Translational Potential

In Chapter 2, we found that inhibition of UXS1 selectively impairs proliferation in UGDH-high cancer cells *in vitro*. And *Doshi et al.* further confirmed the growth defects upon UXS1 reduction using a doxycycline-induced inducible KO system *in vivo*[230]. Analysis of TCGA data revealed that UGDH is consistently over-expressed in lung cancer cells compared to adjacent normal tissues. Collectively, these findings support UXS1 as a promising therapeutic target for UGDH-high cancers. And future development of UXS1 inhibitors could provide a targeted therapeutic strategy for patients exhibiting elevated UGDH expression.

One thing to be considered would be the design of the inhibitor. The intracellular localisation of UXS1 within the Golgi apparatus and ER presents pharmacological challenges, and antibody-based approaches are unlikely to be effective. Thus, a cell-permeable small-molecule inhibitor might be needed. While the crystal structure of human UXS1 has been resolved by *Eixelsberger et al*., revealing a potential druggable pocket at the GDP-mannose 4,6 dehydratase domain as predicted by the Cancer Drug Discovery Platform (canSAR.ai)[231,232], no selective small-molecule inhibitor has been developed. An alternative strategy involves the use of proteolysis-targeting chimaera (PROTAC), which offers advantages by requiring only the target binding but not the enzymatic inhibition. In this case, the bifunctional PROTAC molecule will consist of one UXS1-binding ligand and a recruiter for E3 ubiquitin ligase to induce the degradation of the targeted protein[232].

We also need to address several safety concerns of UXS1 inhibition. Given that UXS1 KO resulted in embryonic lethality in mice[233], the potential side effects associated with the pharmacological inhibition of UXS1 must be carefully evaluated. In addition, UGDH is expressed at relatively high levels in the liver and intestines[234], leading to potential

on-target effects in these healthy tissues. To minimise toxicity risks while maintaining therapeutic efficacy, we propose the use of ADCs, utilising tissue-specific surface markers to deliver UXS1 inhibitors selectively to the tumours while sparing UGDH-high healthy tissues, and the use of tissue-specific PROTACs, utilising a ligand for a tissue-specific E3 ligase to confine UXS1 degradation to the targeted tissues.

In Chapter 3, we found that pharmacological inhibition of type I PRMTs enhanced $CD8^+$ T cell activation and effector function *in vitro*, suggesting the potential applications of PRMT inhibition in adoptive cell therapy. However, knowledge gaps remain regarding the persistence of these effects and the generalisability of the observed phenotypes in *in vivo* systems. Comprehensive *in vivo* studies are needed to evaluate whether PRMT inhibition can sustain T cell anti-tumour activity over extended durations in TME.

Beyond the applications in adoptive cell transfer therapies, systemic PRMT inhibition can also be considered. Higher PRMT expression has been observed in multiple cancer types, including AML, liver cancer, pancreatic cancer, colorectal cancers[235–237], and it is associated with poor prognosis. Mechanistic studies reveal that PRMT inhibition exerts its anti-tumour effects through various pathways. For example, PRMT1 inhibition induces DNA damage via R-loop accumulation in clear cell renal cancer[238]; PRMT3 inhibition increases the expression of methyltransferase 14 (METTL14), leading to GPX4 downregulation which induces ferroptosis in endometrial carcinoma [239]; PRMT3 inhibition also reduces HIF-1a expression, thus reducing glioblastoma cell growth[240]; and pan-type I PRMT inhibition reduced tumour growth through either dysregulated DNA repair pathways [241] or altered RNA splicing pathways [242]. Preclinical studies with pan-type I PRMT inhibitor, MS023 or GSK3368715, have demonstrated improved tumour control and survival in various models, including cancer cell lines, patient-derived xenograft models, and mouse models[240,242,243]. Collectively, these results suggest the potential beneficial effect of systemic PRMT inhibition to treat cancer. Future research should focus on optimising inhibitor

specificity to maximise the therapeutic effect while minimising potential toxicity to normal tissues.

5.2.2 Personalised Medicine

The advancement in NGS techniques has enabled robust molecular profiling to identify predictive and prognostic markers. It is necessary to distinguish which patient groups will benefit from the therapy.

Our findings support a biomarker-driven strategy for UXS1 inhibition, with UGDH expression serving as the predictive marker. This approach is based on three observations: 1) UXS1-dependency is correlated with high UGDH expression, 2) high UGDH expression is associated with poor clinical outcomes, and 3) differential UGDH expression patterns exist between tumours and adjacent normal tissue in some cancer types. Analysis of TCGA data identifies five candidate indications where this therapeutic strategy can be particularly effective, including breast cancer, glioblastoma, lung cancer, uterine cancer, and prostate cancer, as in these cancer types, tumour cells show elevated UGDH expression compared to adjacent normal tissues (**Figure 2.9**).

However, cancer heterogeneity might limit the reliability of the biomarker, as UGDH expression could vary between subclones, creating potential reservoirs of drug-resistant cells. In addition, a mutation detected at the genetic level does not necessarily indicate altered protein expression. Thus, further proteomic data might be required. And the use of patient-derived organoids (PDOs) offers another possible solution to these challenges. Cancer cells can be obtained from patients and maintained in the lab for testing drug efficacy[244]. This approach complements genomic profiling by providing functional validation of drug sensitivity in a patient-specific context.

5.3 Limitations of the current work

The work presented in this thesis is constrained by the reliance on *in vitro* cancer cell lines and *ex vivo* primary mouse cells, which could not fully recapitulate the complex human physiology. Thus, the findings require further validation in appropriate *in vivo* settings before translational studies to explore the clinical implications. In addition, our findings are limited to specific cancer types. For example, we only established UXS1-dependency in NSCLC cells without considering its generalisability across other UGDH-high cancers. Future studies should address these gaps.

Another limitation is the partial mechanistic insights. For example, while we established the toxic accumulation of UDP-GlcUA as the cause of UXS1-dependency in UGDH-high cancer cells, the downstream consequences of this metabolite accumulation remain incompletely understood. *Doshi et al*. demonstrated that UDP-GlcUA accumulation altered Golgi structure and function, thus affecting membrane protein production and trafficking[230]. However, the precise molecular mechanism linking the metabolite build-up and Golgi dysfunction is unclear and requires further exploration. Similarly, while we established that PRMT inhibition increased the effector function of $CD8^+$ T cells, the underlying pathways remain unclear. Furthermore, we did not examine the effects of PRMT inhibition on other immune cells in the TME, such as $CD4^+$ T cells. Determining whether PRMT inhibition can broadly enhance anti-tumour immunity across different immune cell populations would further support the systemic administration of PRMT inhibitors.

5.4 Future directions

In addition to further mechanistic studies, we would like to conduct preclinical and clinical evaluations to translate our scientific findings presented in this thesis into novel cancer therapies.

One last thing to consider is the interplay between three fundamental cancer hallmarks: metabolic reprogramming, epigenetic regulations, and immune surveillance. Our results suggest these systems are deeply interconnected.

The interconnection between metabolic rewiring and epigenetic remodelling operates through reciprocal mechanisms. Epigenetic regulators could control the expression of metabolic enzymes through DNA or histone modifications. In addition, some metabolic enzymes may even serve as the substrates for epigenetic regulators, with their activities regulated directly through epigenetic modifications. Conversely, metabolic shifts actively shape the epigenetic landscape by altering the availability of metabolites that are substrates or co-activators of epigenetic regulators. For example, acetyl-CoA, an intermediate metabolite in glycolysis and FA oxidation for energy production, is also the substrate of histone acetyl transferase (HATs). HATs add the acetyl groups to the histone tails to loosen chromatin structure and promote gene transcription[245]. This interaction between metabolic and epigenetic pathways creates a dynamic regulatory network where changes in one system propagate to the other, enabling cells to rapidly adapt their gene expression profiles to fluctuating nutrient availability and metabolic demands.

Epigenetic remodelling also alters immune response, as we have demonstrated in our findings, where PRMT inhibition changes effector T cell function. In fact, many immune-related genes are regulated by epigenetic regulation, and distinct epigenomic profiles at different activation states are observed in NK cells and T cells[246,247]. For example,

GSK-J4, an inhibitor for histone demethylase JMJD3, reduces the expression of pro-inflammatory cytokines by NK cells[248], while DNMT1 reduction impairs T cell differentiation [249], and the decrease in TET2 promotes the memory T cell phenotype[250].

Epigenetic regulation extends beyond immune cells to influence tumour immunity by modifying critical pathways in cancer cells. For example, a hypermethylation status usually reduces antigen processing and antigen presentation in cancer cells, helping them evade immune surveillance [251–253]. The methylation status within the cancer cells also alters the anti-viral mimicry pathway as demonstrated by *Sheng et al.*, where LSD1 inhibition increased histone methylation, leading to an increased dsRNA expression and inducing type I interferon response [219]. The acetylation status also regulates immunogenicity. For example, HDAC inhibition leads to hyperacetylation and upregulates genes involved in antigen processing and presentation[254]. The reduced efficacy of the HDAC inhibitor in immunocompromised mice suggests that the anti-tumour effect is at least partially via enhanced immune response[255]. Also, HDAC1 inhibition enhances MHC class I expression to increase cytolytic activity of $CD8^+$ T cells in mouse models[256], further supporting the regulatory role of acetylation pattern in immune response.

As interplays between epigenetic regulation and immune regulation have been observed, combining epigenetic regulators with immunotherapies shows promise. For example, HDAC inhibitors enhanced the response to anti-PD1 treatment in *in vivo* mouse xenograft model[257].

Lastly, cross-talks between immune pathways and metabolic pathways have also been reported. For example, T cells at different activation states have distinct metabolic profiles[258], and cancer cells compete with immune cells for essential nutrients in the TME, thus downregulating the anti-tumour immunity. Pharmacological restoration of nutrient availability has been shown to enhance T cell function[259], showing the

functional relevance of this metabolic competition. In addition, cancer cells release immunosuppressive metabolites to TME to downregulate anti-tumour immunity[260]. One example of such metabolites is lactate from the elevated aerobic glycolysis, which modulates the expression of autophagy factor FIP200 in T cells, inducing T cell apoptosis in both primary human cells and mouse models[261].

With the increased understanding of the interplay between metabolism and immunity, potential treatment targeting metabolic pathways and immune pathways could be tested to see whether there will be any synergic effect of targeting both pathways. These findings show the intricate interplay between metabolic and immune pathways and raise the potential benefit of targeting both metabolic and immune pathways simultaneously.

In conclusion, the interplay between these pathways creates both challenges and opportunities for developing novel therapies. Therapeutic targeting of one pathway may have unintended consequences on the others, but coordinated modulation could potentially yield synergistic benefits.

Chapter 6: Methods and Materials

6.1 Cancer cell line culture

B16, LLC, D4M, MC38, HepG2, Hep3B, HEK293T and A549 cells were cultured in DMEM medium (Gibco, 31966-021) containing 10% heat-inactivated foetal bovine serum (FBS) (Gibco, 10500-064) and 1% penicillin/streptomycin (Gibco, 15070-063) in a 5% CO_2 incubator at 37 °C. SNU398, SNU475, NCI-H23, NCI-H647 and LUDLU-1 cells were cultured in RPMI medium (Gibco, 21875-034) containing 10% heat-inactivated FBS and 1% penicillin/streptomycin in a 5% CO_2 incubator at 37 °C. NCI-H1666 cells were cultured in RPMI medium containing 5% heat-inactivated FBS and 1% penicillin/streptomycin in a 5% CO_2 incubator at 37 °C. Hep3B cell line was a gift from Dr Michael McClellan, and HepG2 cell line was a gift from Dr Elizabeth Slee. Both cell lines were originally purchased from ATCC. B16, LLC, D4M, HEK293T, A549, SNU398, SNU475, NCI-H23, NCI-H647 and NCI-H1666 cell lines were purchased from ATCC. LUDLU-1 cell line was purchased from ECACC.

6.2 Primary T cell culture

6.2.1 T cell extraction

Mice were culled with cervical dislocation and dissected to retrieve spleen and lymph node samples. Samples were placed on a 100 μm cell strainer over a 50 ml tube and mashed into single cells with the plunger end of a syringe, flushing with Dulbecco's phosphate buffered saline (PBS) (Gibco, 14190-094). Cell suspension was centrifuged at 1500 rpm for 5 minutes. For spleen samples, the cell pellet was lysed with 1-2 ml/spleen ACK lysis buffer (Gibco, A1049201) for 5 minutes at RT. Reaction was stopped with 10 – 20 ml PBS. Cell suspension was further cleaned up by passing through a 70 μm cell strainer over a 50 ml tube. Cell suspension was then centrifuged at 1500 rpm for 5 minutes, and the cell pellet was resuspended in recommended buffer (PBS with 2% FBS and 1 mM EDTA) or R10 medium (RPMI-1640 + 10% FBS) for

downstream use. For lymph node samples, the cell pellet was resuspended in PBS or recommend buffer for downstream use.

6.2.2 Negative selection of $CD8^+$ T cells

$CD8^+$ T cells from spleen and lymph node samples were enriched using EasySep Mouse $CD8^+$ T Cell Isolation Kit (Stemcell Technologies UK Ltd, 19853) according to the manufacturer's instructions. Briefly, cells were resuspended in recommend buffer at 10^8 cells/ml and incubated with 20 µl/ml EasySep™ FcR Mouse Blocker and 50 µl/ml EasySep™ Mouse $CD8^+$ T Cell Isolation Cocktail for 10 minutes at RT followed by incubation with 125 µl/ml EasySep™ Streptavidin RapidSpheres™ for 5 minutes at RT. The sample was then placed in EasySep™ Magnet for 3 minutes at RT. The enriched $CD8^+$ T cell suspension was poured into a new 50 ml tube for downstream use.

6.2.3 T cell activation and expansion

Primary $CD8^+$ T cells were cultured in RPMI-1640 containing 10% FBS, 1% Penicillin/Streptomycin, 1% L-Glutamine (Gibco, 25030024), 1M HEPES (Gibco, 15630080), 1% MEM non-essential amino acids (Gibco, 11640068), 100mM Sodium pyruvate (Gibco, 11360070) and 50uM 2-mercaptoethanol (Gibco, 31350010). Cells were seeded at 0.2 M cells/200 µl/well with the supplement of 2 ug/ml anti-CD28 (eBioscience, 16-0281-85) and 20 U/ml human-IL-2 (Peprotech, 200-02) on 96-well plate pre-coated with 5 ug/ml anti-CD3 (eBioscience, Cat# 16-0031-85) for activation. Cells were incubated at 37°C with 5% CO_2.

6.3 Gene editing

6.3.1 Cloning

For LSD1 shRNA knock-down plasmids:

pLKO.1-NT shRNA-puro plasmid and pLKO.1-LSD1 shRNA-puro plasmid were gifts from Dr Damayanti Chakraborty. Targeted sequences are listed in **Table 6.1**.

For UXS1 shRNA knock-down plasmids:

UXS1 shRNA oligos was annealed and cloned into a pLKO.1- Puromycin lentiviral vector (Addgene #10878, a gift from David Root). Targeted sequences are listed in **Table 6.1**.

shRNA sequences	
Target genes	Sequences
scramble	CCTAAGGTTAAGTCGCCCTCG
human *LSD1*	GCCTAGACATTAAACTGAATA
human *UXS1* (3' UTR)	GCTTGCTTTAATGAAATGGAT
human *UXS1* (CDS)	CCTCCAAACTACATGTATAAT

Table 6.1 List of shRNA sequences.

For Hk1 gRNA, UXS1 gRNA and UGDH gRNA knock-out plasmids:

The gRNA oligos, with sequences for their respective target genes listed in **Table 6.2**, were annealed, and cloned into lentiCRISPR v2 vector (Addgene #52961, #83480, a gift from Feng Zhang).

For Prmt1 gRNA, Prmt3 gRNA, Prmt4 gRNA, Prmt6 gRNA and Prmt8 gRNA knock-out plasmids:

The gRNA oligos, with sequences for their respective target genes listed in **Table 6.2**, were annealed, and cloned into pMSCV-U6sgRNA (BbsI)-PGKpuro2ABFP vector (Addgene #102796, a gift from Sarah Teichmann).

gRNA sequences	
Target genes	Sequences
mouse *Hk1* #1	CTCCCGGGATTATAACCCAA
mouse *Hk1* #2	CTACTGGTAAAGATCCGTAG
mouse *Hk1* #3	CCGACAATCCAAAATAGACG
human *UXS1* #1	GTAGGGCTGGCAAAACGAGT
human *UXS1* #2	GTCCGGATGCAGATAACAGG
human *UXS1* #3	GGATTATACATGTAGTTTGG
human *UGDH* #1	GCATTGTGCAAAACTCAAAT
human *UGDH* #2	GTGCTCATATACAGCACACA
mouse *Prmt1* #1	AAAGCCAACAAGTTAGACCA
mouse *Prmt1* #2	CCCCTCTTCTAGGTTTCCTG
mouse *Prmt3* #1	CCAGTCTGAAATCCTCTACC
mouse *Prmt3* #2	TCTGTGCGTACTTTGTCCTA
mouse *Prmt4* #1	GAGACAGAGTGCAGTCGTGT
mouse *Prmt4* #2	ATGCAGGACTATGTGCGGAC
mouse *Prmt6* #1	TTAGCGACCAGATGCTCGAG
mouse *Prmt6* #2	GGCAAGACGGTGCTGGACGT
mouse *Prmt8* #1	ACTTACCAACCACTTGTCCC
mouse *Prmt8* #2	ACATGGTGGACACATTGCAC

Table 6.2 List of gRNA sequences.

For Hk2 over-expression plasmids:

Expression vector with puromycin selection, pHAGE-CMV-Flag-HA-LSD1, was a gift from Dr Wanqiang Sheng. The vector was cut with restriction enzyme XbaI (NEB, R0145S) and SalI (NEB, R0138S). Mouse HK2 transcript sequence was amplified using PCR primer sequences listed in **Table 6.3** from cDNA library reverse transcribed from total RNA of B16. Mouse HK2 transcript sequence was cloned into pHAGE-CMV-FLAG-HA vector using T4 ligase (NEB, M0202L).

For UGDH, UXS1, EGFP over-expression plasmids:

UGDH gRNA-resistant transcript sequence was synthesised by Genscript. The UXS1 transcript sequence was amplified from cDNA library reversed-transcribed from total RNA of NCI-H23. The EGFP transcript sequence was synthesised by IDT. EGFP, UXS1, WT/enzyme-dead UGDH (C276G) with/without nuclear localisation sequence

were cloned into pCMV-neomycinR lentiviral vector (Addgene #92194, a gift from Huda Zoghbi) by using Gibson assembly kit (NEB #E5510S) and site-directed mutagenesis kit (NEB #E0554S).

Primers for generating FLAG-UXS1 expression construct	
Primer labels	Sequences
h-FLAG-UXS1-F	GAAGACACCGGCGGCCTAGCGCTGCCACCATGGACTACAAAGACCATGACGG
h-FLAG-UXS1-R	ATAGGGAGAGGATCAGTTATCTAGATTCAGCTGTGGCGAGTCCGTC

Primers for generating Hk2 expression construct	
Primer labels	Sequences
m-Hk2-F	GTCGAC CATGATCGCCTCGCATATGAT
m-Hk2-R	TCTAGACTATCTCTGCCCGGCCT

Table 6.3 List of oligos used for cloning.

6.3.2 Virus production

For lentivirus carrying over-expressed transcript, shRNA, or gRNA:

Lentivirus was produced by co-transfecting HEK293T cells with over-expression plasmids or pLKO.1 plasmid or lentiCRISPRv2 plasmid and two envelope plasmids, psPAX2 (Addgene, #12260) and pMD2.G-VSVG (Addgene, #12259). Both plasmids were gifts from Didier Trono. Viral supernatant was harvested after 48 hours and 72 hours by passing through a 0.45 mm filter. Collected lentivirus was used directly to infect cells or frozen at – 80°C for later use.

For retrovirus carrying gRNA:

Retrovirus carrying gRNA was produced by co-transfecting HEK293T cells with pMSCV-U6sgRNA (BbsI)-PGKpuro2ABFP plasmids and envelop plasmid, pCL-ECO (addgene,12371, a gift from Inder Verma). Viral supernatant was harvested after 48 hours and 72 hours by passing through a 0.45 mm filter. Collected retrovirus was used directly to infect cells or frozen at – 80°C for later use.

6.3.3 Viral infection and selection

For cancer cell lines:

Cells were seeded at 3.5 x 10^5 cells/well on the 6-well plate the day before viral infection. Cells were infected with 1 ml viral supernatant and 8 μg/ml polybrene (Merck Life Science, TR-1003-G). After 24-hour incubation at 37 C with 5% CO_2, 1 ml culture medium was added to the cell. After another 24-hour incubation, cells were selected with puromycin (Merck Life Science, P4512), blasticidin (Life Technologies, R21001) or G418 solution (Roche, 4727894001) for 5 days before being used for downstream analysis.

For primary T cells:

5 x 10^5 primary T cells were seeded in each well on the 12-well plate after 24-hour activation. 1 ml retroviral supernatant was added to each well with 10 μg/ml polybrene. The plate was centrifuged at 2000 rpm for 90 minutes at 30°C followed by incubation at 37°C with 5% CO_2 for 4 hours. 1 ml culture medium was added to each well. After 24-hour incubation, primary T cells were selected with 2 μg/ml puromycin for two days before being used for downstream analysis.

6.4 Cell proliferation assays

6.4.1 Cell-Titer Glo assay

Cells were seeded at 1000 to 3000 cells/well on white walled 96-well plate. Cell proliferation was measured with Cell-Titer Glo Luminescent Cell Viability Assay (Promega, G7571) according to the manufacturer's manual.

6.4.2 CyQuant assay

3500 cells/well were seeded on 96-well plate for cell growth assay. 8 days later, relative cell number was assessed by using the CyQUANT NF cell proliferation kit (Invitrogen, C35006) according to the manufacturer's instructions.

6.4.3 BrdU assay

BrdU cell growth assay was performed with BrdU assay kit (Merck, #QIA58) according to the manufacturer's instructions. In brief, 1 x 10^4 NCI-H23/A549 cells were seeded in each well of 96-well plate for cell growth assay in 100 µl volume followed by adding 20 µl BrdU label. 24 hours later, the plate was fixed and stained with BrdU antibody.

6.4.4 Colony formation assay

B16 cells were seeded at 200 cells/well on 12-well plate. After 7-10 days, the culture medium was removed, and cells were fixed with methanol for 20 minutes at RT. Cells were then stained with crystal violet solution (0.5% w/v crystal violet, 25% methanol) and incubated at RT for 40 minutes. Plates were washed with dH_2O and left to dry overnight. Crystal violet stain was dissolved with 10% acetic acid. Absorbance at 595 nm was measured with a plate reader.

6.5 Seahorse assay

B16 cells were seeded at 15,000 cells/well on 96-well Seahorse cell plates the day before the assay. On the day, culture medium was removed and replaced by 180 ul/well Seahorse XF base medium (Agilent Technologies, 103335-100) supplemented with pyruvate (Agilent Technologies, 103578-100) and glutamine (Agilent Technologies, 103579-50). Cartridges were loaded with 20 µL 100 mM glucose (Agilent Technologies, 103577-100) in port A, 22 µl 10 µM oligomycin (Sigma-Aldrich, 04876) in port B, 25 µl 10 µM FCCP (Sigma-Aldrich, C2920) in port C, and 27 µl 5 µM rotenone (Sigma-Aldrich, R8875) and antimycin A (Sigma-Aldrich, A8674) in port D. Assay was done using Seahorse XFe system. Relative cell number was obtained with CyQUANT NF proliferation assay kit (Life Technologies Ltd, C35006) according to the manufacturer's manual.

6.6 Cytokine production assay

T cells were transferred to a U-bottom 96-well plate. Cells were incubated with 200 ul/well eBioscience™ Cell Stimulation Cocktail plus protein transport inhibitors (Invitrogen, 00-4975-03, 1:500 dilution in T cell culture medium) in the incubator at 37°C with 5% CO2 for four hours. Samples were stained and analysed with BD LSRFortessaX20 system.

6.7 Killing assay

OT-1 expressing $CD8^+$ T cells recognising OVA-expressing tumour cells were obtained from OT-1 mice spleens and lymph nodes and enriched with EasySep Mouse CD8+ T Cell Isolation Kit. T cells were cultured in T cell medium at 0.2 M/well on a 96-well plate and activated with CD3, CD28 and IL-2 for 24 hrs. After that, $CD8^+$ T cells were collected and counted to co-culture with 0.1 M/well OVA-expressing tumour cells pre-labelled with CellTrace Far Red (Invitrogen, C34564) at ratio of 2:1, 1:1 or 1:2 for 16 or 48 hours in U-bottom 96-well plate. After incubation, T cells and tumour cells were collected, washed with FACS buffer (PBS with 2% FBS and 2 mM EDTA), and stained with Fixable Viability Dye eFluor™ 506 (eBioscience, 65-0866-14, 1:1000) in FACS buffer for 20 minutes at 4°C. Cell were analysed with BD LSRFortessaX20 system.

6.8 Flow cytometry

6.8.1 Sample staining

Samples were transferred to 96-well plate for staining. Cells were washed with fluorescence-activated cell sorting (FACS) buffer (PBS with 2% FBS and 5 mM Ethylenediaminetetraacetic acid, EDTA) followed by blocking with anti-FcR antibody (BioLegend, 156604, 1:200) for 10 minutes at 4 C. Samples were stained with surface antibodies listed in Table S2 for 30 minutes at 4 C followed by two washes with FACS

buffer. For surface panel, samples were resuspended in 200 ul/well FACS buffer and analysed with BD LSRFortessaX20 system. For intracellular panel, samples were fixed and permeabilized with eBioscience™ Foxp3 / Transcription Factor Staining Buffer Set-1 kit (Life technologies, 00-5523-00) according to the manufacturer's instruction. Briefly, cells were incubated in fixation/permeabilization working solution for 30 minutes at 4°C followed by two washes with perm/wash buffer. Cells were then stained with intracellular antibodies listed in Table S2 for 30 minutes at 4°C followed by two washes with perm/wash buffer. Samples were resuspended in 200 ul/well perm/wash buffer and analyzed with BD LSRFortessaX20 system.

6.8.2 Antibodies

Antibodies used in flow cytometry analysis are listed in **Table 6.4**.

Target protein	Colour	Supplier	Catologue number	Clone number
Anti-mouse CD8a	BUV395	BD	563786	53-6.7
Anti-mouse CD8a	FITC	Biolegend	100706	53-6.7
Anti-mouse CD8a	APC	Biolegend	100712	53-6.7
anti-mouse CD8a	BUV395	Thermo-fisher	363-0081-82	53-6.7
anti-mouse CD8a	PerCP-Cy5.5	BioLegend	100734	53-6.7
anti-mouse/human CD44	FITC	BioLegend	103006	IM7
anti-mosue CD62L	APC-Cy7	Biolegend	104428	MEL-14
anti-mouse CD45	FITC	BioLegend	103107	30-F11
anti-mouse CD45	BUV805	Thermo-fisher	368-0451-82	30-F11
anti-mouse CD45.1	FITC	BioLegend	110706	A20
anti-mouse CD183 (CXCR3)	PE/Cy7	BioLegend	126516	CXCR3-173
anti-mouse CD183 (CXCR3)	BV421	BioLegend	126522	CXCR3-173
anti-mouse CD107a (LAMP-1)	PE/Cy7	BioLegend	121620	1D4B
anti-mouse IFNg	BV785	BioLegend	505837	XMG1.2
anti-mouse IFNg	APC	BioLegend	505810	XMG1.2
anti-mouse TNFa	PerCP-Cy5.5	BioLegend	506322	MP6-XT22
anti-mouse TNFa	FITC	BioLegend	506304	MP6-XT22
anti-mouse TNFα	BV650	BioLegend	506333	MP6-XT22
anti-mouse IL-2	AF700	BioLegend	503818	JES6-5H4
anti-mouse IL-2	PE	BioLegend	503808	JES6-5H4
anti-mouse IL-2	PerCP-Cy5.5	BioLegend	503822	JES6-5H4
anti-mouse GzmB	APC	BioLegend	372204	QA16A02
anti-mouse GzmB	PE	BioLegend	372208	QA16A02
anti-mouse Perforin	APC	BioLegend	154304	S16009A
anti-mouse Ki-67	AF700	BioLegend	652420	16A8

Table 6.4 List of antibodies for flow cytometry experiments.

6.9 RNA extraction and qPCR

6.9.1 RNA extraction

Total RNA was isolated from cells with TRIzol reagent (Fisher Scientific UK Ltd, 12034977) following manufacturer's instructions. Briefly, 1 M cells were collected. The cell pellet was resuspended in 500 ul TRIzol, and the suspension was incubated for 5 minutes at room temperature. 100 ul chloroform was added and mixed by vertexing. The sample was centrifuged at 12,000 xg at 4°C for 15 minutes followed by RNA precipitation of the aqueous phase with 250 ul isopropanol. The RNA pellet was washed with 1 ml 75% ethanol and resuspended in 30 ul RNase-free water.

6.9.2 RT-qPCR

The extracted RNA was reversely transcribed into cDNA using the PrimeScript™ RT Master Mix (Perfect Real Time) (Takara Bio UK Ltd, RR036A) according to the manufacturer's instructions. The obtained cDNA samples were diluted and used for real-time quantitative PCR (RT-qPCR). SYBR™ Select Master Mix (Life Technologies Ltd, 4472908) and gene specific primers with sequences listed in **Table 6.5** were used for PCR amplification. The reaction was done on a QuantStudio3 real-time PCR system (Applied Biosystems). The RT-qPCR data were normalized to GAPDH or b-actin and presented as fold changes of gene expression in the test sample compared to the control.

RT-qPCR primer sequences		
Taget genes	Primer labels	Sequences
mouse *Ifnα1*	m-Ifnα1-qPCR-F	CGGTGCTGAGCTACTGGC
	m-Ifnα1-qPCR-R	TTTGTACCAGGAGTGTCAAGG
mouse *Ifnβ*	m-Ifnβ-qPCR-F	GGTGGAATGAGACTATTGTTG
	m-Ifnβ-qPCR-R	AGGACATCTCCCACGTC
mouse *Ifnl2* (IL-28)	m-Il-28B-qPCR-F	AGCTGCAGGTCCAAGAGCG
	m-Il-28B-qPCR-R	GGTGGTCAGGGCTGAGTCATT
mouse *Isg*15	m-Isg15-qPCR-F	GGTGTCCGTGACTAACTCCAT
	m-Isg15-qPCR-R	TGGAAAGGGTAAGACCGTCCT
mouse ERV-L	m-ERV-L-qPCR-F	TTTCTCAAGGCCCACCAATAGT
	m-ERV-L-qPCR-R	GACACCTTTTTTAACTATGCGAGCT
mouse *Hk1*	m-Hk1-qPCR-F	GAAAGGAGACCAACAGCAGAGC
	m-Hk1-qPCR-R	TTCGTTCCTCCGAGATCCAAGG
mouse *Hk2*	m-Hk2-qPCR-F	CCCTGTGAAGATGTTGCCCACT
	m-Hk2-qPCR-R	CCTTCGCTTGCCATTACGCACG
mouse *Gapdh*	m-Gapdh-qPCR-F	TGACCTCAACTACATGGTCTACA
	m-Gapdh-qPCR-R	CTTCCCATTCTCGGCCTTG
mouse *β-actin*	m-bactin qPCR_F	GGCTGTATTCCCCTCCATCG
	m-bactin qPCR_R	CCAGTTGGTAACAATGCCATGT
human *UXS1*	h-UXS1-qPCR-F	CAACCGCAGGAGGATGAAGC
	h-UXS1-qPCR-R	CCTGGATAGACCTGTTGAGTAGAA
human *UGDH*	h-UGDH-qPCR-F	CTTGCCCAGAGAATAAGCAG
	h-UGD-qPCR-R	CAAATTCAGAACATCCTTTTGGA
human *GAPDH*	h-GAPDH-qPCR-F	AACGGGAAGCTTGTCATCAA
	h-GAPDH-qPCR-R	TGGACTCCACGACGTACTCA
human *TGFβR1*	h-TGFβR1 qPCR_F	CCCATCAGTTGAAGAAATGAGAA
	h-TGFβR1 qPCR_R	CCTGTTGACTGAGTTGCGATAA

Table 6.5 List of RT-qPCR primer sequences.

6.10 Protein extraction and immunoblot analysis

6.10.1 Protein extraction

Cells in culture were collected with trypsin digestion. Cell pellets were washed with ice-cold PBS twice to remove residual medium completely. Lysis buffer (50 mM Tris pH 7.4, 200 mM NaCl, 0.1% NP-40, 10% glycerol) supplemented with protease inhibitor (Roche, 4693116001) and phosphatase inhibitor (Roche, 4906837001) was directly added to the cell pellets. Cell lysates were incubated on ice for 30 minutes before being cleared by top-speed centrifugation.

6.10.2 Protein quantification

Protein concentration was determined using the BCA protein assay kit (Fisher Scientific, 10678484) following the manufacturer's instructions. Samples were adjusted to reach the same protein concentration with the lysis buffer.

6.10.3 Immunoblot

4x NuPAGE™ LDS Sample Buffer (Life Technologies, NP0007) and 10x NuPAGE™ sample reducing agent (Life Technologies, NP0009) were added to the sample, followed by boiling at 95 ºC for 10 minutes. Samples were loaded into each well of NuPAGE™ 4 to 12% Bis-Tris Mini Protein Gel (Life Technologies, NP0323BOX). The blot was run at 200 V for 30 minutes followed by semi-dry transfer onto the membrane with Bio-Rad Transblot Turbo Transfer pack (BioRad, 1704159). The membrane was blocked with 5% skimmed milk in PBS-T (0.1% Tween-20) at room temperature for 60 minutes and probed with primary antibody at 4ºC overnight. The next day, the membrane was washed three times with PBS-T and probed with secondary antibody at room temperature for 60 minutes. The membrane was washed three times with PBS-T before visualisation with Clarity Max ECL Substrate (BioRad, 1704159).

6.10.4 Antibodies

Antibodies used include anti-LSD1 (Cell Signalling Technology #2139S, 1:1000), anti-HK1 (Cell Signalling Technology #2024S, 1:1000), anti-HK2 (Cell Signalling Technology #2867S, 1:1000 for western blot), UGDH (Atlas Antibodies #HPA036656, 1:2000), UGDH (GeneTex #104993, 1:2000), vinculin (Invitrogen #700062, 1:1000) anti-rabbit secondary (Cell Signalling Technology #7074S, 1:10000), and anti-mouse secondary (Cell Signalling Technology #7076S, 1:10000).

6.11 Immunostaining

Cells were seeded on coverslips coated with 0.01% poly-L-lysine the day before staining. On the day, cells were fixed with 2% Paraformaldehyde and permeabilised

with 0.2% Triton-X. Samples were then washed and stained with UGDH antibody (Atlas Antibodies #HPA036656, 1:200) overnight followed by secondary anti-rabbit 488A (Invitrogen, A32731) antibody. Slides were visualized with LSM980 confocal microscope.

6.12 HPLC-MS/MS analysis

The analysis was conducted with a method previously established at the Kriaucionis group[262]. Cells were seeded on a 60 mm dish the day before metabolite extraction. On the day, the dish was washed with PBS twice and dipped in liquid nitrogen. Methanol: acetonitrile (50% v/v) was added to the dish, and cell extracts were collected with a cell scraper. Samples were centrifuged at 13,000 rpm at 4 ºC for 30 minutes. Supernatants were collected and stored at – 80 ºC until analysis. Standards used were UDP-glucose (Promega, V7091) and UDP-glucuronic acid (Sigma-Aldrich, U6751). The analysis was done on 6495 Triple Quad LC/MS system (Agilent Technologies) with a Ultisil HILIC Amphion, 5um, 2.1×150mm II column (Chromex Scientific, H00274, 31014).

6.13 Statistical analysis

The data are presented as mean ± SD. The statistical significance of differences between the control and experimental groups was calculated using the unpaired Mann-Whitney test. P values < 0.05 were considered significant.

Chapter 7: References

1. Gong L, Zhang Y, Liu C, Zhang M, Han S. Application of radiosensitizers in cancer radiotherapy. *Int J Nanomedicine*. 2021;16:1083-1102. doi:10.2147/IJN.S290438
2. Deacon J, Peckham MJ, Steel GG. *The Radioresponsiveness of Human Tumours and the Initial Slope of the Cell Survival Curve*. Vol 2.; 1984.
3. Franzone P, Fiorentino A, Barra S, et al. Image-guided radiation therapy (IGRT): practical recommendations of Italian Association of Radiation Oncology (AIRO). *Radiol Med*. 2016;121(12):958-965. doi:10.1007/s11547-016-0674-x
4. Lind J. *Principles of Cytotoxic Chemotherapy*.; 2007.
5. Pommier Y. Topoisomerase I inhibitors: Camptothecins and beyond. In: *Nature Reviews Cancer*. Vol 6. ; 2006:789-802. doi:10.1038/nrc1977
6. Li Y, Zhang C, Tang D, et al. Identification of a ligand-binding site on tubulin mediating the tubulin-RB3 interaction. *Proc Natl Acad Sci U S A*. 2025;122(11). doi:10.1073/pnas.2424098122
7. Chu E, Gollerkeri A. *Resistance to Inhibitor Compounds of Thymidylate Synthase*.; 2002.
8. Barreto JN, McCullough KB, Ice LL, Smith JA. Antineoplastic agents and the associated myelosuppressive effects: A review. *J Pharm Pract*. 2014;27(5):440-446. doi:10.1177/0897190014546108
9. Hu J, Wang Z, Wang X, Xie S. Side-effects of hyperthermic intraperitoneal chemotherapy in patients with gastrointestinal cancers. *PeerJ*. 2023;11. doi:10.7717/peerj.15277
10. Hunter C, Smith R, Cahill DP, et al. A hypermutation phenotype and somatic MSH6 mutations in recurrent human malignant gliomas after alkylator chemotherapy. *Cancer Res*. 2006;66(8):3987-3991. doi:10.1158/0008-5472.CAN-06-0127

11. Cahill DP, Levine KK, Betensky RA, et al. Loss of the mismatch repair protein MSH6 in human glioblastomas is associated with tumor progression during temozolomide treatment. *Clinical Cancer Research*. 2007;13(7):2038-2045. doi:10.1158/1078-0432.CCR-06-2149
12. RALLIS KS, YAU THL, SIDERIS M. Chemoradiotherapy in cancer treatment: Rationale and clinical applications. *Anticancer Res*. 2021;41(1):1-7. doi:10.21873/anticanres.14746
13. Henderson BE, Feigelson HS. Hormonal carcinogenesis. *Carcinogenesis*. 2000;21(3):427-433. doi:10.1093/carcin/21.3.427
14. Clusan L, Ferrière F, Flouriot G, Pakdel F. A Basic Review on Estrogen Receptor Signaling Pathways in Breast Cancer. *Int J Mol Sci*. 2023;24(7):6834. doi:10.3390/ijms24076834
15. Fairchild A, Tirumani SH, Rosenthal MH, et al. Hormonal therapy in oncology: A primer for the radiologist. *American Journal of Roentgenology*. 2015;204(6):W620-W630. doi:10.2214/AJR.14.13604
16. Garrido-Castro AC, Lin NU, Polyak K. Insights into molecular classifications of triple-negative breast cancer: Improving patient selection for treatment. *Cancer Discov*. 2019;9(2):176-198. doi:10.1158/2159-8290.CD-18-1177
17. Wilson CA, Ramos L, Villaseñor MR, et al. *Localization of Human BRCA1 and Its Loss in High-Grade, Non-Inherited Breast Carcinomas*.; 1999. http://www.med.ucla.edu/ora/manuscripts.htm
18. Li Y, Zhan Z, Yin X, Fu S, Deng X. Targeted Therapeutic Strategies for Triple-Negative Breast Cancer. *Front Oncol*. 2021;11. doi:10.3389/fonc.2021.731535
19. Xie C, Luo J, He Y, Jiang L, Zhong L, Shi Y. BRCA2 gene mutation in cancer. *Medicine*. 2022;101(45):e31705. doi:10.1097/MD.0000000000031705
20. Barchiesi G, Roberto M, Verrico M, Vici P, Tomao S, Tomao F. Emerging Role of PARP Inhibitors in Metastatic Triple Negative Breast Cancer. Current Scenario and Future Perspectives. *Front Oncol*. 2021;11. doi:10.3389/fonc.2021.769280

21. André F, Ciruelos E, Rubovszky G, et al. Alpelisib for PIK3CA -Mutated, Hormone Receptor–Positive Advanced Breast Cancer . *New England Journal of Medicine*. 2019;380(20):1929-1940. doi:10.1056/nejmoa1813904

22. Davies H, Bignell GR, Cox C, et al. *Mutations of the BRAF Gene in Human Cancer*.; 2002. www.nature.com/nature

23. Zhang W, Liu HT, Tu H. *MAPK Signal Pathways in the Regulation of Cell Proliferation in Mammalian Cells*.; 2002. http://www.cell-research.com

24. Gambardella V, Tarazona N, Cejalvo JM, et al. Personalized medicine: Recent progress in cancer therapy. *Cancers (Basel)*. 2020;12(4). doi:10.3390/cancers12041009

25. Smyth LM, Piha-Paul SA, Won HH, et al. Efficacy and determinants of response to her kinase inhibition in her2-mutant metastatic breast cancer. *Cancer Discov*. 2020;10(2):198-213. doi:10.1158/2159-8290.CD-19-0966

26. Hyman DM, Piha-Paul SA, Won H, et al. HER kinase inhibition in patients with HER2-and HER3-mutant cancers. *Nature*. 2018;554(7691):189-194. doi:10.1038/nature25475

27. Dighe AS, Richards E, Old LJ, Schreiber RD. Enhanced in vivo growth and resistance to rejection of tumor cells expressing dominant negative IFNγ receptors. *Immunity*. 1994;1(6):447-456. doi:10.1016/1074-7613(94)90087-6

28. Kaplan DH, Shankaran V, Dighe AS, et al. Demonstration of an interferon γ-dependent tumor surveillance system in immunocompetent mice. *Proceedings of the National Academy of Sciences*. 1998;95(13):7556-7561. doi:10.1073/pnas.95.13.7556

29. Schreiber RD, Old LJ, Smyth MJ. *Cancer Immunoediting: Integrating Immunity's Roles in Cancer Suppression and Promotion*. https://www.science.org

30. Vesely MD, Kershaw MH, Schreiber RD, Smyth MJ. Natural innate and adaptive immunity to cancer. *Annu Rev Immunol*. 2011;29:235-271. doi:10.1146/annurev-immunol-031210-101324

31. Zhang Y, Zhang Z. The history and advances in cancer immunotherapy: understanding the characteristics of tumor-infiltrating immune cells and their therapeutic implications. *Cell Mol Immunol*. 2020;17(8):807-821. doi:10.1038/s41423-020-0488-6

32. Freeman GJ, Long AJ, Iwai Y, et al. *Engagement of the PD-1 Immunoinhibitory Receptor by a Novel B7 Family Member Leads to Negative Regulation of Lymphocyte Activation*. Vol 192.; 2000. http://www.jem.org/cgi/content/full/192/7/1027

33. Hirano F, Kaneko K, Tamura H, et al. Blockade of B7-H1 and PD-1 by monoclonal antibodies potentiates cancer therapeutic immunity. *Cancer Res*. 2005;65(3):1089-1096.

34. Brahmer JR, Tykodi SS, Chow LQM, et al. Safety and Activity of Anti–PD-L1 Antibody in Patients with Advanced Cancer. *New England Journal of Medicine*. 2012;366(26):2455-2465. doi:10.1056/nejmoa1200694

35. Walunas TL, Lenschow DJ, Bakker CY, et al. *CTLA-4 Can Function as a Negative Regulator of T Cell Activation*. Vol 1.

36. Leach DR, Krummel MF, Allison JP. Enhancement of Antitumor Immunity by CTLA-4 Blockade. *Science (1979)*. 1996;271(5256):1734-1736. doi:10.1126/science.271.5256.1734

37. Pardoll D. Releasing the brakes on antitumor immune response. *Science*. 1996;271(5256):1691. doi:10.1126/science.271.5256.1691

38. Hodi FS, O'Day SJ, McDermott DF, et al. Improved Survival with Ipilimumab in Patients with Metastatic Melanoma. *New England Journal of Medicine*. 2010;363(8):711-723. doi:10.1056/nejmoa1003466

39. Ledford H. Melanoma drug wins US approval. *Nature*. 2011;471(7340):561. doi:10.1038/471561a

40. Rosenberg SA, Restifo NP. *Adoptive Cell Transfer as Personalized Immunotherapy for Human Cancer*. https://www.science.org

41. Lee DW, Kochenderfer JN, Stetler-Stevenson M, et al. T cells expressing CD19 chimeric antigen receptors for acute lymphoblastic leukaemia in children and young adults: A phase 1 dose-escalation trial. *The Lancet*. 2015;385(9967):517-528. doi:10.1016/S0140-6736(14)61403-3

42. D'Angelo SP, Araujo DM, Abdul Razak AR, et al. Afamitresgene autoleucel for advanced synovial sarcoma and myxoid round cell liposarcoma (SPEARHEAD-1): an international, open-label, phase 2 trial. *The Lancet*. 2024;403(10435):1460-1471. doi:10.1016/S0140-6736(24)00319-2

43. Kantoff PW, Higano CS, Shore ND, et al. Sipuleucel-T Immunotherapy for Castration-Resistant Prostate Cancer. *New England Journal of Medicine*. 2010;363(5):411-422. doi:10.1056/nejmoa1001294

44. Waldmann TA. Cytokines in cancer immunotherapy. *Cold Spring Harb Perspect Biol*. 2018;10(12). doi:10.1101/cshperspect.a028472

45. Jiang T, Zhou C, Ren S. Role of IL-2 in cancer immunotherapy. *Oncoimmunology*. 2016;5(6). doi:10.1080/2162402X.2016.1163462

46. Shalhout SZ, Miller DM, Emerick KS, Kaufman HL. Therapy with oncolytic viruses: progress and challenges. *Nat Rev Clin Oncol*. 2023;20(3):160-177. doi:10.1038/s41571-022-00719-w

47. Corrigan PA, Beaulieu C, Patel RB, Lowe DK. Talimogene Laherparepvec: An Oncolytic Virus Therapy for Melanoma. *Annals of Pharmacotherapy*. 2017;51(8):675-681. doi:10.1177/1060028017702654

48. McGranahan N, Swanton C. Biological and therapeutic impact of intratumor heterogeneity in cancer evolution. *Cancer Cell*. 2015;27(1):15-26. doi:10.1016/j.ccell.2014.12.001

49. Dagogo-Jack I, Shaw AT. Tumour heterogeneity and resistance to cancer therapies. *Nat Rev Clin Oncol*. 2018;15(2):81-94. doi:10.1038/nrclinonc.2017.166

50. Harbst K, Lauss M, Cirenajwis H, et al. Multiregion whole-exome sequencing uncovers the genetic evolution and mutational heterogeneity of early-stage

metastatic melanoma. *Cancer Res*. 2016;76(16):4765-4774. doi:10.1158/0008-5472.CAN-15-3476

51. Piotrowska Z, Niederst MJ, Karlovich CA, et al. Heterogeneity underlies the emergence of EGFRT790wild-type clones following treatment of T790M-positive cancers with a third-generation EGFR inhibitor. *Cancer Discov*. 2015;5(7):713-723. doi:10.1158/2159-8290.CD-15-0399
52. Das Thakur M, Salangsang F, Landman AS, et al. Modelling vemurafenib resistance in melanoma reveals a strategy to forestall drug resistance. *Nature*. 2013;494(7436):251-255. doi:10.1038/nature11814
53. Gottesman MM, Fojo T, Bates SE. Multidrug resistance in cancer: Role of ATP-dependent transporters. *Nat Rev Cancer*. 2002;2(1):48-58. doi:10.1038/nrc706
54. Yardley DA. Drug Resistance and the Role of Combination Chemotherapy in Improving Patient Outcomes. *Int J Breast Cancer*. 2013;2013:1-15. doi:10.1155/2013/137414
55. Balkwill FR, Capasso M, Hagemann T. The tumor microenvironment at a glance. *J Cell Sci*. 2012;125(23):5591-5596. doi:10.1242/jcs.116392
56. Bilotta MT, Antignani A, Fitzgerald DJ. Managing the TME to improve the efficacy of cancer therapy. *Front Immunol*. 2022;13. doi:10.3389/fimmu.2022.954992
57. Campbell DJ, Koch MA. T reg cells: Patrolling a dangerous neighborhood. *Nat Med*. 2011;17(8):929-930. doi:10.1038/nm.2433
58. Mauri C, Bosma A. Immune regulatory function of B cells. *Annu Rev Immunol*. 2012;30:221-241. doi:10.1146/annurev-immunol-020711-074934
59. Grzywa TM, Sosnowska A, Matryba P, et al. Myeloid Cell-Derived Arginase in Cancer Immune Response. *Front Immunol*. 2020;11. doi:10.3389/fimmu.2020.00938
60. Shih C, Padhy LC, Murray M, Weinberg RA. Transforming genes of carcinomas and neuroblastomas introduced into mouse fibroblasts. *Nature*. 1981;290(5803):261-264. doi:10.1038/290261a0

61. Sukumar S, Notario V, Martin-Zanca D, Barbacid M. *Induction of Mammary Carcinomas in Rats by Nitroso-Methylurea Involves Malignant Activation of H-Ras-I Locus by Single Point Mutations*. Vol 306.; 1983.

62. Stratton MR, Campbell PJ, Futreal PA. The cancer genome. *Nature*. 2009;458(7239):719-724. doi:10.1038/nature07943

63. Thierry F, Benotmane MA, Demeret C, Mori M, Teissier S, Desaintes C. A Genomic Approach Reveals a Novel Mitotic Pathway in Papillomavirus Carcinogenesis. *Cancer Res*. 2004;64(3):895-903. doi:10.1158/0008-5472.CAN-03-2349

64. Futreal PA, Coin L, Marshall M, et al. A census of human cancer genes. *Nat Rev Cancer*. 2004;4(3):177-183. doi:10.1038/nrc1299

65. Rheinbay E, Nielsen MM, Abascal F, et al. Analyses of non-coding somatic drivers in 2,658 cancer whole genomes. *Nature*. 2020;578(7793):102-111. doi:10.1038/s41586-020-1965-x

66. Comprehensive genomic characterization defines human glioblastoma genes and core pathways. *Nature*. 2008;455(7216):1061-1068. doi:10.1038/nature07385

67. Levine AJ. *P53, the Cellular Gatekeeper Review for Growth and Division*. Vol 88.; 1997.

68. El-Deiry WS, Tokino T, Velculescu VE, et al. *WAR, a Potential Mediator of ~53 Tumor Suppression*. Vol 75.; 1993.

69. Miyashita T, Reed JC. *Tumor Suppressor P53 Is a Direct Transcriptional Activator of the Human Bax Gene*. Vol 80.; 1995.

70. Buckbinder L, Talbott R, Velasco-Miguel S, et al. Induction of the growth inhibitor IGF-binding protein 3 by p53. *Nature*. 1995;377(6550):646-649. doi:10.1038/377646a0

71. Hassin O, Oren M. Drugging p53 in cancer: one protein, many targets. *Nat Rev Drug Discov*. 2023;22(2):127-144. doi:10.1038/s41573-022-00571-8

72. Yamada KM, Araki M. Tumor suppressor PTEN: modulator of cell signaling, growth, migration and apoptosis. *J Cell Sci*. 2001;114(13):2375-2382. doi:10.1242/jcs.114.13.2375

73. Simanshu DK, Nissley D V., McCormick F. RAS Proteins and Their Regulators in Human Disease. *Cell*. 2017;170(1):17-33. doi:10.1016/j.cell.2017.06.009

74. Lim TKH, Skoulidis F, Kerr KM, et al. KRAS G12C in advanced NSCLC: Prevalence, co-mutations, and testing. *Lung Cancer*. 2023;184. doi:10.1016/j.lungcan.2023.107293

75. Canon J, Rex K, Saiki AY, et al. The clinical KRAS(G12C) inhibitor AMG 510 drives anti-tumour immunity. *Nature*. 2019;575(7781):217-223. doi:10.1038/s41586-019-1694-1

76. Hanahan D, Weinberg RA. The Hallmarks of Cancer. *Cell*. 2000;100(1):57-70. doi:10.1016/S0092-8674(00)81683-9

77. Hanahan D, Weinberg RA. Hallmarks of cancer: The next generation. *Cell*. 2011;144(5):646-674. doi:10.1016/j.cell.2011.02.013

78. Hanahan D. Hallmarks of Cancer: New Dimensions. *Cancer Discov*. 2022;12(1):31-46. doi:10.1158/2159-8290.CD-21-1059

79. Warburg O. The Metabolism of Carcinoma Cells. *J Cancer Res*. 1925;9(1):148-163. doi:10.1158/jcr.1925.148

80. Gomes AS, Ramos H, Soares J, Saraiva L. p53 and glucose metabolism: an orchestra to be directed in cancer therapy. *Pharmacol Res*. 2018;131:75-86. doi:10.1016/j.phrs.2018.03.015

81. Matés JM, Campos-Sandoval JA, Santos-Jiménez J de los, Márquez J. Dysregulation of glutaminase and glutamine synthetase in cancer. *Cancer Lett*. 2019;467:29-39. doi:10.1016/j.canlet.2019.09.011

82. Wise DR, Deberardinis RJ, Mancuso A, et al. *Myc Regulates a Transcriptional Program That Stimulates Mitochondrial Glutaminolysis and Leads to Glutamine Addiction*.; 2008. www.pnas.org/cgi/content/full/

83. Koundouros N, Poulogiannis G. Reprogramming of fatty acid metabolism in cancer. *Br J Cancer*. 2020;122(1):4-22. doi:10.1038/s41416-019-0650-z

84. Snaebjornsson MT, Janaki-Raman S, Schulze A. Greasing the Wheels of the Cancer Machine: The Role of Lipid Metabolism in Cancer. *Cell Metab*. 2020;31(1):62-76. doi:10.1016/j.cmet.2019.11.010

85. Santos CR, Schulze A. Lipid metabolism in cancer. *FEBS J*. 2012;279(15):2610-2623. doi:10.1111/j.1742-4658.2012.08644.x

86. Yang M, Vousden KH. Serine and one-carbon metabolism in cancer. *Nat Rev Cancer*. 2016;16(10):650-662. doi:10.1038/nrc.2016.81

87. Shuvalov O, Petukhov A, Daks A, Fedorova O, Vasileva E, Barlev NA. *One-Carbon Metabolism and Nucleotide Biosynthesis as Attractive Targets for Anticancer Therapy*. www.impactjournals.com/oncotarget

88. Schiliro C, Firestein BL. Mechanisms of metabolic reprogramming in cancer cells supporting enhanced growth and proliferation. *Cells*. 2021;10(5). doi:10.3390/cells10051056

89. Russell JH, Ley TJ. Lymphocyte-mediated cytotoxicity. *Annu Rev Immunol*. 2002;20:323-370. doi:10.1146/annurev.immunol.20.100201.131730

90. Ostroumov D, Fekete-Drimusz N, Saborowski M, Kühnel F, Woller N. CD4 and CD8 T lymphocyte interplay in controlling tumor growth. *Cellular and Molecular Life Sciences*. 2018;75(4):689-713. doi:10.1007/s00018-017-2686-7

91. Blank C, Gajewski TF, Mackensen A. Interaction of PD-L1 on tumor cells with PD-1 on tumor-specific T cells as a mechanism of immune evasion: Implications for tumor immunotherapy. *Cancer Immunology, Immunotherapy*. 2005;54(4):307-314. doi:10.1007/s00262-004-0593-x

92. Iwai Y, Ishida M, Tanaka Y, Okazaki T, Honjo T, Minato N. *Involvement of PD-L1 on Tumor Cells in the Escape from Host Immune System and Tumor Immunotherapy by PD-L1 Blockade*. www.pnas.orgcgidoi10.1073pnas.192461099

93. Rabinovich GA, Gabrilovich D, Sotomayor EM. Immunosuppressive strategies that are mediated by tumor cells. *Annu Rev Immunol*. 2007;25:267-296. doi:10.1146/annurev.immunol.25.022106.141609

94. Mclane LM, Abdel-Hakeem MS, Wherry EJ. CD8 T Cell Exhaustion During Chronic Viral Infection and Cancer. Published online 2025. doi:10.1146/annurev-immunol-041015

95. Recillas-Targa F. Cancer Epigenetics: An Overview. *Arch Med Res*. 2022;53(8):732-740. doi:10.1016/j.arcmed.2022.11.003

96. Jones PA. Functions of DNA methylation: Islands, start sites, gene bodies and beyond. *Nat Rev Genet*. 2012;13(7):484-492. doi:10.1038/nrg3230

97. Hur K, Cejas P, Feliu J, et al. Hypomethylation of long interspersed nuclear element-1 (LINE-1) leads to activation of protooncogenes in human colorectal cancer metastasis. *Gut*. 2014;63(4):635-646. doi:10.1136/gutjnl-2012-304219

98. Greger V, Passarge E, H□pping W, Messmer E, Horsthemke B. Epigenetic changes may contribute to the formation and spontaneous regression of retinoblastoma. *Hum Genet*. 1989;83(2):155-158. doi:10.1007/BF00286709

99. Tessarz P, Kouzarides T. Histone core modifications regulating nucleosome structure and dynamics. *Nat Rev Mol Cell Biol*. 2014;15(11):703-708. doi:10.1038/nrm3890

100. Bender S, Tang Y, Lindroth AM, et al. Reduced H3K27me3 and DNA Hypomethylation Are Major Drivers of Gene Expression in K27M Mutant Pediatric High-Grade Gliomas. *Cancer Cell*. 2013;24(5):660-672. doi:10.1016/j.ccr.2013.10.006

101. Lewis PW, Müller MM, Koletsky MS, et al. Inhibition of PRC2 Activity by a Gain-of-Function H3 Mutation Found in Pediatric Glioblastoma. *Science (1979)*. 2013;340(6134):857-861. doi:10.1126/science.1232245

102. Pajovic S, Siddaway R, Bridge T, et al. Epigenetic activation of a RAS/MYC axis in H3.3K27M-driven cancer. *Nat Commun*. 2020;11(1):6216. doi:10.1038/s41467-020-19972-7

103. Versteege I, Sévenet N, Lange J, et al. Truncating mutations of hSNF5/INI1 in aggressive paediatric cancer. *Nature*. 1998;394(6689):203-206. doi:10.1038/28212

104. Glaros S, Cirrincione GM, Palanca A, Metzger D, Reisman D. Targeted Knockout of *BRG1* Potentiates Lung Cancer Development. *Cancer Res*. 2008;68(10):3689-3696. doi:10.1158/0008-5472.CAN-07-6652

105. Short NJ, Kantarjian H. Hypomethylating agents for the treatment of myelodysplastic syndromes and acute myeloid leukemia: Past discoveries and future directions. *Am J Hematol*. 2022;97(12):1616-1626. doi:10.1002/ajh.26667

106. Suraweera A, O'Byrne KJ, Richard DJ. Combination Therapy With Histone Deacetylase Inhibitors (HDACi) for the Treatment of Cancer: Achieving the Full Therapeutic Potential of HDACi. *Front Oncol*. 2018;8. doi:10.3389/fonc.2018.00092

107. Mullard A. FDA approves an inhibitor of a novel 'epigenetic writer.' *Nat Rev Drug Discov*. 2020;19(3):156-156. doi:10.1038/d41573-020-00024-0

108. Tsherniak A, Vazquez F, Montgomery PG, et al. Defining a Cancer Dependency Map. *Cell*. 2017;170(3):564-576.e16. doi:10.1016/j.cell.2017.06.010

109. Chang L, Ruiz P, Ito T, Sellers WR. Targeting pan-essential genes in cancer: Challenges and opportunities. *Cancer Cell*. 2021;39(4):466-479. doi:10.1016/j.ccell.2020.12.008

110. McDonald ER, de Weck A, Schlabach MR, et al. Project DRIVE: A Compendium of Cancer Dependencies and Synthetic Lethal Relationships Uncovered by Large-Scale, Deep RNAi Screening. *Cell*. 2017;170(3):577-592.e10. doi:10.1016/j.cell.2017.07.005

111. Zhou C, Huang H, Wang Y, Sendinc E, Shi Y. Selective regulation of tuft cell-like small cell lung cancer by novel transcriptional co-activators C11orf53 and COLCA2. *Cell Discov*. 2022;8(1). doi:10.1038/s41421-022-00470-7

112. Szczepanski AP, Tsuboyama N, Watanabe J, Hashizume R, Zhao Z, Wang L. *POU2AF2/C11orf53 Functions as a Coactivator of POU2F3 by Maintaining Chromatin Accessibility and Enhancer Activity*. Vol 8.; 2022.

113. Wu XS, He XY, Ipsaro JJ, et al. OCA-T1 and OCA-T2 are coactivators of POU2F3 in the tuft cell lineage. *Nature*. 2022;607(7917):169-175. doi:10.1038/s41586-022-04842-7

114. Zhou C, Huang H, Wang Y, Sendinc E, Shi Y. Selective regulation of tuft cell-like small cell lung cancer by novel transcriptional co-activators C11orf53 and COLCA2. *Cell Discov*. 2022;8(1). doi:10.1038/s41421-022-00470-7

115. Zimmer BM, Barycki JJ, Simpson MA. Integration of Sugar Metabolism and Proteoglycan Synthesis by UDP-glucose Dehydrogenase. *Journal of Histochemistry and Cytochemistry*. 2021;69(1):13-23. doi:10.1369/0022155420947500

116. Eames BF, Singer A, Smith GA, et al. UDP xylose synthase 1 is required for morphogenesis and histogenesis of the craniofacial skeleton. *Dev Biol*. 2010;341(2):400-415. doi:10.1016/j.ydbio.2010.02.035

117. García-García MJ, Anderson K V. *Essential Role of Glycosaminoglycans in Fgf Signaling during Mouse Gastrulation Charide Polymer Side Chains. Proteoglycans of the He-Paran Sulfate Family Can Bind a Variety of Growth Factors, Including Members of the TGF, Wnt, and Fgf Families*. Vol 114.; 2003. http://mouse.ski.mskcc.org/;

118. Spicer AP, Kaback LA, Smith TJ, Seldin MF. Molecular cloning and characterization of the human and mouse UDP- glucose dehydrogenase genes. *Journal of Biological Chemistry*. 1998;273(39):25117-25124. doi:10.1074/jbc.273.39.25117

119. Clarkin CE, Allen S, Kuiper NJ, Wheeler BT, Wheeler-Jones CP, Pitsillides AA. Regulation of UDP-glucose dehydrogenase is sufficient to modulate hyaluronan production and release, control sulfated GAG synthesis, and promote chondrogenesis. *J Cell Physiol*. 2011;226(3):749-761. doi:10.1002/jcp.22393

120. Sen PLMJ, Mulder GJ, Burchell3 B, Bock4 KW. *SDecial Article New Developments in Glucuronidation Research: Report of a Workshop on "Glucuronidation, Its Role in Health and Disease."*

121. Wang X, Liu R, Zhu W, et al. UDP-glucose accelerates SNAI1 mRNA decay and impairs lung cancer metastasis. *Nature*. 2019;571(7763):127-131. doi:10.1038/s41586-019-1340-y

122. Huang D, Casale GP, Tian J, et al. UDP-glucose dehydrogenase as a novel field-specific candidate biomarker of prostate cancer. *Int J Cancer*. 2010;126(2):315-327. doi:10.1002/ijc.24820

123. Arnold JM, Gu F, Ambati CR, et al. *UDP-Glucose 6-Dehydrogenase Regulates Hyaluronic Acid Production and Promotes Breast Cancer Progression Corresponding Author HHS Public Access*. http://www.nature.com/authors/editorial_policies/license.html#terms

124. Wang TP, Pan YR, Fu CY, Chang HY. Down-regulation of UDP-glucose dehydrogenase affects glycosaminoglycans synthesis and motility in HCT-8 colorectal carcinoma cells. *Exp Cell Res*. 2010;316(17):2893-2902. doi:10.1016/j.yexcr.2010.07.017

125. Taieb M, Ghannoum D, Barré L, Ouzzine M. Xylosyltransferase I mediates the synthesis of proteoglycans with long glycosaminoglycan chains and controls chondrocyte hypertrophy and collagen fibers organization of in the growth plate. *Cell Death Dis*. 2023;14(6). doi:10.1038/s41419-023-05875-0

126. Rustad CF, Backe PH, Jin C, et al. A monoallelic UXS1 variant associated with short-limbed short stature. *Mol Genet Genomic Med*. 2024;12(6). doi:10.1002/mgg3.2472

127. Teoh ST, Ogrodzinski MP, Lunt SY. UDP-glucose 6-dehydrogenase knockout impairs migration and decreases in vivo metastatic ability of breast cancer cells. *Cancer Lett*. 2020;492:21-30. doi:10.1016/j.canlet.2020.07.031

128. Abughanimeh O, Kaur A, El Osta B, Ganti AK. Novel targeted therapies for advanced non-small lung cancer. *Semin Oncol*. 2022;49(3-4):326-336. doi:10.1053/j.seminoncol.2022.03.003

129. Soria JC, Ohe Y, Vansteenkiste J, et al. Osimertinib in Untreated EGFR -Mutated Advanced Non–Small-Cell Lung Cancer . *New England Journal of Medicine*. 2018;378(2):113-125. doi:10.1056/nejmoa1713137

130. Peters S, Camidge DR, Shaw AT, et al. Alectinib versus Crizotinib in Untreated ALK -Positive Non–Small-Cell Lung Cancer . *New England Journal of Medicine*. 2017;377(9):829-838. doi:10.1056/nejmoa1704795

131. Skoulidis F, Li BT, Dy GK, et al. Sotorasib for Lung Cancers with KRAS p.G12C Mutation . *New England Journal of Medicine*. 2021;384(25):2371-2381. doi:10.1056/nejmoa2103695

132. Drilon A, Siena S, Dziadziuszko R, et al. Entrectinib in ROS1 fusion-positive non-small-cell lung cancer: integrated analysis of three phase 1–2 trials. *Lancet Oncol*. 2020;21(2):261-270. doi:10.1016/S1470-2045(19)30690-4

133. Robert C, Grob JJ, Stroyakovskiy D, et al. Five-Year Outcomes with Dabrafenib plus Trametinib in Metastatic Melanoma. *New England Journal of Medicine*. 2019;381(7):626-636. doi:10.1056/nejmoa1904059

134. Olivares-Hernández A, González del Portillo E, Tamayo-Velasco Á, et al. Immune checkpoint inhibitors in non-small cell lung cancer: from current perspectives to future treatments—a systematic review. *Ann Transl Med*. 2023;11(10):354-354. doi:10.21037/atm-22-4218

135. Chen S, Zhang Z, Zheng X, et al. Response Efficacy of PD-1 and PD-L1 Inhibitors in Clinical Trials: A Systematic Review and Meta-Analysis. *Front Oncol*. 2021;11. doi:10.3389/fonc.2021.562315

136. Mizuno T, Katsuya Y, Sato J, Koyama T, Shimizu T, Yamamoto N. Emerging PD-1/PD-L1 targeting immunotherapy in non-small cell lung cancer: Current status and future perspective in Japan, US, EU, and China. *Front Oncol*. 2022;12. doi:10.3389/fonc.2022.925938

137. Ran FA, Hsu PD, Wright J, Agarwala V, Scott DA, Zhang F. Genome engineering using the CRISPR-Cas9 system. *Nat Protoc*. 2013;8(11):2281-2308. doi:10.1038/nprot.2013.143

138. Wang X, Liu R, Zhu W, et al. UDP-glucose accelerates SNAI1 mRNA decay and impairs lung cancer metastasis. *Nature*. 2019;571(7763):127-131. doi:10.1038/s41586-019-1340-y

139. Doshi MB, Lee N, Tseyang T, et al. Disruption of sugar nucleotide clearance is a therapeutic vulnerability of cancer cells. *Nature*. 2023;623(7987):625-632. doi:10.1038/s41586-023-06676-3

140. Vigetti D, Ori M, Viola M, et al. Molecular cloning and characterization of UDP-glucose dehydrogenase from the amphibian Xenopus laevis and its involvement in hyaluronan synthesis. *Journal of Biological Chemistry*. 2006;281(12):8254-8263. doi:10.1074/jbc.M508516200

141. Lu P, Takai K, Weaver VM, Werb Z. Extracellular Matrix degradation and remodeling in development and disease. *Cold Spring Harb Perspect Biol*. 2011;3(12). doi:10.1101/cshperspect.a005058

142. Tang T, Li L, Tang J, et al. A mouse knockout library for secreted and transmembrane proteins. *Nat Biotechnol*. 2010;28(7):749-755. doi:10.1038/nbt.1644

143. Eames BF, Singer A, Smith GA, et al. UDP xylose synthase 1 is required for morphogenesis and histogenesis of the craniofacial skeleton. *Dev Biol*. 2010;341(2):400-415. doi:10.1016/j.ydbio.2010.02.035

144. Lee N, Spears ME, Carlisle AE, Kim D. Endogenous toxic metabolites and implications in cancer therapy. *Oncogene*. 2020;39(35):5709-5720. doi:10.1038/s41388-020-01395-9

145. Carlisle AE, Lee N, Matthew-Onabanjo AN, et al. Selenium detoxification is required for cancer-cell survival. *Nat Metab*. 2020;2(7):603-611. doi:10.1038/s42255-020-0224-7

146. Kim D, Fiske BP, Birsoy K, et al. SHMT2 drives glioma cell survival in ischaemia but imposes a dependence on glycine clearance. *Nature*. 2015;520(7547):363-367. doi:10.1038/nature14363

147. Kaech SM, Cui W. Transcriptional control of effector and memory CD8+ T cell differentiation. *Nat Rev Immunol*. 2012;12(11):749-761. doi:10.1038/nri3307

148. Wherry EJ, Kurachi M. Molecular and cellular insights into T cell exhaustion. *Nat Rev Immunol*. 2015;15(8):486-499. doi:10.1038/nri3862

149. VanderWalde A, Bellasea SL, Kendra KL, et al. Ipilimumab with or without nivolumab in PD-1 or PD-L1 blockade refractory metastatic melanoma: a randomized phase 2 trial. *Nat Med*. 2023;29(9):2278-2285. doi:10.1038/s41591-023-02498-y

150. Cascone T, Awad MM, Spicer JD, et al. Perioperative Nivolumab in Resectable Lung Cancer. *New England Journal of Medicine*. 2024;390(19):1756-1769. doi:10.1056/nejmoa2311926

151. Choueiri TK, Tomczak P, Park SH, et al. Adjuvant Pembrolizumab after Nephrectomy in Renal-Cell Carcinoma. *New England Journal of Medicine*. 2021;385(8):683-694. doi:10.1056/nejmoa2106391

152. Monk BJ, Colombo N, Tewari KS, et al. First-Line Pembrolizumab + Chemotherapy Versus Placebo + Chemotherapy for Persistent, Recurrent, or Metastatic Cervical Cancer: Final Overall Survival Results of KEYNOTE-826. *Journal of Clinical Oncology*. 2023;41(36):5505-5511. doi:10.1200/JCO.23.00914

153. Schmid P, Cortes J, Pusztai L, et al. Pembrolizumab for Early Triple-Negative Breast Cancer. *New England Journal of Medicine*. 2020;382(9):810-821. doi:10.1056/nejmoa1910549

154. Baker DJ, Arany Z, Baur JA, Epstein JA, June CH. CAR T therapy beyond cancer: the evolution of a living drug. *Nature*. 2023;619(7971):707-715. doi:10.1038/s41586-023-06243-w

155. Abramson JS. Anti-CD19 CAR T-Cell Therapy for B-Cell Non-Hodgkin Lymphoma. *Transfus Med Rev*. 2020;34(1):29-33. doi:10.1016/j.tmrv.2019.08.003

156. Maude SL, Laetsch TW, Buechner J, et al. Tisagenlecleucel in Children and Young Adults with B-Cell Lymphoblastic Leukemia. *New England Journal of Medicine*. 2018;378(5):439-448. doi:10.1056/nejmoa1709866

157. Fowler NH, Dickinson M, Dreyling M, et al. Tisagenlecleucel in adult relapsed or refractory follicular lymphoma: the phase 2 ELARA trial. *Nat Med*. 2022;28(2):325-332. doi:10.1038/s41591-021-01622-0

158. Groom JR, Luster AD. CXCR3 in T cell function. *Exp Cell Res*. 2011;317(5):620-631. doi:10.1016/j.yexcr.2010.12.017

159. Chow MT, Ozga AJ, Servis RL, et al. Intratumoral Activity of the CXCR3 Chemokine System Is Required for the Efficacy of Anti-PD-1 Therapy. *Immunity*. 2019;50(6):1498-1512.e5. doi:10.1016/j.immuni.2019.04.010

160. Carty SA, Gohil M, Banks LB, et al. The Loss of TET2 Promotes CD8+ T Cell Memory Differentiation. *The Journal of Immunology*. 2018;200(1):82-91. doi:10.4049/jimmunol.1700559

161. Jain N, Zhao Z, Feucht J, et al. TET2 guards against unchecked BATF3-induced CAR T cell expansion. *Nature*. 2023;615(7951):315-322. doi:10.1038/s41586-022-05692-z

162. Fraietta JA, Nobles CL, Sammons MA, et al. Disruption of TET2 promotes the therapeutic efficacy of CD19-targeted T cells. *Nature*. 2018;558(7709):307-312. doi:10.1038/s41586-018-0178-z

163. Ghoneim HE, Fan Y, Moustaki A, et al. De Novo Epigenetic Programs Inhibit PD-1 Blockade-Mediated T Cell Rejuvenation. *Cell*. 2017;170(1):142-157.e19. doi:10.1016/j.cell.2017.06.007

164. Prinzing B, Zebley CC, Petersen CT, et al. *Deleting DNMT3A in CAR T Cells Prevents Exhaustion and Enhances Antitumor Activity*. Vol 13.; 2021. https://www.science.org

165. Jain N, Zhao Z, Koche RP, et al. Disruption of SUV39H1-Mediated H3K9 Methylation Sustains CAR T-cell Function. *Cancer Discov*. 2024;14(1):142-157. doi:10.1158/2159-8290.CD-22-1319

166. Qiu F, Jiang P, Zhang G, et al. Priming with LSD1 inhibitors promotes the persistence and antitumor effect of adoptively transferred T cells. *Nat Commun*. 2024;15(1):4327. doi:10.1038/s41467-024-48607-4

167. Wolf SS. The protein arginine methyltransferase family: An update about function, new perspectives and the physiological role in humans. *Cellular and Molecular Life Sciences*. 2009;66(13):2109-2121. doi:10.1007/s00018-009-0010-x

168. Tewary SK, Zheng YG, Ho MC. Protein arginine methyltransferases: insights into the enzyme structure and mechanism at the atomic level. *Cellular and Molecular Life Sciences*. 2019;76(15):2917-2932. doi:10.1007/s00018-019-03145-x

169. Yang Y, Bedford MT. Protein arginine methyltransferases and cancer. *Nat Rev Cancer*. 2013;13(1):37-50. doi:10.1038/nrc3409

170. Cheung N, Chan LC, Thompson A, Cleary ML, So CWE. Protein arginine-methyltransferase-dependent oncogenesis. *Nat Cell Biol*. 2007;9(10):1208-1215. doi:10.1038/ncb1642

171. Shih AH, Abdel-Wahab O, Patel JP, Levine RL. The role of mutations in epigenetic regulators in myeloid malignancies. *Nat Rev Cancer*. 2012;12(9):599-612. doi:10.1038/nrc3343

172. Boisvert FM, Rhie A, Richard S, Doherty AJ. The GAR motif of 53BP1 is arginine methylated by PRMT1 and is necessary for 53BP1 DNA binding activity. *Cell Cycle*. 2005;4(12):1834-1841. doi:10.4161/cc.4.12.2250

173. Yu Z, Vogel G, Yan C, et al. The MRE11 GAR motif regulates DNA double-strand break processing and ATR activation. *Cell Res*. 2012;22(2):305-320. doi:10.1038/cr.2011.128

174. Cheung N, Fung TK, Zeisig BB, et al. Targeting Aberrant Epigenetic Networks Mediated by PRMT1 and KDM4C in Acute Myeloid Leukemia. *Cancer Cell*. 2016;29(1):32-48. doi:10.1016/j.ccell.2015.12.007

175. Hwang JW, Cho Y, Bae GU, Kim SN, Kim YK. Protein arginine methyltransferases: promising targets for cancer therapy. *Exp Mol Med*. 2021;53(5):788-808. doi:10.1038/s12276-021-00613-y

176. Wu H, Siarheyeva A, Zeng H, et al. Crystal structures of the human histone H4K20 methyltransferases SUV420H1 and SUV420H2. *FEBS Lett*. 2013;587(23):3859-3868. doi:10.1016/j.febslet.2013.10.020

177. Wang Hengbin, Wang Liangjun, Erdjument-Bromage Hediye, et al. Role of histone H2A ubiquitination in Polycomb silencing. *Nature*. 2004;431(7010):873-878. doi:10.1038/nature02935

178. Chen Y, Fu LL, Wen X, et al. Sirtuin-3 (SIRT3), a therapeutic target with oncogenic and tumor-suppressive function in cancer. *Cell Death Dis*. 2014;5(2). doi:10.1038/cddis.2014.14

179. Wang F, Marshall CB, Ikura M. Transcriptional/epigenetic regulator CBP/p300 in tumorigenesis: Structural and functional versatility in target recognition. *Cellular and Molecular Life Sciences*. 2013;70(21):3989-4008. doi:10.1007/s00018-012-1254-4

180. Wang ZQ, Zhang ZC, Wu YY, et al. Bromodomain and extraterminal (BET) proteins: biological functions, diseases, and targeted therapy. *Signal Transduct Target Ther*. 2023;8(1). doi:10.1038/s41392-023-01647-6

181. He R, Liu B, Geng B, Li N, Geng Q. The role of HDAC3 and its inhibitors in regulation of oxidative stress and chronic diseases. *Cell Death Discov*. 2023;9(1). doi:10.1038/s41420-023-01399-w

182. Lee J, Xia Y, Son MY, et al. A novel small molecule facilitates the reprogramming of human somatic cells into a pluripotent state and supports the maintenance of an undifferentiated state of human pluripotent stem cells. *Angewandte Chemie - International Edition*. 2012;51(50):12509-12513. doi:10.1002/anie.201206691

183. Uhlmann T, Geoghegan VL, Thomas B, Ridlova G, Trudgian DC, Acuto O. A method for large-scale identification of protein arginine methylation. *Molecular and Cellular Proteomics*. 2012;11(11):1489-1499. doi:10.1074/mcp.M112.020743

184. Geoghegan V, Guo A, Trudgian D, Thomas B, Acuto O. Comprehensive identification of arginine methylation in primary T cells reveals regulatory roles in cell signalling. *Nat Commun*. 2015;6. doi:10.1038/ncomms7758

185. Mowen KA, Schurter BT, Fathman JW, David M, Glimcher LH. *Arginine Methylation Regulates Subcellular Localization*. Vol 15. Yun and Fu; 2004.

186. Daniels MA, Luera D, Teixeiro E. NFκB signaling in T cell memory. *Front Immunol*. 2023;14. doi:10.3389/fimmu.2023.1129191

187. Tikhanovich I, Kuravi S, Artigues A, et al. Dynamic arginine methylation of tumor necrosis factor (TNF) receptor-associated factor 6 regulates toll-like receptor signaling. *Journal of Biological Chemistry*. 2015;290(36):22236-22249. doi:10.1074/jbc.M115.653543

188. Veazey KJ, Cheng D, Lin K, et al. CARM1 inhibition reduces histone acetyltransferase activity causing synthetic lethality in CREBBP/EP300-mutated lymphomas. *Leukemia*. 2020;34(12):3269-3285. doi:10.1038/s41375-020-0908-8

189. Veazey KJ, Cheng D, Lin K, et al. CARM1 inhibition reduces histone acetyltransferase activity causing synthetic lethality in CREBBP/EP300-mutated lymphomas. *Leukemia*. 2020;34(12):3269-3285. doi:10.1038/s41375-020-0908-8

190. Hwang JW, Cho Y, Bae GU, Kim SN, Kim YK. Protein arginine methyltransferases: promising targets for cancer therapy. *Exp Mol Med*. 2021;53(5):788-808. doi:10.1038/s12276-021-00613-y

191. Stein C, Riedl S, Rüthnick D, Nötzold RR, Bauer UM. The arginine methyltransferase PRMT6 regulates cell proliferation and senescence through

transcriptional repression of tumor suppressor genes. *Nucleic Acids Res*. 2012;40(19):9522-9533. doi:10.1093/nar/gks767

192. Wang C, Jiang H, Jin J, et al. Development of Potent Type I Protein Arginine Methyltransferase (PRMT) Inhibitors of Leukemia Cell Proliferation. *J Med Chem*. 2017;60(21):8888-8905. doi:10.1021/acs.jmedchem.7b01134
193. He X, Zhu Y, Lin YC, et al. PRMT1-mediated FLT3 arginine methylation promotes maintenance of FLT3-ITD+ acute myeloid leukemia. *Blood*. 2019;134(6):548-560. doi:10.1182/blood.2019001282
194. Inoue F, Sone K, Toyohara Y, et al. Histone arginine methyltransferase CARM1 selective inhibitor TP-064 induces apoptosis in endometrial cancer. *Biochem Biophys Res Commun*. 2022;601:123-128. doi:10.1016/j.bbrc.2022.02.086
195. Liu Y, Liu H, Ye M, et al. Methylation of BRD4 by PRMT1 regulates BRD4 phosphorylation and promotes ovarian cancer invasion. *Cell Death Dis*. 2023;14(9). doi:10.1038/s41419-023-06149-5
196. Shi Y, Lan F, Matson C, et al. Histone demethylation mediated by the nuclear amine oxidase homolog LSD1. *Cell*. 2004;119(7):941-953. doi:10.1016/j.cell.2004.12.012
197. Mao F, Shi YG. Targeting the LSD1/KDM1 Family of Lysine Demethylases in Cancer and Other Human Diseases. In: ; 2023:15-49. doi:10.1007/978-3-031-38176-8_2
198. Shi YJ, Matson C, Lan F, Iwase S, Baba T, Shi Y. Regulation of LSD1 histone demethylase activity by its associated factors. *Mol Cell*. 2005;19(6):857-864. doi:10.1016/j.molcel.2005.08.027
199. Sun G, Alzayady K, Stewart R, et al. Histone Demethylase LSD1 Regulates Neural Stem Cell Proliferation. *Mol Cell Biol*. 2010;30(8):1997-2005. doi:10.1128/MCB.01116-09
200. Yokoyama A, Takezawa S, Schüle R, Kitagawa H, Kato S. Transrepressive Function of TLX Requires the Histone Demethylase LSD1. *Mol Cell Biol*. 2008;28(12):3995-4003. doi:10.1128/mcb.02030-07

201. Wang Y, Zhang H, Chen Y, et al. LSD1 Is a Subunit of the NuRD Complex and Targets the Metastasis Programs in Breast Cancer. *Cell*. 2009;138(4):660-672. doi:10.1016/j.cell.2009.05.050

202. Hu X, Li X, Valverde K, et al. *LSD1-Mediated Epigenetic Modification Is Required for TAL1 Function and Hematopoiesis*. www.pnas.org/cgi/content/full/

203. Metzger E, Wissmann M, Yin N, et al. LSD1 demethylates repressive histone marks to promote androgen-receptor- dependent transcription. *Nature*. 2005;437(7057):436-439. doi:10.1038/nature04020

204. Laurent B, Ruitu L, Murn J, et al. A Specific LSD1/KDM1A Isoform Regulates Neuronal Differentiation through H3K9 Demethylation. *Mol Cell*. 2015;57(6):957-970. doi:10.1016/j.molcel.2015.01.010

205. Huang J, Sengupta R, Espejo AB, et al. p53 is regulated by the lysine demethylase LSD1. *Nature*. 2007;449(7158):105-108. doi:10.1038/nature06092

206. Wang J, Hevi S, Kurash JK, et al. The lysine demethylase LSD1 (KDM1) is required for maintenance of global DNA methylation. *Nat Genet*. 2009;41(1):125-129. doi:10.1038/ng.268

207. Kontaki H, Talianidis I. Lysine Methylation Regulates E2F1-Induced Cell Death. *Mol Cell*. 2010;39(1):152-160. doi:10.1016/j.molcel.2010.06.006

208. Yang J, Huang J, Dasgupta M, et al. Reversible methylation of promoter-bound STAT3 by histone-modifying enzymes. *Proc Natl Acad Sci U S A*. 2010;107(50):21499-21504. doi:10.1073/pnas.1016147107

209. Chen Y, Kim J, Zhang R, et al. Histone Demethylase LSD1 Promotes Adipocyte Differentiation through Repressing Wnt Signaling. *Cell Chem Biol*. 2016;23(10):1228-1240. doi:10.1016/j.chembiol.2016.08.010

210. Fuentes P, Cánovas J, Berndt FA, Noctor SC, Kukuljan M. CoREST/LSD1 control the development of pyramidal cortical neurons. *Cerebral Cortex*. 2012;22(6):1431-1441. doi:10.1093/cercor/bhr218

211. Choi J, Jang H, Kim H, et al. Modulation of lysine methylation in myocyte enhancer factor 2 during skeletal muscle cell differentiation. *Nucleic Acids Res*. 2014;42(1):224-234. doi:10.1093/nar/gkt873

212. Kerenyi MA, Shao Z, Hsu YJ, et al. Histone demethylase Lsd1 represses hematopoietic stem and progenitor cell signatures during blood cell maturation. *Elife*. 2013;2013(2). doi:10.7554/eLife.00633

213. Højfeldt JW, Agger K, Helin K. Histone lysine demethylases as targets for anticancer therapy. *Nat Rev Drug Discov*. 2013;12(12):917-930. doi:10.1038/nrd4154

214. Scoumanne A, Chen X. The lysine-specific demethylase 1 is required for cell proliferation in both p53-dependent and -independent manners. *Journal of Biological Chemistry*. 2007;282(21):15471-15475. doi:10.1074/jbc.M701023200

215. Sun L, Fang J. Epigenetic regulation of epithelial–mesenchymal transition. *Cellular and Molecular Life Sciences*. 2016;73(23):4493-4515. doi:10.1007/s00018-016-2303-1

216. Hino S, Kohrogi K, Nakao M. Histone demethylase LSD1 controls the phenotypic plasticity of cancer cells. *Cancer Sci*. 2016;107(9):1187-1192. doi:10.1111/cas.13004

217. Sakamoto A, Hino S, Nagaoka K, et al. Lysine demethylase LSD1 coordinates glycolytic and mitochondrial metabolism in hepatocellular carcinoma cells. *Cancer Res*. 2015;75(7):1445-1456. doi:10.1158/0008-5472.CAN-14-1560

218. Kosumi K, Baba Y, Sakamoto A, et al. Lysine-specific demethylase-1 contributes to malignant behavior by regulation of invasive activity and metabolic shift in esophageal cancer. *Int J Cancer*. 2016;138(2):428-439. doi:10.1002/ijc.29714

219. Sheng W, LaFleur MW, Nguyen TH, et al. LSD1 Ablation Stimulates Anti-tumor Immunity and Enables Checkpoint Blockade. *Cell*. 2018;174(3):549-563.e19. doi:10.1016/j.cell.2018.05.052

220. A S PrN, Howard Kaizen BM, ROBEirt SCHIMKE AT. *BIOCHEAiJSTRI: KATZEN .LNI) SCHIAXKE MULTIPLE FORMS OF HEXOKINASE IN THE RAT: TISSUE DISTRIBUTION, AGE DEPENDENCY, AND PROPERTIES*. Vol 51. Academic Press; 1964. https://www.pnas.org

221. Wilson JE. Isozymes of mammalian hexokinase: Structure, subcellular localization and metabolic function. *Journal of Experimental Biology*. 2003;206(12):2049-2057. doi:10.1242/jeb.00241

222. Li H, Song J, He Y, et al. CRISPR/Cas9 Screens Reveal that Hexokinase 2 Enhances Cancer Stemness and Tumorigenicity by Activating the ACSL4-Fatty Acid β-Oxidation Pathway. *Advanced Science*. 2022;9(21). doi:10.1002/advs.202105126

223. Wang J, Shao F, Yang Y, et al. A non-metabolic function of hexokinase 2 in small cell lung cancer: promotes cancer cell stemness by increasing USP11-mediated CD133 stability. *Cancer Commun*. 2022;42(10):1008-1027. doi:10.1002/cac2.12351

224. Yan H, Wang Z, Teng D, et al. Hexokinase 2 senses fructose in tumor-associated macrophages to promote colorectal cancer growth. *Cell Metab*. Published online October 24, 2024. doi:10.1016/j.cmet.2024.10.002

225. Ludvik AE, Pusec CM, Priyadarshini M, et al. HKDC1 Is a novel hexokinase involved in Whole-Body glucose use. *Endocrinology*. 2016;157(9):3452-3461. doi:10.1210/en.2016-1288

226. DeWaal D, Nogueira V, Terry AR, et al. Hexokinase-2 depletion inhibits glycolysis and induces oxidative phosphorylation in hepatocellular carcinoma and sensitizes to metformin. *Nat Commun*. 2018;9(1). doi:10.1038/s41467-017-02733-4

227. Liu Y, Debo B, Li M, Shi Z, Sheng W, Shi Y. LSD1 inhibition sustains T cell invigoration with a durable response to PD-1 blockade. *Nat Commun*. 2021;12(1). doi:10.1038/s41467-021-27179-7

228. Batlle E, Massagué J. Transforming Growth Factor-β Signaling in Immunity and Cancer. *Immunity*. 2019;50(4):924-940. doi:10.1016/j.immuni.2019.03.024

229. Sheng W, Liu Y, Chakraborty D, Debo B, Shi Y. Simultaneous inhibition of lsd1 and tgfb enables eradication of poorly immunogenic tumors with anti–pd-1 treatment. *Cancer Discov*. 2021;11(8):1970-1981. doi:10.1158/2159-8290.CD-20-0017

230. Doshi MB, Lee N, Tseyang T, et al. Disruption of sugar nucleotide clearance is a therapeutic vulnerability of cancer cells. *Nature*. 2023;623(7987):625-632. doi:10.1038/s41586-023-06676-3

231. Eixelsberger T, Sykora S, Egger S, et al. Structure and mechanism of human UDP-xylose synthase: Evidence for a promoting role of sugar ring distortion in a three-step catalytic conversion of UDP-glucuronic acid. *Journal of Biological Chemistry*. 2012;287(37):31349-31358. doi:10.1074/jbc.M112.386706

232. Békés M, Langley DR, Crews CM. PROTAC targeted protein degraders: the past is prologue. *Nat Rev Drug Discov*. 2022;21(3):181-200. doi:10.1038/s41573-021-00371-6

233. Tang T, Li L, Tang J, et al. A mouse knockout library for secreted and transmembrane proteins. *Nat Biotechnol*. 2010;28(7):749-755. doi:10.1038/nbt.1644

234. Uhlén M, Fagerberg L, Hallström BM, et al. Tissue-based map of the human proteome. *Science (1979)*. 2015;347(6220). doi:10.1126/science.1260419

235. Thiebaut C, Eve L, Poulard C, Le Romancer M. Structure, Activity, and Function of PRMT1. *Life*. 2021;11(11):1147. doi:10.3390/life11111147

236. Hsu SH, Hung WC. Protein arginine methyltransferase 3: A crucial regulator in metabolic reprogramming and gene expression in cancers. *Cancer Lett*. 2023;554:216008. doi:10.1016/j.canlet.2022.216008

237. Suresh S, Huard S, Dubois T. CARM1/PRMT4: Making Its Mark beyond Its Function as a Transcriptional Coactivator. *Trends Cell Biol*. 2021;31(5):402-417. doi:10.1016/j.tcb.2020.12.010

238. Walton J, Ng ASN, Arevalo K, et al. PRMT1 inhibition perturbs RNA metabolism and induces DNA damage in clear cell renal cell carcinoma. *Nat Commun*. 2024;15(1):8232. doi:10.1038/s41467-024-52507-y

239. Wang Y, Wang C, Guan X, et al. PRMT3-Mediated Arginine Methylation of METTL14 Promotes Malignant Progression and Treatment Resistance in Endometrial Carcinoma. *Advanced Science*. 2023;10(36). doi:10.1002/advs.202303812

240. Liao Y, Luo Z, Lin Y, et al. PRMT3 drives glioblastoma progression by enhancing HIF1A and glycolytic metabolism. *Cell Death Dis*. 2022;13(11):943. doi:10.1038/s41419-022-05389-1

241. Li Y, Dobrolecki LE, Sallas C, et al. PRMT blockade induces defective DNA replication stress response and synergizes with PARP inhibition. *Cell Rep Med*. 2023;4(12):101326. doi:10.1016/j.xcrm.2023.101326

242. Wu Q, Nie DY, Ba-Alawi W, et al. PRMT inhibition induces a viral mimicry response in triple-negative breast cancer. *Nat Chem Biol*. 2022;18(8):821-830. doi:10.1038/s41589-022-01024-4

243. Fedoriw A, Rajapurkar SR, O'Brien S, et al. Anti-tumor Activity of the Type I PRMT Inhibitor, GSK3368715, Synergizes with PRMT5 Inhibition through MTAP Loss. *Cancer Cell*. 2019;36(1):100-114.e25. doi:10.1016/j.ccell.2019.05.014

244. Vlachogiannis G, Hedayat S, Vatsiou A, et al. *Patient-Derived Organoids Model Treatment Response of Metastatic Gastrointestinal Cancers*. https://www.science.org

245. Kaelin WG, McKnight SL. Influence of metabolism on epigenetics and disease. *Cell*. 2013;153(1):56-69. doi:10.1016/j.cell.2013.03.004

246. Lau CM, Adams NM, Geary CD, et al. Epigenetic control of innate and adaptive immune memory. *Nat Immunol*. 2018;19(9):963-972. doi:10.1038/s41590-018-0176-1

247. Scharer CD, Barwick BG, Youngblood BA, Ahmed R, Boss JM. Global DNA Methylation Remodeling Accompanies CD8 T Cell Effector Function. *The*

Journal of Immunology. 2013;191(6):3419-3429. doi:10.4049/jimmunol.1301395

248. Cribbs A, Hookway ES, Wells G, et al. Inhibition of histone H3K27 demethylases selectively modulates inflammatory phenotypes of natural killer cells. *J Biol Chem*. 2018;293(7):2422-2437. doi:10.1074/jbc.RA117.000698
249. Lee PP, Fitzpatrick DR, Beard C, et al. A Critical Role for Dnmt1 and DNA Methylation in T Cell Development, Function, and Survival. *Immunity*. 2001;15(5):763-774. doi:10.1016/S1074-7613(01)00227-8
250. Carty SA, Gohil M, Banks LB, et al. The Loss of TET2 Promotes CD8+ T Cell Memory Differentiation. *The Journal of Immunology*. 2018;200(1):82-91. doi:10.4049/jimmunol.1700559
251. Serrano A, Tanzarella S, Lionello I, et al. Rexpression of HLA class I antigens and restoration of antigen-specific CTL response in melanoma cells following 5-aza-2?-deoxycytidine treatment. *Int J Cancer*. 2001;94(2):243-251. doi:10.1002/ijc.1452
252. Almstedt M, Blagitko-Dorfs N, Duque-Afonso J, et al. The DNA demethylating agent 5-aza-2′-deoxycytidine induces expression of NY-ESO-1 and other cancer/testis antigens in myeloid leukemia cells. *Leuk Res*. 2010;34(7):899-905. doi:10.1016/j.leukres.2010.02.004
253. Adair SJ, Hogan KT. Treatment of ovarian cancer cell lines with 5-aza-2′-deoxycytidine upregulates the expression of cancer-testis antigens and class I major histocompatibility complex-encoded molecules. *Cancer Immunology, Immunotherapy*. 2009;58(4):589-601. doi:10.1007/s00262-008-0582-6
254. West AC, Johnstone RW. New and emerging HDAC inhibitors for cancer treatment. *Journal of Clinical Investigation*. 2014;124(1):30-39. doi:10.1172/JCI69738
255. West AC, Mattarollo SR, Shortt J, et al. An intact immune system is required for the anticancer activities of histone deacetylase inhibitors. *Cancer Res*. 2013;73(24):7265-7276. doi:10.1158/0008-5472.CAN-13-0890

256. Murakami T, Sato A, Chun NAL, et al. Transcriptional modulation using HDACi depsipeptide promotes immune cell-mediated tumor destruction of murine B16 melanoma. *J Invest Dermatol*. 2008;128(6):1506-1516. doi:10.1038/sj.jid.5701216

257. Woods DM, Sodré AL, Villagra A, Sarnaik A, Sotomayor EM, Weber J. HDAC Inhibition Upregulates PD-1 Ligands in Melanoma and Augments Immunotherapy with PD-1 Blockade. *Cancer Immunol Res*. 2015;3(12):1375-1385. doi:10.1158/2326-6066.CIR-15-0077-T

258. Pearce EL, Poffenberger MC, Chang CH, Jones RG. Fueling Immunity: Insights into Metabolism and Lymphocyte Function. *Science (1979)*. 2013;342(6155). doi:10.1126/science.1242454

259. Guerra L, Bonetti L, Brenner D. Metabolic Modulation of Immunity: A New Concept in Cancer Immunotherapy. *Cell Rep*. 2020;32(1):107848. doi:10.1016/j.celrep.2020.107848

260. Harmon C, O'Farrelly C, Robinson MW. The Immune Consequences of Lactate in the Tumor Microenvironment. In: ; 2020:113-124. doi:10.1007/978-3-030-43093-1_7

261. Wei H, Guan JL. Pro-tumorigenic function of autophagy in mammary oncogenesis. *Autophagy*. 2012;8(1):129-131. doi:10.4161/auto.8.1.18171

262. Spingardi P. *Investigating the Roles of CDA and DCTD in Cancer Nucleotide Metabolism.* . 2021.

Appendices

Appendix 1: Inhibitors used in the drug screen in Chapter 3

Number	Inhibitor	Target
1	SB939	HDAC inhibitor
2	PCI 34051	HDAC8 inhibitor
3	4-iodo-SAHA	HDAC inhibitor
4	Sulforaphane	HDAC inhibitor
5	Sirtinol	Sirtuin deacetylase inhibitor
6	C646	HAT p300 inhibitor
7	Garcinol	HAT inhibitor (natural compound)
8	Ellagic Acid	Multiple pathways (naturally occruing polyphenol)
14	JGB1741	SIRT1 inhibitor
15	I-BET762	Bromodomain and extra-terminal domain (BET) protein inhibitor
9	Scriptaid	HDAC inhibitor
10	Suberohydroxamic Acid	HDAC inhibitor
11	Apicidin	HDAC inhibitor
12	Cl-Amidine (hydrochloride)	Protein-arginine deiminase (PAD) inhibitor
13	F-Amidine (trifluoroacetate salt)	PAD inhibitor
16	UNC0638	HMT inhibitor
17	UNC669	Malignant brain tumour (MBT) domain protein inhibitor
18	CAY10669	HAT p300/CBP-associated factor (PCAF) inhibitor
19	Zebularine	DNA methyltransferase inhibitor
20	Delphinidin (chloride)	EGFR inhibitor and HAT inhibitor
21	ITF 2357	HDAC inhibitor
22	UNC0631	HMT inhibitor
23	UNC0646	HMT inhibitor
24	2,4-Pyridinedicarboxylic Acid (hydrate)	JmjC domain-containing histone demethylase (JHDM) inhibitor
25	PFI-1	BETprotein inhibitor
26	5-Azacytidine	DNA methyltransferase inhibitor
27	SGI-1027	DNA methyltransferase inhibitor
28	Decitabine	Nucleic acid synthesis inhibitor
29	I-BET151	BRD inhibitor
30	(+)-JQ1	BET protein inhibitor
31	Sodium 4-Phenylbutyrate	HDAC inhibitor
32	IOX1	2-oxoglutarate oxygenase inhibitor
33	Gemcitabine	Nucleic acid synthesis inhibitor
34	Daminozide	KDM2/7 histone demethylase inhibitor
35	GSK-J1 (sodium salt)	Jumonji domain-containing protein 3 (JMJD3) inhibitor and KDM6A inhibitor
36	GSK-J4 (hydrochloride)	H3K27 histone demethylase inhibitor
37	CI-994	HDAC inhibitor
38	CPTH2 (hydrochloride)	HAT inhibitor
39	Butyrolactone 3	HAT inhibitor
40	Valproic Acid (sodium salt)	Class I HDAC inhibitor
41	Tenovin-1	p53 activator
42	Tenovin-6 (hydrochloride)	p53 activator
43	BIX01294 (hydrochloride hydrate)	HMT inhibitor
44	Anacardic Acid	HAT inhibitor
45	AGK2	SIRT2 inhibitor
46	CAY10603	HDAC6 inhibitor
47	Splitomicin	Yeast HDAC inhibitor
48	CBHA	HDAC6 inhibitor
49	Salermide	Sirtuin inhibitor
50	Pimelic Diphenylamide 106	Class I HDAC inhibitor
51	Panobinostat	HDAC inhibitor
52	MS-275	HDAC inhibitor
53	HNHA	HDAC inhibitor
54	RG108	DNA methyltransferase inhibitor
55	2',3',5'-triacetyl-5-Azacytidine	DNA methyltransferase inhibitor
56	UNC0224	HAT inhibitor
57	Chidamide	HDAC inhibitor
58	3-Deazaneplanocin A	EZH2 inhibitor
59	5-Nitroso-8-quinolinol	HDAC inhibitor
60	Pyroxamide	HDAC inhibitor
61	N-Oxalylglycine	Jumonji domain-containing protein 2 (JMJD2) inhibitor
62	AMI-1 (sodium salt)	Type I PRMT inhibitor
63	EPZ005687	EZH2 inhibitor
64	SGC0946	HMT DOT1L inhibitor
65	UNC1215	MBT domain protein inhibitor

66	AK-7	SIRT2 inhibitor
67	JNJ-26481585 (hydrochloride)	HDAC inhibitor
68	GSK343	EZH2 inhibitor
69	Bromosporine	BRD inhibitor
70	GSK2801	BRD inhibitor
71	Plumbagin	Naphthoquinone (natural compound)
72	SIRT1/2 Inhibitor IV	SIRT1/2 inhibitor
73	I-CBP112 (hydrochloride)	p300 and CBP inhibitor
74	SGC-CBP30	BRD inhibitor
75	UNC0642	HMT inhibitor
76	UNC1999	EZH2 inhibitor
77	(R)-PFI-2 (hydrochloride)	HMT SET7/9 inhibitor
78	LMK 235	HDAC4 and HDAC5 inhibitor
79	HPOB	HDAC6 inhibitor
80	HDAC6 Inhibitor	HDAC6 inhibitor
81	2-hexyl-4-Pentynoic Acid	HDAC inhibitor
82	PFI-3	BRD inhibitor
83	JIB-04	JMJD inhibitor
84	CAY10683	HDAC inhibitor
85	GSK126	EZH2 inhibitor
86	CPI-203	BRD inhibitor
87	SP2509	LSD1 inhibitor
88	6-Thioguanine	DNA methylation inhibitor
89	Tubastatin A	HDAC6 inhibitor
90	OTX015	BRD inhibitor
91	A-366	HMT inhibitor
92	OICR-9429	WD repeat domain 5 (WDR5) inhibitor
93	EPZ004777 (formate)	HMT DOT1L inhibitor
94	EPZ6438	EZH2 inhibitor
95	EPZ5676	HMT DOT1L inhibitor
96	MC 1568	Class IIa HDAC inhibitor
97	PBIT	KDM5 family protein inhibitor
98	Octyl-α-hydroxyglutarate	Cell-permeable form of metabolite 2-Hydroxyglutarate (2-HG)
99	α-Hydroxyglutaric Acid (sodium salt)	Metavbolite α-hydroxy acid, methylation regulation
100	UNC0379	HMT SET8 inhibitor
101	RVX-208	BRD inhibitor
102	CUDC-101	EGFR inhibitor, HDAC inhibitor and HER2 inhibitor
103	LAQ824	HDAC inhibitor
104	GSK-LSD1 (hydrochloride)	LSD1 inhibitor
105	BVT 948	Protein tyrosine phosphatases inhibitor
106	RGFP966	HDAC3 inhibitor
107	BG45	HDAC3 inhibitor
108	UMB-32	BRD inhibitor
109	EPZ015666	PRMT5 inhibitor
110	BI-2536	Polo-like kinase 1 (PLK1) inhibitor
111	BAZ2-ICR	BRD inhibitor
112	OG-L002	LSD1 inhibitor
113	ML-324	JMJD2 inhibitor
114	GSK484 (hydrochloride)	Peptidylarginine deiminase 4 (PAD4) inhibitor
115	Resminostat (hydrochloride)	HDAC inhibitor
116	NI-57	BRD inhibitor
117	PFI-4	BRD inhibitor
118	Tasquinimod	S100A9 inhibitor (anti-cancer compound)
119	MM-102	WDR5/ mixed lineage leukemia (MLL) interaction inhibitor
120	TC-E 5003	PRMT1 inhibitor
121	L002	HAT p300 inhibitor
122	BI-9564	BRD inhibitor
123	RN-1 (hydrochloride)	LSD1 inhibitor
124	Mocetinostat	HDAC inhibitor
125	A-196	HMT SUV420H1 and SUV420H2 inhibitor
126	MS049 (hydrochloride)	PRMT4/PRMT6 inhibitor
127	GSK591	PRMT5 inhibitor
128	MS023 (hydrochloride)	Type I PRMT inhibitor
129	PRT4165	PRC1 ubiquitin ligase inhibitor
130	EPZ020411	PRMT6 inhibitor
131	GSK2879552	LSD1 inhibitor
132	Cyproheptadine (hydrochloride hydrate)	Interferon regulatory factor 6 (IRF6) regulation
133	CPTH6 (hydrobromide)	HAT Gcn5 and pCAF inhibitor
134	CeMMEC1	BRD inhibitor
135	PCI 24781	HDAC inhibitor
136	BML-278	SIRT1, SIRT2, and SIRT3 activator
137	CeMMEC13	BRD inhibitor

138	4'-bromo-Resveratrol	SIRT1 and SIRT3 inhibitor
139	AZD 5153	BRD4 inhibitor
140	Todralazine (hydrochloride)	β2-adrenergic receptor inhibitor
141	HDAC3 Inhibitor	HDAC3 inhibitor
142	NCH-51	HDAC inhibitor
143	UF010	Class I HDAC inhibitor
144	RGFP109	HDAC inhibitor
145	C-7280948	PRMT1 inhibitor
146	EED226	PRC2 inhibitor
147	CAY10722	SIRT3 inhibitor
148	PAOA	Selective HDAC1/3 inhibitor
149	TMP-195	Class IIa HDAC inhibitor
150	Bufexamac	Class IIb HDAC inhibitor
151	Trichostatin A	HDAC inhibitor
152	CAY10398	HDAC inhibitor
153	RSC-133	DNMT1 inhibitor
154	BML-210	HDAC inhibitor
155	CAY10591	SIRT1 activator
156	(±)-EX-527	SIRT1 inhibitor
157	SAHA	HDAC inhibitor
158	Tranylcypromine (hydrochloride)	LSD1 inhibitor